UNIVERSIDADE FEDERAL DO RIO GRANDE DO SUL

CENTRO ESTADUAL EM PESQUISAS DE SENSORIAMENTO REMOTO E METEOROLOGIA

PROGRAMA DE PÓS-GRADUAÇÃO EM SENSORIAMENTO REMOTO

MÉTODO PARA QUANTIFICAÇÃO E MAPEAMENTO DA COMPLEMENTARIDADE ESPACIAL NO TEMPO

ALFONSO RISSO

Orientação:

Profa. Dra. RITA DE CASSIA MARQUES ALVES

Prof. Dr. ALEXANDRE BELUCO

Porto Alegre,

Dezembro de 2019

UNIVERSIDADE FEDERAL DO RIO GRANDE DO SUL

CENTRO ESTADUAL EM PESQUISAS DE SENSORIAMENTO REMOTO E METEOROLOGIA

PROGRAMA DE PÓS-GRADUAÇÃO EM SENSORIAMENTO REMOTO

Alfonso Risso

MÉTODO PARA QUANTIFICAÇÃO E MAPEAMENTO DA COMPLEMENTARIDADE ESPACIAL NO TEMPO

Tese de Doutorado apresentada ao Programa de Pós-Graduação em Sensoriamento Remoto, do Centro Estadual de Pesquisas em Sensoriamento Remoto e Meteorologia, da Universidade Federal do Rio Grande do Sul, como parte dos requisitos para a obtenção do título de Doutor por Defesa Direta de Tese pelos requisitos estabelecidos pela Resolução 56/98 do CEPE da UFRGS.

Orientação:

Profa. Dra. RITA DE CASSIA MARQUES ALVES

Prof. Dr. ALEXANDRE BELUCO

Porto Alegre,

Dezembro de 2019

Risso, Alfonso
MÉTODO PARA QUANTIFICAÇÃO E MAPEAMENTO DA COMPLEMENTARIDADE ESPACIAL NO TEMPO
/Alfonso Risso

-- 2018.
xxx f.

Orientador: Alexandre Beluco.

Tese (Doutorado) -- Universidade Federal do Rio Grande do Sul, Instituto de Pesquisas Hidráulicas, Programa de Pós-Graduação em Recursos Hídricos e Saneamento Ambiental, Porto Alegre, BR-RS, 2015.

1. Complementaridade Energética. 2. Recursos Renováveis. 3. Sistemas Híbridos. 4. Geoprocessamento. 5. HOMER. 6. ViPOR
I. Alves, Rita de Cassia Marques, Beluco, Alexandre, orient. II. Título.

Alfonso Risso

MÉTODO PARA QUANTIFICAÇÃO E MAPEAMENTO DA COMPLEMENTARIDADE ESPACIAL NO TEMPO

Tese de Doutorado apresentada ao Programa de Pós-Graduação em Sensoriamento Remoto, do Centro Estadual de Pesquisas em Sensoriamento Remoto e Meteorologia, da Universidade Federal do Rio Grande do Sul, como parte dos requisitos para a obtenção do título de Doutor por Defesa Direta de Tese pelos requisitos estabelecidos pela Resolução 56/98 do CEPE da UFRGS.

Banca Examinadora:

_____

Prof. Dr. José de Souza – Fundação Liberato DPPI

_____

Prof. Dr. Elton Rossini – UERGS

_____

Prof. Dr. André Silveira – UFRGS

_____

Profa. Dra. Tatiana S. da Silva – UFRGS

Porto Alegre
Dezembro de 2019

AGRADECIMENTOS

Às vezes é difícil enxergar a luz no fim do túnel, porém na maioria das vezes, basta observar de um outro ponto de vista.

O meu mais profundo agradecimento a todos que de alguma forma contribuíram ao longo desta interessante e intensa jornada. Aos que acreditaram e aos que não acreditaram meu sincero obrigado.

Uma etapa cumprida e um sonho alcançado acompanhado de pessoas muito importantes na minha vida.

- Aos meus orientadores e amigos Prof. Alexandre e Profª Rita. O primeiro, por me fazer acreditar que eu poderia contribuir na área de pesquisa de energias renováveis e a Profª Rita por me acolher tão gentilmente no Centro Estadual de Pesquisas e Sensoriamento Remoto da UFRGS.
- Aos professores da banca pelas suas avaliações e contribuições
- Ao Programa de Pós-Graduação em Sensoriamento Remoto da UFRGS, por permitir e apoiar o desenvolvimento desta Tese de Doutorado.
- Ao Centro Estadual de Pesquisa em Sensoriamento Remoto e Meteorologia pela oportunidade da realização deste trabalho, aos funcionários pela amizade e apoio dedicado;
- Aos meus colegas professores e amigos do Instituto de Pesquisas Hidráulicas que com sua camaradagem, me incentivaram e contribuíram para minha formação profissional e sanidade mental;
- Aos meus alunos que sempre torceram por mim. Em especial à Mariana Tosi Correa que contribuiu de forma dedicada na elaboração de alguns dos artigos apresentados neste trabalho.
- Aos meus amigos da Overboxe Academia pelo apoio e incentivo.
- Finalmente e com muito amor a minha família. Ao meu filho por me puxar as orelhas nos momentos certos e por sua parceria única. A minha irmã e minha sobrinha Maria Clara, pela paciência e carinho. A minha mãe Stella pelo seu amor e dedicação. Também não posso deixar de agradecer ao meu pai, “Don Cacho Risso”, que apesar não estar mais neste plano, sempre acreditou nos seus filhos e dedicou a nós toda sua vida.

Aos que vieram, estão e virão, o meu muito obrigado e um abraço a todos.

MÉTODO PARA QUANTIFICAÇÃO E MAPEAMENTO DA COMPLEMENTARIDADE ESPACIAL NO TEMPO

RESUMO

Esta tese tem por objetivo desenvolver uma ferramenta que permita compreender a complementaridade energética, dando ênfase a complementaridade temporal em um domínio espacial, de forma a permitir o mapeamento de seus parâmetros descritores. A metodologia para o desenvolvimento desta ferramenta, se adequa perfeitamente ao ambiente de um Sistema de Informações Geográficas – SIG, permitindo o armazenamento, manejo e representação espacial da complementaridade energética através de técnicas de análise espacial, disponíveis na maioria das plataformas de geoprocessamento. Na composição desta tese são apresentados seis artigos e um capítulo de livro, os quais descrevem as diferentes abordagens metodológicas desenvolvidas para a obtenção de uma ferramenta que permita representar espacialmente a complementaridade temporal em um domínio espacial, assim como permitir o engajamento de aplicativos (HOMER e ViPOR) para gestão e tomada de decisões sobre os cenários obtidos a partir do mapeamento da complementaridade energética de sistemas híbridos de recursos renováveis. O mapeamento, através de uma matriz regular de células hexagonais e de gráficos de roseta acoplados, para a visualização da natureza das diferentes fontes de recursos energéticos em um sistema híbrido e a sua complementaridade, mostrou ser uma forma muito eficiente para a compreensão dos múltiplos parâmetros envolvidos na complementaridade temporal no domínio espacial.

PALAVRAS-CHAVE: 1. Complementaridade Energética. 2. Recursos Renováveis. 3. Sistemas Híbridos. 4. Geoprocessamento. 5. HOMER. 6. ViPOR.

A METHOD FOR QUANTIFICATION OF SPACE COMPLEMENTARITY IN TIME AND ITS GRAPHIC EXPRESSION THROUGH MAPS

ABSTRACT

This thesis intends to develop a tool that allows to understand the energy complementarity, emphasizing the temporal complementarity in a spatial domain, in order to allow the mapping of its descriptor parameters. The methodology for the development of this tool is perfectly suited to the environment of a Geographic Information System - GIS, allowing the storage, management and spatial representation of energy complementarity through spatial analysis techniques, available in most geoprocessing platforms. In the composition of this thesis six articles and a book chapter are presented, describing the different methodological approaches developed to obtain a tool that allows to represent the temporal complementarity in a spatial domain, as well as to allow the engagement of applications (HOMER and ViPOR) for management. and decision making on scenarios obtained from the mapping of energy complementarity of hybrid renewable resource systems. Mapping, through a regular matrix of hexagonal cells and coupled rosette graphs, to visualize the nature of the different sources of energy resources in a hybrid system and their complementarity, proved to be a very efficient way to understand the multiple parameters involved in the temporal complementarity of the system.

KEYWORDS: 1. Energetic Complementarity. 2. Renewable Resources. 3. Hybrid Systems. 4. Geoprocessing. 5. HOMER. 6. ViPOR.

SUMÁRIO

LISTA DE FIGURAS

LISTA DE TABELAS

1. INTRODUÇÃO

O Brasil possui o privilégio de possuir uma matriz energética onde os sistemas de geração baseados em recursos renováveis se destacam (Fig. 1.1), com ênfase para energia hidrelétrica (63%). Concomitantemente, observa-se nos últimos anos o crescimento de outras fontes renováveis como eólica, solar entre outras e a redução do uso de fontes não renováveis. Por outro lado, de acordo com EPE (2018) [1-1], observa-se uma taxa positiva anual de crescimento de consumo de energia de 1,3 % entre os anos de 2011 -2017, decorrente de fatores como crescimento populacional e qualidade de vida, expansão da rede de abastecimento, etc. Estas tendências, implicam numa necessidade de crescimento e otimização do sistema de geração de energia.

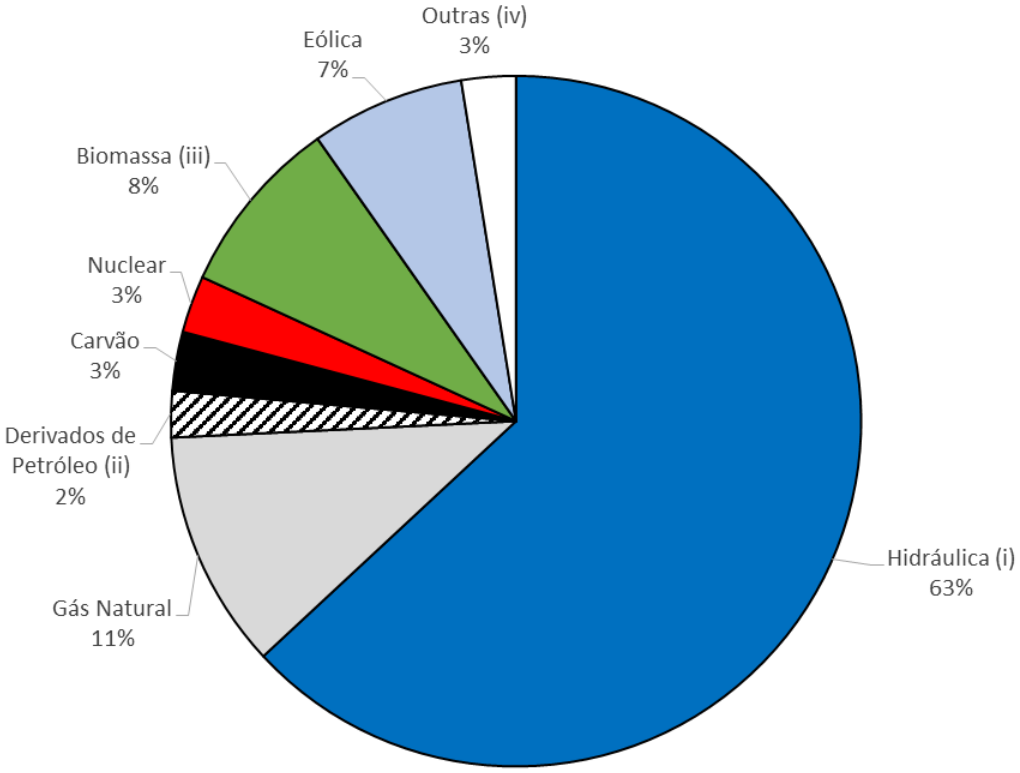

Fig. 1.1. Geração elétrica por fonte no Brasil (GWh).
(Fonte: EPE (2018) [1-1]).

Os sistemas de geração de energia baseados em recursos renováveis vêm se tornando alternativas viáveis em uma quantidade crescente de oportunidades. Tanto pelas novas tecnologias disponíveis para os recursos que já apresentam maturidade técnica e econômica, como a energia hidrelétrica, a energia eólica e a energia solar em algumas aplicações, quanto

os recursos renováveis em fase de desenvolvimento, como a energia de ondas e a energia de marés.

Neste sentido, se faz presente a necessidade de dispor ferramentas que embasem decisões de priorização de investimentos aos gestores responsáveis pelo gerenciamento dos recursos energéticos disponíveis. Entre as novas ferramentas para tomada de decisão está a complementaridade energética, que pode contribuir para a priorização de investimentos já que sistemas baseados em recursos complementares podem ser mostrar mais eficientes. A complementaridade pode ser verificada entre recursos energéticos em um mesmo local e entre locais diferentes. A complementaridade temporal pode ser dividida em três componentes: a complementaridade no tempo, a complementaridade de energia e a complementaridade entre amplitudes.

Sendo assim, este trabalho contribui para um melhor entendimento da complementaridade energética e, especificamente, para um melhor entendimento da complementaridade em um domínio espacial.

1.1 Organização

Nos capítulos iniciais deste trabalho, é feita uma descrição sucinta e objetiva dos conceitos fundamentais de complementaridade energética no espaço e no tempo, revisando algumas pesquisas prévias.

Também são descritos os materiais e métodos utilizados pelo autor que resultaram na confecção de seis artigos e um capítulo de livro listados a seguir:

- Bases for a Methodology Assessing Time Complementarity in Space. Energy and Power Engineering (2017). Ed. Scientific Research Publishing. Autores: Alfonso Risso e Alexandre Beluco.
- Complementarity Roses Evaluating Spatial Complementarity in Time between Energy Resources. Energies (2018). MDPI. Autores: Alfonso Risso, Alexandre Beluco e Rita de Cássia Marques Alves.
- Compatibilization Between ISLSCP II UNH/GRDC Composite Monthly Runoff Model and HYDROBASINS Base for Long-Term Flow Estimation in Rio Grande do Sul (2019). Journal of Hydrology. ELSEVIER Editorial. Autores: Alfonso Risso; Mariana Tosi Corrêa; Alexandre Beluco, Rita de Cássia Marques Alves e Laurindo Guasselli.
- Qualitative Evaluation of Spatial Complementarity between Renewable Energy Resources with Complementarity Roses (2019). Publicado no periódico

MethodsX. ELSEVIER Editorial. Autores: Alfonso Risso, Alexandre Beluco e Rita de Cássia Marques Alves.

- Ponderadores de Distância para Parâmetros de Complementaridade Espacial entre Recursos Energéticos Renováveis no Estado do Rio Grande Do Sul. Anuário do Instituto de Geociências (2019). Instituto de Geociências da Universidade Federal do Rio de Janeiro. Autores: Alfonso Risso; Mariana Tosi Corrêa; Alexandre Beluco e Rita de Cássia Marques Alves.
- A PV Wind Hydro Hybrid System with Pumped Storage Capacity Installed in Linha Sete, Aparados da Serra, Southern Brazil. Modeling and Dynamic Behaviour of Hydropower Plants – Ch 10 (2016). Ed. The Institution of Engeneering and Technology. Autores Alfonso Risso, Fausto A. Canales, Alexandre Beluco e Elton G. Rossini.
- Some Effects Of Spatial Complementarity In Time On The Design Of A Medium-Sized Wind Hydro Hybrid System. Renewable Energy (2019). ELSEVIER Editorial.Autores: Alfonso Risso, Alexandre Beluco e a Rita de Cássia Marques Alves.

Os artigos primeiro, segundo e quarto, se articulam na proposição de um método para quantificação de complementaridade energética espacial no tempo e para sua expressão através de mapas, com base na elaboração de rosas de complementaridade que expressam as complementaridades no tempo entre diferentes locais, mostrando informações de direção, de distância entre os locais comparados e de intensidade de complementaridade no tempo.

O terceiro artigo, apresenta uma metodologia para validar dos valores da composição mensal de escoamento superficial (Composite Monthly Runoff) acoplados a um modelo de direção de fluxo com 250 m de resolução, derivado do Shuttle Radar Topography Mission descrito por Farr et al (2000) [1-2]. Uma vez validados, foi possível estimar a distribuição espacial dos meses de máximas e mínimas vazões mínimas na área de estudo.

O quinto artigo apresenta a consolidação da metodologia de quantificação e mapeamento da complementaridade energética no espaço, ajustado a funções de ponderação que visam atenuar o efeito de complementaridade com a distância entre os diferentes recursos energéticos.

No capítulo de livro, é avaliada a influência da complementaridade espacial sobre a performance de um sistema híbrido de geração de médio porte, conectando usinas hidrelétricas, fazendas eólicas e uma usina fotovoltaica a algumas cidades do litoral norte do estado do Rio Grande do Sul. O trabalho apresenta um mapa do Estado do Rio Grande do Sul, indicando a

complementaridade espacial no tempo entre um conjunto de usinas hidrelétricas e um conjunto de fazendas eólicas, espalhadas ao longo do território do Estado.

No último artigo é descrita uma aplicação do programa ViPOR, onde são dimensionadas linhas de transmissão para dois cenários, sem e com complementaridade espacial no tempo, visando comprovar a otimização de custos de implantação da rede no cenário com complementaridade. Ao final, são tecidos comentários sobre a continuidade deste trabalho.

1.2 Referencias

[1-1] EPE, Empresa de Pesquisa Energética (2018). Anuário Estatístico de Energia Elétrica 2018 ano base 2017. Ministério de Minas e Energia. URL: http://www.epe.gov.br.

[1-2] Farr, T. G., and M. Kobrick (2000), Shuttle Radar Topography Mission produces a wealth of data, *Eos Trans. AGU*, *81*(48), 583, 585.

2. OBJETIVOS

2.1 Objetivo geral

O principal objetivo deste trabalho é a proposição e avaliação de ferramentas e métodos que permitam uma melhor compreensão da complementaridade espaço/temporal em uma matriz de geração de energia híbrida baseada em recursos energéticos renováveis.

2.2 Objetivos específicos

I. Melhorar o entendimento da complementaridade energética no espaço como ferramenta de planejamento e gestão;

II. Identificação de formas que permitam representar adequadamente a distribuição espacial da complementaridade dos diferentes sistemas energéticos renováveis;

III. Propor um método para avaliação quantitativa da complementaridade espacial no tempo e que permita o seu mapeamento;

IV. Compreender a influência da complementaridade espacial no tempo sobre a performance de sistemas híbridos baseados em recursos energéticos renováveis

3. JUSTIFICATIVA

A compreensão da complementaridade de diferentes matrizes de recursos energéticos renováveis, através de ferramentas que permitam a sua quantificação e mapeamento, fornece subsídios para projetistas, gestores e operadores ligados à geração de energia elétrica, respondendo a questões como:

- Identificar a distância e localização entre recursos complementares.
- Projetar sistemas energéticos que se aproveitem das informações de complementaridade, otimizando custos de implantação e operação.
- Identificar locais ideais para implantação de novos sistemas geração para diferentes recursos renováveis.

4. COMPLEMENTARIDADE

Complementaridade é uma habilidade verificada quando duas ou mais fontes de recursos energéticos conseguem se completar um ao outro ao longo do tempo. A complementaridade pode ser:

- Pontual → complementaridade temporal;
- Multi-pontual → complementaridade espacial.

Este segundo caso é mais complexo do que a complementaridade em um mesmo local, exigindo uma abordagem específica para sua quantificação.

Nos ultimos anos, destacam-se alguns trabalhos publicados previamente neste contexto.

Dentro de um enfoque estatístico, [4-3] e [4-4] apresentaram estudos de mapas de complementaridade espaço-tempo por correlção estatística sobre unidades espaciais irregulares. O estudo de [4-3] abordou a complementaridade de sistemas hidro eólicos e [4-4] estudou complementaridade entre sistemas hidro e eólico offshore

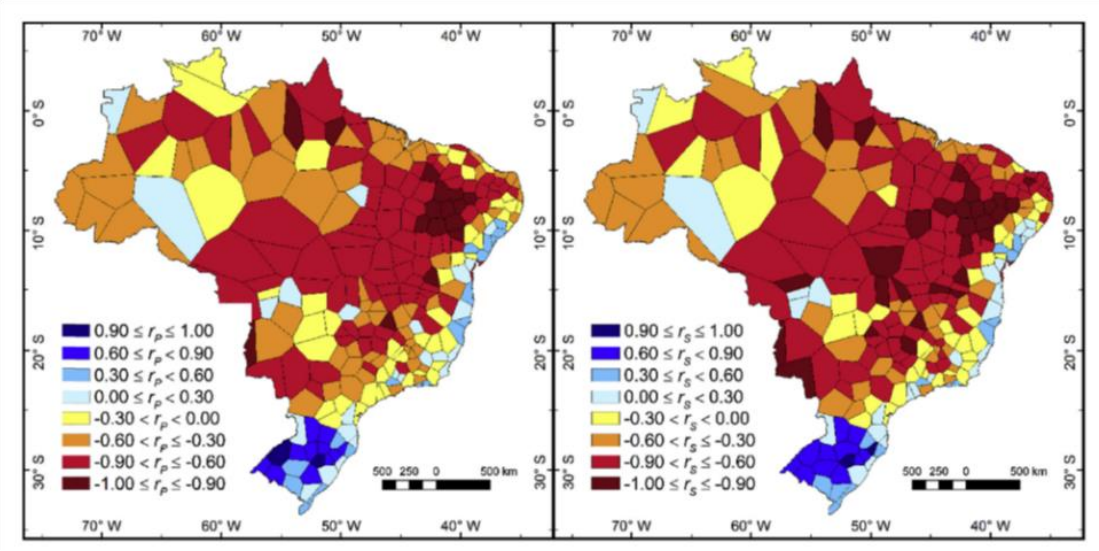

Fig. 4.1. Complementaridade de sistemas hidro eólicos. (Fonte: [4-3]).

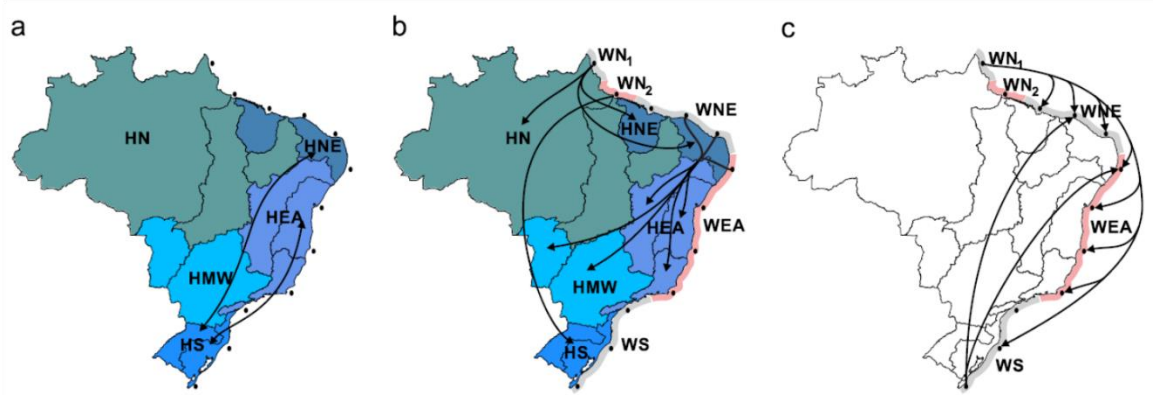

Fig. 4.2. Complementaridade (a) hídrico-hídrico offshore, (b) hídrico-eólica e (c) eólica-eólica offshore. (Fonte: [4-4]).

São apresentaods por [4-1] e [4-2], um conjunto de artigos sobre complementaridade energética, com ênfase na abordagem temporal (pontual), cujos fundamentos são apresentados no ítem a seguir e que serviram para o desenvolvimento desta tese.

4.1 Fundamentos da Complementaridade Temporal

Segundo Beluco (2008) a complementaridade temporal (Eq. 4.1) entre diferentes recursos energéticos renováveis, pode ser estimada a partir três componentes (*tempo, energia* e *amplitude*) extraídos da sua séries temporais. A Fig. 4.3 apresenta um exemplo de máxima complementaridde temporal.

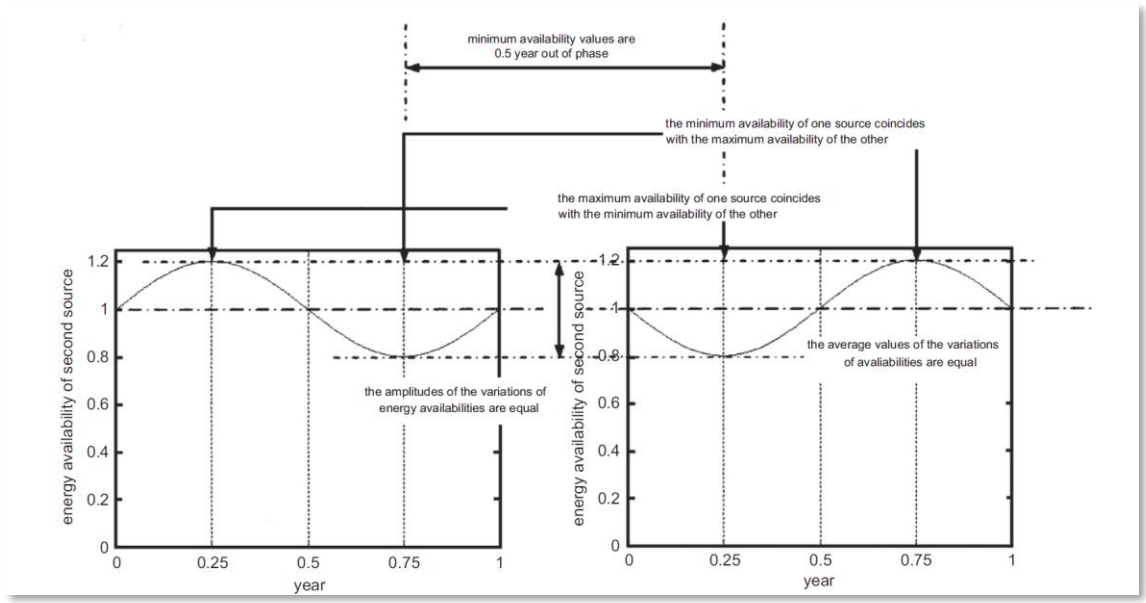

Fig. 4.3. Máxima complementaridade ao longo de um ano.

(Fonte: [4-1])

$$K = K_t K_e K_a \qquad \text{Eq. 4.1}$$

Onde:

K é o índice de complementaridade no tempo;

K_t é o índice parcial de complementaridade no tempo;

K_e é o índice parcial de complementaridade de energia e

K_a é o índice parcial de complementaridade de amplitude.

Sendo que a Eq. 4.2 representa o índice parcial de compementaridade no tempo.

$$K_t = \frac{|d_h - d_s|}{\sqrt{[D_h - d_h]|D_s - d_s|}} \qquad \text{Eq. 4.2}$$

Onde:

D_h é o dia com máxima disponibilidade de energia hidráulica;

d_h é o dia com a mínima disponibilidade de energia hidráulica;

D_s é o dia com máxima disponibilidade de energia solar e

d_s é o dia com a mínima disponibilidade de energia solar.

A Eq. 4.3 representa o índice parcial de complementaridade de energia.

$$K_e = 1 - \sqrt{\left(\frac{E_h - E_s}{E_h + E_s}\right)^2} \qquad \text{Eq. 4.3}$$

Onde:

E_h é a energia hidráulica total em um ano;

E_s é a energia solar total em um ano.

E a Eq. 4.4 representa índice parcial de complementaridade de amplitude.

$$K_a = \begin{cases} \left[1 - \frac{(\delta_h - \delta_s)^2}{(1-\delta_s)^2}\right] \; para \;\; \delta_h \leq \delta_s \\ \left[\frac{(1-\delta_s)^2}{(1-\delta_s)^2 + (\delta_h - \delta_s)^2}\right] para \;\; \delta_h > \delta_s \end{cases} \quad \text{Eq. 4.4}$$

Onde:

δ_h é a diferença entre a máxima e a mínima energia hidráulica disponível em um ano;

δ_s é a diferença entre a máxima e a mínima energia solar disponível em um ano.

4.2 Referencias

[4-1] Beluco, A., Kroeff, P.K., Krenzinger, A. (2008) A dimensionless index evaluating the time complementarity between solar and hydraulic energies. Renewable Energy, 33, 10, 2157-2165. http://dx.doi.org/10.1016/j.renene.2008.01.019

[4-2] Beluco, A. Souza, P.K. Krenzinger, A. (2012) A method to evaluate the effect of complementarity in time between hydro and solar energy on the performance of hybrid hydro PV generating plants. Renewable Energy, v.45, p.24-30.

[4-3] Cantão, M. P., Bessa, M. R., Bettega, R., Detzel, D. H. M., Lima, J. M. (2017). Evaluation of hydro-wind complementarity in the Brazilian territory by means of correlation maps. Renewable Energy , v. 101, p. 1215-1225.

[4-4] Silva, A. R., Pimenta, F.M., Assireu, A.T., Spyrides, M.H.C. (2016). Complementarity of Brazil s hydro and offshore wind power. Renewable and Sustainable Energy Reviews, Elsevier, v. 56, p. 413–427, 2016.

5. METODOLOGIA

Para o mapeamento da complementaridade espacial no tempo, foi desenvolvida uma metodologia constituida de 6 etapas:

I. Discretização o espaço geográfico (células hexagonais);

II. Integração as diferentes matrizes energéticas as células;

III. Estimativa dos meses mínimos e máximos de disponibilidade energética em cada célula;

IV. Estimativa das localizações e distâncias entre as células das diferentes matrizes energéticas;

V. Cálculo das complementaridades espaciais no tempo entre as matrizes energéticas;

VI. Construção de Rosas de Complementaridade.

5.1 Células Hexagonais

A opção de uma matriz regular de células hexagonais para discretização da distribuição espacial dos recursos energéticos e sua complementaridade se deu pelos seguintes motivos:

- Normalizar a discretização do espaço: Obter uma unidade geométrica discreta única para representar a distribuição dos recursos energéticos e sua complementaridade.
- Encaixe perfeito: As unidades geométricas discretas não devem apresentar espaços vazios (gaps) entre sí.

Estas duas propriedades espaciais são possíveis de serem obtidas utilizando matrizes regulares com células triangulares e retangulares. No entanto, uma matriz hexagonal apresenta as seguintes vantagens:

- Redução do efeito de "pixelização": Os padrões lineares nos hexágonos não são tão aparentes, o que torna as formas "mais suaves" quando os contornos fiquem viziveis.
- Mesma distância de seu vizinho mais próximo em todas as direções: Em uma célula retangular os vizinhos diagonais diferem na distância dos vizinhos cardeais, o que em análise espacial pode reduzir efeitos de tendenciosidade (efeito de preconceito).
- Melhor ajuste a estrutura do gráfico de rosetas: Os gráficos de rosetas são utilizados neste trabalho com o objetivo de representar espacialmente, propriedades como, distância, direção e magnitude da complementaridade energética entre duas fontes de recursos energéticos situados em diferentes locais. Para este tipo de estrutura, as células hexagonais são as que apresentam um melhor ajuste espacial.

Uma análise comparativa mais detalhada sobre as vantagens e desvantagens entre estruturas de matrizes retangulares e hexagonais em análise espacial pode ser vista em [5-1].

5.2 Diagrama de Roseta

Um diagrama de roseta, também conhecido como gráfico polar, é uma estrutura espacial bastante utilizada em geologia e meteorologia, com a finalidade de representar múltiplos atributos espaciais associados a uma localização. No caso de aplicações em geologia, esta estrutura é normalmente utilizada para descrever as características tectônicas de um ponto, tais como, frequência de lineamento na vizinhança, suas direções, classes de comprimento, etc. Em meteorologia, este tipo de estrutura é muito utilizado para representar, as frequências de direção, intensidade e probabilidade de ocorrência de ventos e graus contaminação atmosférica por exemplo.

Desta forma, o uso de diagramas de roseta atende as necessidades de representar graficamente os múltiplos atributos descritivos, associados a complementaridade temporal no espaço entre dois recursos energéticos (direção, frequência, distância e magnitude). Por outro lado, a capacidade de acoplar este tipo de representação as células de uma matriz hexagonal, tornou este tipo de estrutura a mais adequada para esse fim. A **Fig. 5.1** apresenta os elementos do gráfico de roseta, denominado nesta tese de "rosas de complementaridade".

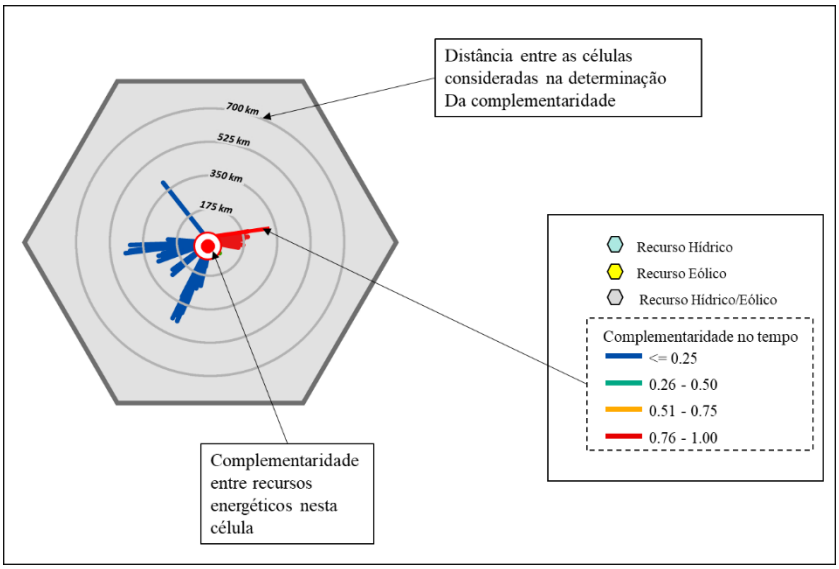

Fig. 5.1. Elementos descritivos de uma célula hexagonal com a sus rosa de complementaridade acoplada.

5.3 Distribuição Espacial das Matrizes Energéticas

Um fator importante a ser considerado na análise da complementaridade espacial dos recursos energéticos é o seu padrão de distribuição espacial.

Os sistemas de geração de Energia Hidrelétrica apresentam um padrão espacial **Pontual/Linear**. Em outras palavras, a disponibilidade desse recurso energético é definida por uma localização pontual que depende de uma diferença potencial gravitacional (queda d'água) e uma área de contribuição (bacia hidrográfica), sendo esta localização situada em um determinado curso d'água (feição linear). No capítulo 9 descreve a técnica utilizada para mapear o potencial hídrico neste tipo de padrão espacial, através da acoplagem de um modelo de disponibilidade hídrica superficial difuso e um modelo digital de elevações hidrologicamente consistido.

Já a disponibilidade dos recursos energéticos eólicos e fotovoltaico apresentam um padrão **Difuso/Superficial**. Nesse caso o seu padrão de distribuição apresenta um gradiente de variabilidade gradual no espaço, isto é, todos os pontos da área analisada apresentarão algum valor de disponibilidade energética.

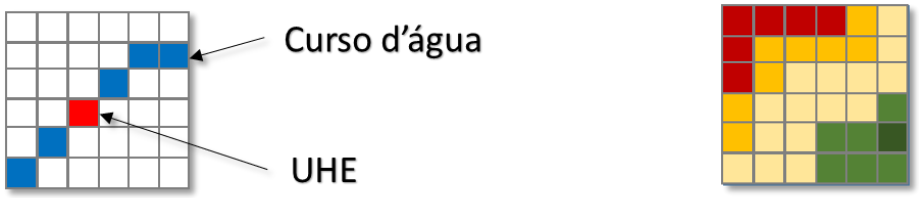

(a) (b)

Fig. 5.2. (a) Energia hidrelétrica → Pontual/Linear; (b) Energia eólica e fotovoltaica → Difusa/Superficial.

5.4 Dados Espaciais

Para a implementação das ferramentas para estimativa de complementaridade espacial no tempo, neste trabalho, foram utilizadas três bases de dados georreferenciados contendo informações de infraestrutura, recursos hídricos e clima.

5.4.1 Infraestrutura Nacional de Geração de Energia Elétrica

A base utilizada com os dados referentes a Infraestrutura Nacional de Geração de Energia Elétrica é a disponibilizada no Sistema de Informações Geográficas do Setor Elétrico

[5-5] (Fig. 5.3). Foram baixadas camadas Shapefile (ESRI) do endereço: https://sigel.aneel.gov.br/Down/.

As camadas baixadas consistiram planos de informação referentes a:

- Aproveitamentos Hidrelétricos (Usinas, PCHs e Centrais de Geração);
- Aproveitamentos Eolioelétricos.

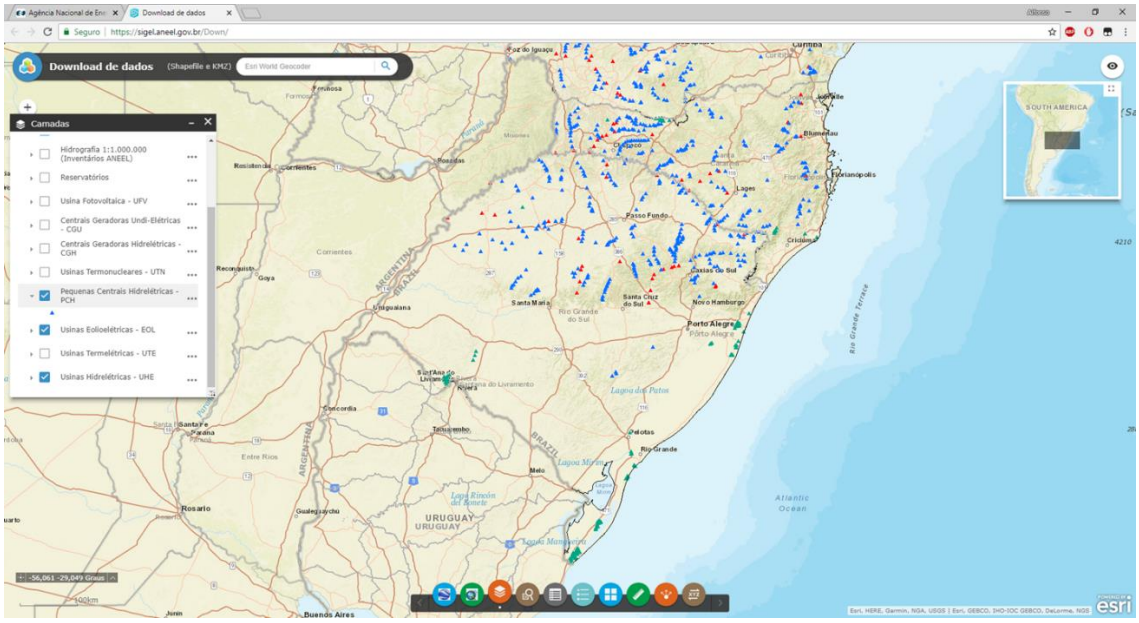

Fig. 5.3. Janela de consulta e download dos planos de informação do sistema SIGEL – ANEEL. (Fonte: [5-5])

5.4.2 Recursos Hídricos

Para identificar a disponibilidade de recursos hídricos superficiais para geração de hidrelétrica, foram utilizados os dados da base georreferenciada do International Satellite Land Surface Climatology Project (ISLSCP II) - University of New Hampshire [5-4]. Os planos de informação utilizados pertencem ao módulo: Hidrologia e Solos → ISLSCP II UNH/GRDC Composite Monthly Runoff. Estes dados de escoamento composto combinam estimativas médias mensais de escoamento de um modelo de balanço hídrico simulado derivadas de dados climáticas com descarga fluvial monitorada. Estes dados espaciais são apresentados com as seguintes características:

- Resolução Espacial do Conjunto de Dados: 1,0 grau e 0,5 grau em latitude e longitude

- Extensão temporal do conjunto de dados: 1986 a 1995.

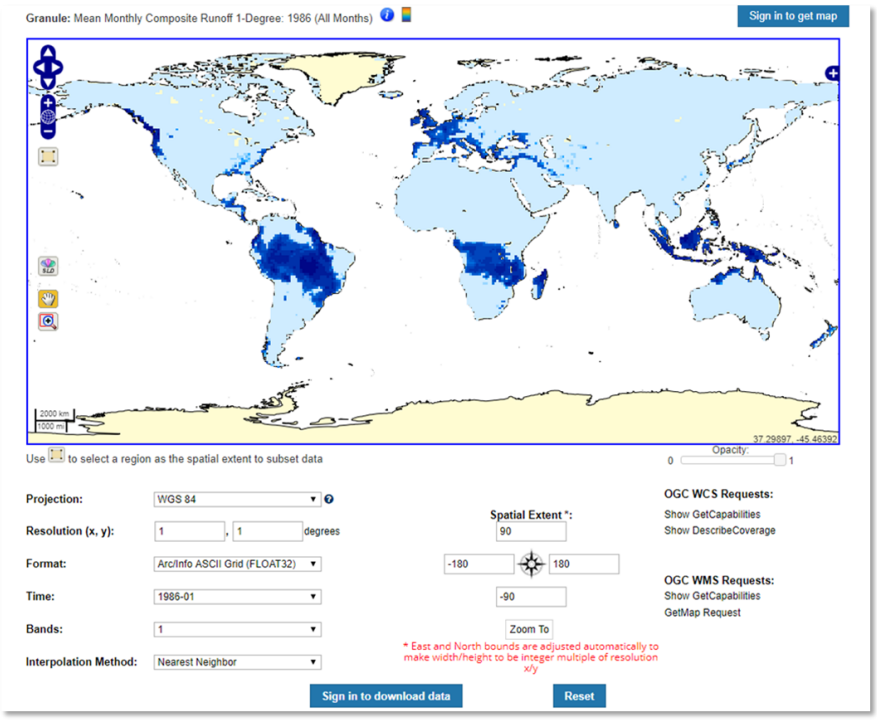

Fig. 5.4. Janela de consulta e download dos dados espaciais do ISLSCP II.

(Fonte: [5-4])

A Fig. 5.5 apresenta os meses de mínima e máxima disponibilidade hídrica integrados a base de células hexagonais. A escolha de uma área de 500 km² para as células hexagonais foi definida tendo em vista permitir uma melhor visualização para avaliar a eficiência do método de mapeamento da complementaridade e seus parâmetros, sem um custo computacional elevado. Por outro lado, esta resolução espacial para as células hexagonais, também deverá permitir a visualização das rosas de complementaridade.

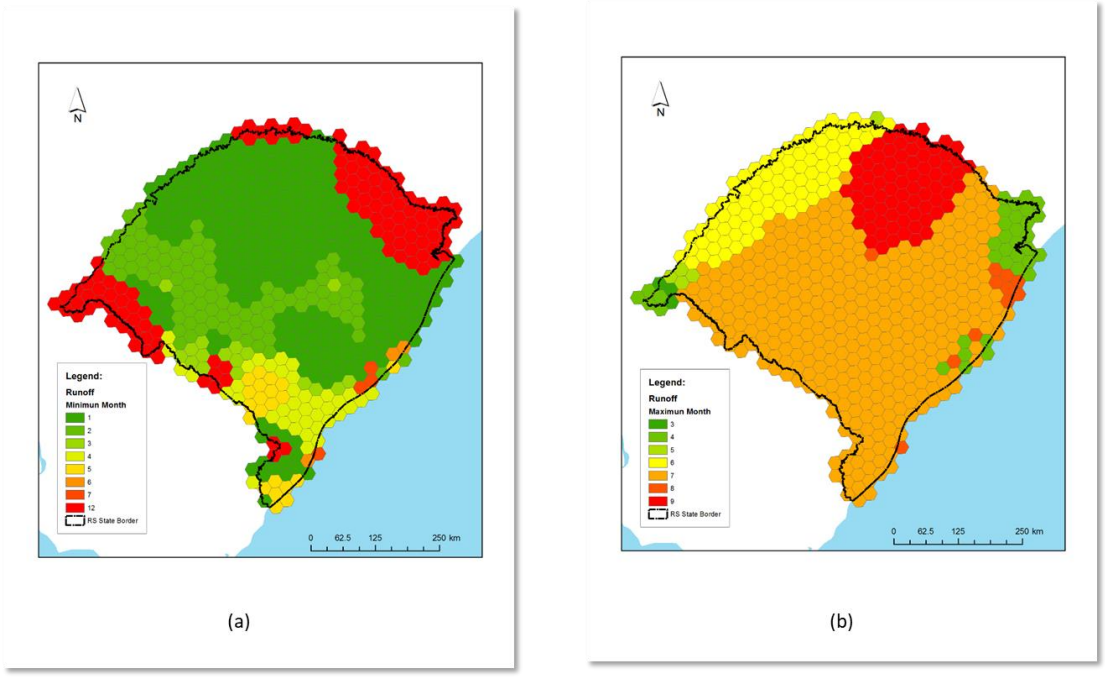

Fig. 5.5. Meses de mínima (a) e máxima (b) disponibilidade hídrica.

A Fig. 5.6 apresenta as células hexagonais com os meses de mínima e máxima disponibilidade hídrica que possuam infraestrutura de geração hidrelétrica.

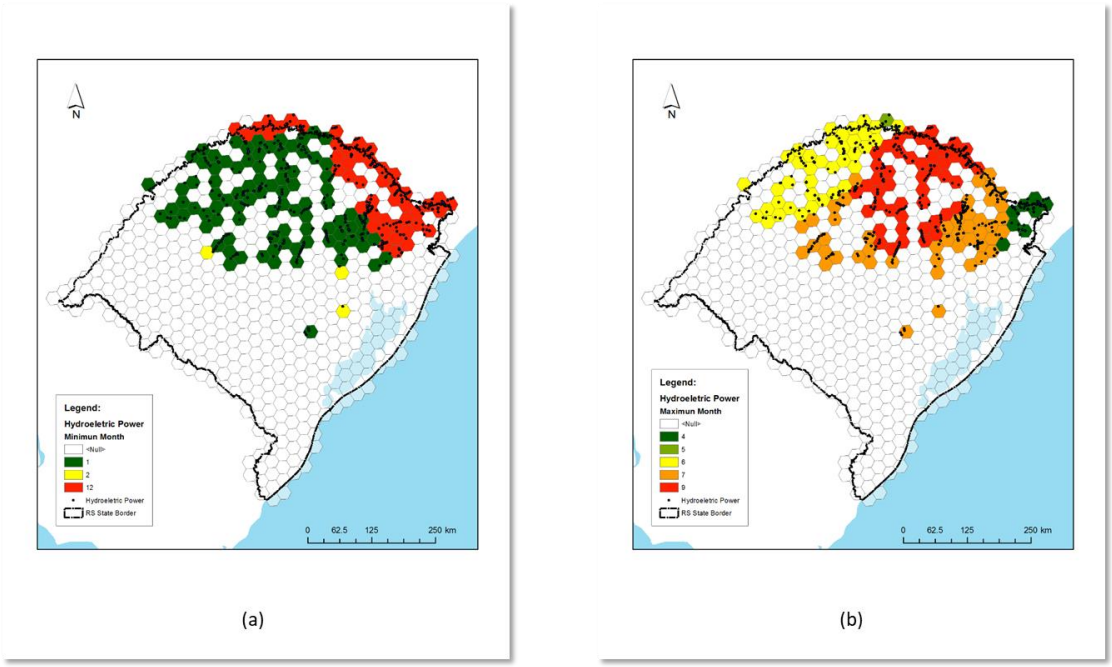

Fig. 5.6. Meses de mínima (a) e máxima (b) disponibilidade hídrica em células que possuam infraestrutura de geração hidrelétrica.

5.4.3 Clima → Vento e Radiação Solar

Para avaliar a disponibilidade de energia eólica e solar foram utilizados os dados da base georreferenciada do Climatic Research Unit (University of East Anglia), baixadas na forma de grades regulares de alta resolução [5-2].

Estes dados espaciais são apresentados com as seguintes características:

- Resolução Espacial do Conjunto de Dados: 10 minutos e 0,5 grau em latitude e longitude
- Extensão temporal do conjunto de dados: 1961 a 1990

A Fig. 5.7 apresenta os meses de mínima e máxima disponibilidade eólica integrados a base de células hexagonais (500 km²).

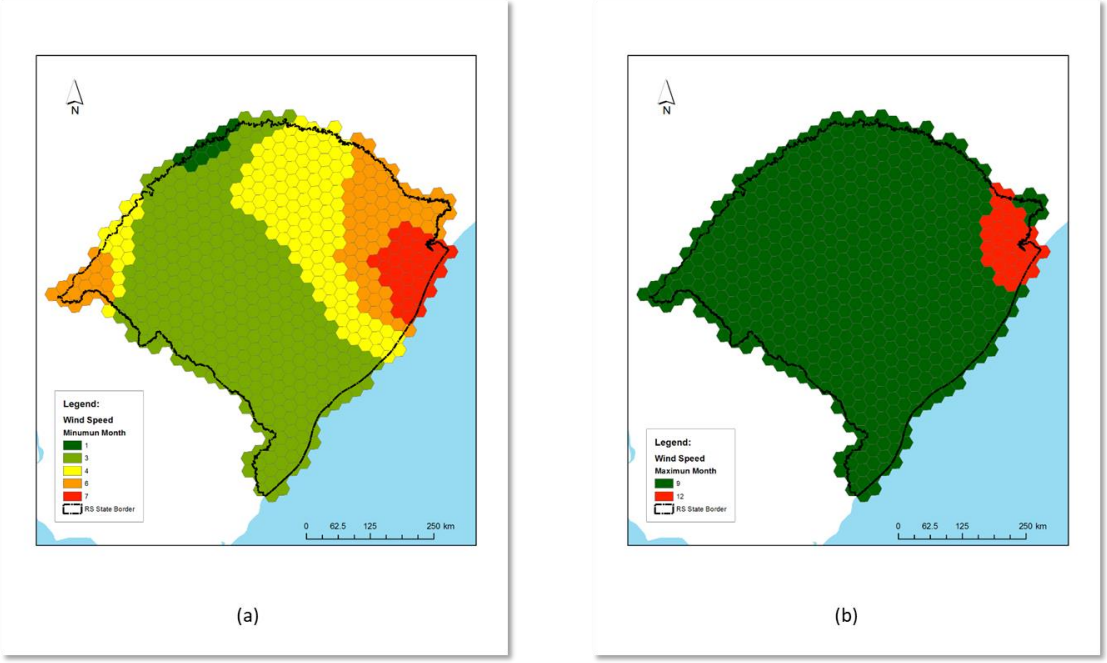

Fig. 5.7. Meses de mínima (a) e máxima (b) disponibilidade eólica.

A Fig. 5.8 apresenta as células hexagonais com os meses de mínima e máxima disponibilidade eólica que possuam infraestrutura de geração hidrelétrica.

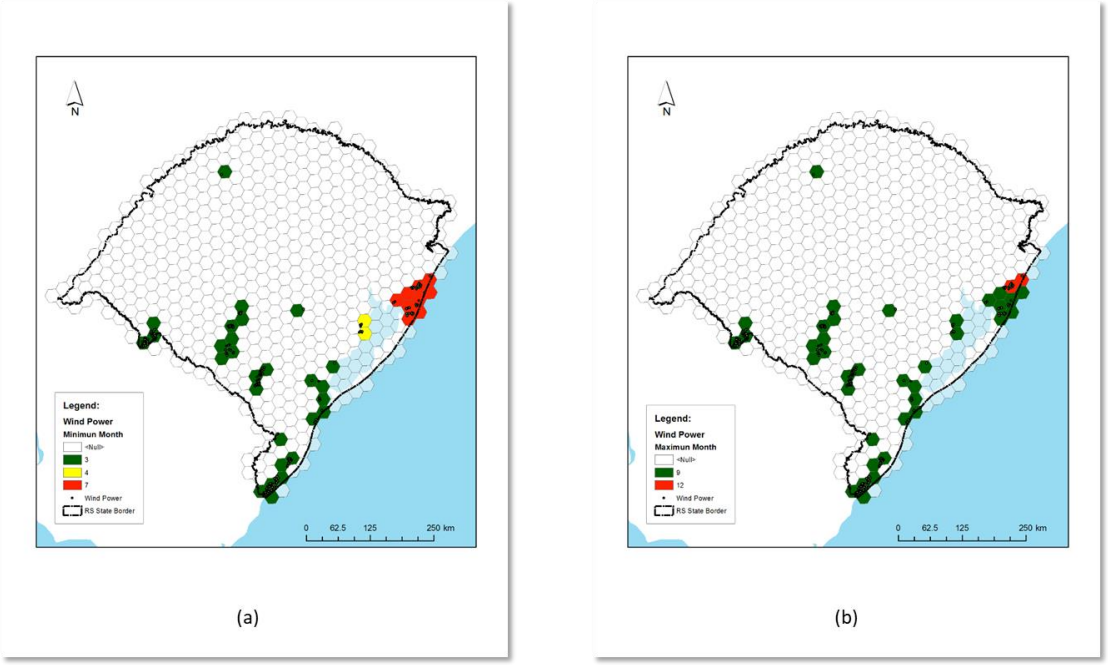

Fig. 5.8. Meses de mínima (a) e máxima (b) disponibilidade hídrica em células que possuam infraestrutura de geração eólica.

5.5 Referências

[5-1] Birch, C.P.D., Oom, S.P., Beecham, J. A. (2007). Rectangular and hexagonal grids used for observation, experiment, and simulation in ecology. Ecological Modelling, Vol. 206, Elsevier. No. 3–4, pp. 347–359.

[5-2] CRU, 2018. Climatic Research Unit, da Universidade de East Anglia. Disponível em: <https://crudata.uea.ac.uk/cru/data/hrg/>. Acesso em: 18. set. 2018.

[5-3] IBGE, 2018. Instituto Brasileiro de Geografia e Estatística. Disponível em: <https://cidades. ibge.gov.br/brasil/rs/panorama>. Acesso em: 10 nov. 2018.

[5-4] ISLSCP II, 2018. International Satellite Land Surface Climatology Project, da Universidade de New Hampshire. Disponível em: <https://daac.ornl.gov/ISLSCP_II/guides/comp_ runoff_monthly_xdeg.html>. Acesso em: 18. set. 2018.

[5-5] SIGEL-ANNEL, 2018. Sistema de Informações Geográficas do Setor Elétrico, da Agência Nacional de Energia Elétrica. Disponível em: <https://sigel.aneel.gov.br/>

6. PRODUTOS

As primeiras avaliações da efetividade das ferramentas de mapeamento da complementaridade espacial, foram efetuadas em arranjos de células hexagonais com poucos elementos, de forma a manter um controle mais efetivo das análises.

Na Fig. 6.1 é apresentado um arranjo de células hexagonais, mostrando uma combinação de duas fontes de recursos energéticos renováveis (hidrelétrico e eólico) com os meses de mínima disponibilidade.

Uma vez estimadas as localizações e distâncias entre as células das diferentes matrizes energética (W e H), são foram estimados os valores do índice parcial de complementaridade temporal (Kt) conforme a Eq. 4.2. A Fig. 6.2 representa o índice K_t entre a célula marcada em azul (H 29), contendo usinas hidrelétricas e as outras células da rede contendo usinas eólicas.

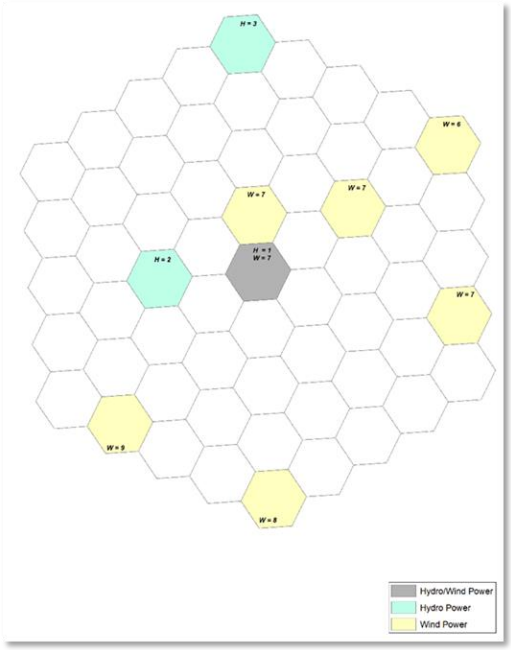

Fig. 6.1. Meses de mínima disponibilidade para duas diferentes matrizes energéticas H e W.

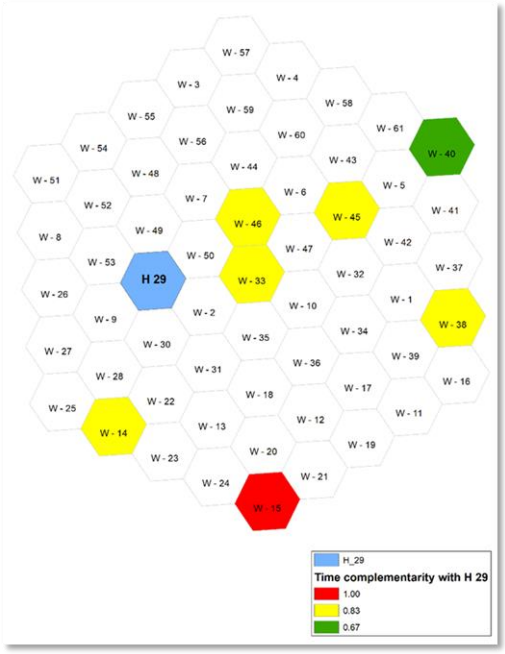

Fig. 6.2. Índice K_t das cálulas com sistemas eólicos com relação a célula H 29 (hidrelétrica).

Foram identificadas as conexões entre as matrizes energéticas a partir da localização dos centroides das células hexagonais de cada recurso e utilizando funções de análise espacial entre pontos, foram estimadas as distâncias, orientações de conexão entre as células complementares e grau de complementaridade temporal mínimas e máximas. Os resultados das análises e armazenada em uma estrutura tabular georreferenciada (tabela de atributo) como apresentada na Fig. 6.3.

ID_Hidro	ID_Wind	DISTANCE	H_Min	W_Min	X_H	Y_H	X_W	Y_W	KT_min	D_Norm	Octante	anti_Octante	XfHK	YfHK	XfWK	YfWK	XfHD
1	1	41617,9146	1	7	892784,3	208194,2	871975,4	172152,0	1,000	2	SW	NE	886777,3	197789,7	877982,4	182556,5	8905
1	3	41617,9146	1	7	892784,3	208194,2	913593,3	172152,0	1,000	2	SE	NW	898791,3	197789,7	907586,3	182556,5	8950
1	2	24028,1142	1	7	892784,3	208194,2	892784,3	184166,0	1,000	1	S	N	892784,3	196180,1	892784,3	196180,1	8927
2	1	83235,82898	1	7	830357,4	244236,3	871975,4	172152,0	1,000	4	SE	NW	836364,4	233831,8	865968,4	182556,5	8348
2	3	110110,6519	1	7	830357,4	244236,3	913593,3	172152,0	1,000	5	SE	NW	839439,2	236371,3	904511,5	180017,0	8394
2	2	86634,59759	1	7	830357,4	244236,3	892784,3	184166,0	1,000	4	SE	NW	839014,5	235906,1	884127,2	192496,2	8371
3	1	86634,59761	12	7	851166,4	256250,4	871975,4	172152,0	0,833	4	S	N	853571,1	246531,8	869570,7	181870,6	8534
3	3	104736,1214	12	7	851166,4	256250,4	913593,3	172152,0	0,833	5	SE	NW	857133,8	248211,4	907625,9	180191,0	8579
3	2	83235,82903	12	7	851166,4	256250,4	892784,3	184166,0	0,833	4	SE	NW	856172,3	247580,0	887778,4	192836,4	8557

Fig. 6.3. Tabela com os atributos de complementaridade temporal, posição e orientação relativa.

A representação espacial dos atributos de complementaridade temporal (magnitude, distância, orientação e fonte energética) se deu na forma de Rosas de Complementaridade .

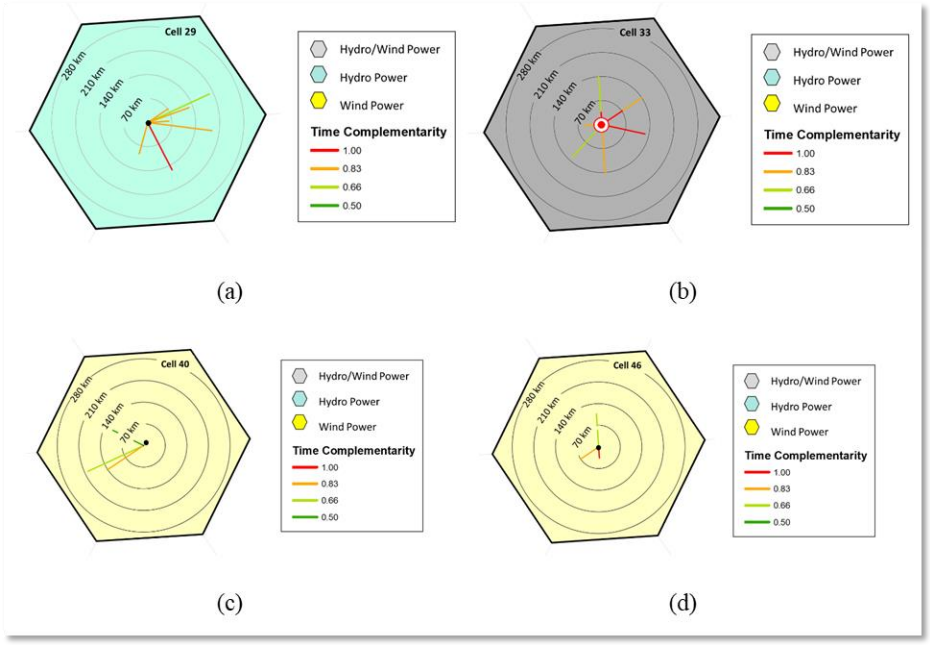

Fig. 6.4. Rosas de complementaridade para as células (a) H-29, (b) W-33, (c) W-40 e (d) W-46.

7. BASES PARA UMA METODOLOGIA PARA AVALIAÇÃO DA COMPLEMENTARIDADE TEMPORAL NO ESPAÇO

7.1 Apresentação

Este capítulo, apresenta o trabalho *"Bases for a Methodology Assessing Time Complementarity in Space"* submetido e publicado na revista "Energy and Power Engineering", em 2017, pela editora Scientific Research Publishing, tendo como autores o Prof. Alfonso Risso e o Prof. Alexandre Beluco.

Abstract

Energetic complementarity has been studied in recent years and can be an important tool for managers to decide on the design and operation of hybrid systems based on renewable energy resources. Complementarity is an ability presented by two or more energy resources to complement each other over time. Complementarity can be verified in one place or at different places. This second case can be termed as spatial complementarity and is more complex than the complementarity in the same place, requiring a specific approach for its quantification This paper discusses concepts related to energetic complementarity and presents the basis for a method to evaluate energetic time-complementarity across space, applying the concepts presented to the northern coast of the state of Rio Grande do Sul, the southernmost state of Brazil.

Keywords

Energetic complementarity, Energetic complementarity in time, Energetic complementarity in space, Hydro energy, Wind power.

7.2 Introduction

Energetic complementarity, as considered in this work, is a capacity presented by two energy resources to complement each other (completely or partially) in time and-or space. Beluco et al [7-1] proposed a dimensionless index that allows quantifying the temporal complementarity, dividing it into three components: time, energy and amplitude. This paper deals only with the application of the first of these three components.

This concept was designed to initially assess energetic complementarity in one place. However, complementarity can be verified between power plants located in the same location (or near each other), but also between power plants located far from each other. This second case extends the applicability of the concept of energetic complementarity and requires a method to express this spatial complementarity with maps.

This paper presents the basis for a method that allows quantifying complementarity throughout space and presents its application to a region in the State of Rio Grande do Sul. This paper also discusses some limitations of this method and next steps to be followed to improve the understanding of spatial complementarity. This paper clearly establishes basic concepts for the future layout of spatial complementarity maps.

7.3 Complementarity in time across space

Beluco et. al. 0-0 proposed a dimensionless index evaluating complementarity between two energy resources and defined its three components. The time-complementary index was defined as shown in Eq. (1), where κt is the partial energetic complementarity in time, where maximum and minimum availability of hydraulic energy occur, respectively, on Julian day number D_h and d_h (likewise D_s and d_s refer to the same days regarding solar energy). Note that if the differences $|D - d|$ equal 180, then $\kappa_t = |d_h - d_s|/180$, so that $\kappa_t = 1$ if the maxima are 180 days apart, and $\kappa_t = 0$ if the maxima coincide.

$$\kappa_t = \frac{|d_h - d_s|}{\sqrt{|D_h - d_h||D_s - d_s|}} \quad (1)$$

On this work, spatial complementarity will be evaluated from the calculation of this temporal index, with the difference that the index will be calculated with resource data at different locations and no longer with data from two sources in the same place, as estimated by Beluco et al. 0.

So, for clarity of concepts, in this paper the complementarity calculated in only one place applying the index proposed by ref. [7-1] will be referred to as temporal complementarity.

In turn, the complementarity calculated even by the index proposed by ref. [7-1] but considering two different locations in space will be termed as spatial complementarity.

7.4 A graphical method assessing complementarity in space

This section will initially present a graphical method for evaluating spatial complementarity and will then describe some examples designed to demonstrate its applicability.

The proposed method for evaluating spatial complementarity in a given region consists of the following four steps: [7-1] establish a network of hexagonal cells over the region to be studied; [7-2] calculate the complementarity in time, applying Eq. (1) above, among all the cells of that network; [7-3] compare the obtained results in order to associate for each distance the maximum value obtained for the complementarity in time; [7-4] plot the results of maximum complementarity in time as a function of the distance between the cells.

The study of spatial complementarity requires the establishment of a region to be studied and its modeling with a network of cells. In this paper, a network of hexagonal cells will be adopted, as they allow a better coverage of the surface. Each cell in this network will be assigned power generation information resulting from the added effect of all power plants in its area of influence. This step will be better understood in the next section, when a real case is analyzed.

The size and arrangement of the cells can be established according to the nature of the available energy resources or characteristics of the region to be studied. Once the data associated with the generating units of the study region are known, temporal complementarity can be determined with the application of Eq. (1).

Just for simplicity, the examples described in this section throughout the next figures will consider the case where the differences shown below in Eq. (1) are equal to 6. Thus, the months corresponding to the availability minima can be directly applied to upper part of this equation, leading to the evaluation of complementarity in time.

Fig. 7.1 shows a hexagonal cell network used for determination of spatial complementarity. This network can have the dimensions of its cells adapted to the conditions

of the region under study or to the number of plants operating in that region. It is appropriate to set up one network for each type of energy resource used.

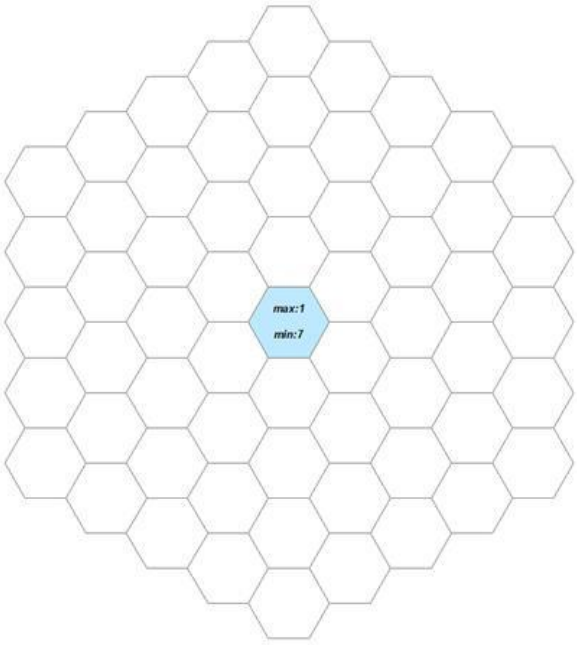

Fig. 7.1. A net with hexagonal cells containing power plants in the center position.

In this network, there are plants only in the central cell, which appears marked with a specific color, and there are indications of the months of the year in which maximum and minimum energy availability occurs. In the case of only one plant, the corresponding months of the energy resources available for this plant will be indicated. In case this cell contains more than one plant, the months of maximum and minimum energy availability corresponding to the joint effect of the plants of that cell should be indicated.

Fig. 7.2 shows two networks side by side, showing hypothetical generation information for two energy resources. The network on the left shows information for hydroelectric power and the grid on the right for wind energy. The network on the left indicates hydroelectric plants only in the central cell, while the network on the right affects plants in the two cross-hatched cells. So only three cells in this region include power plants. The network shown on the left is identical to the network shown in Fig. 7.1.

A trivial situation, considering the determination of complementarity index, would be obtained by comparing two such networks, mounted to a region in which the compared plants were both located in the central cell. It would be equivalent to the calculation already known

for the temporal complementarity in just one place. Results for such a case can lead to complementarity maps such as those presented by Beluco et al. 0 for the State of Rio Grande do Sul.

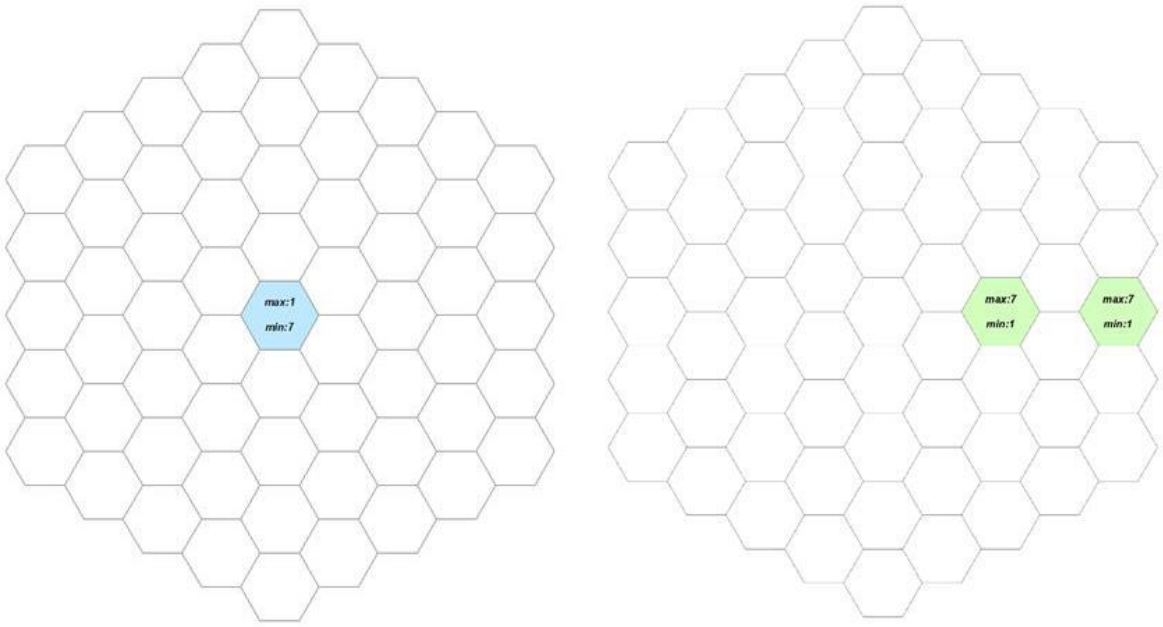

Fig. 7.2. Nets with hexagonal cells indicating hydroelectric plants (left) and wind plants (right) in the region under consideration.

The central cell of the left network indicates that the maximum availability occurs in January (month 1, from 1 to 12) while the minimum in the month of July (month 7). The cells on the right network indicate that maximum availability occurs in July while the minimum occurs in January. As the months of minimum availability of hydropower and wind energy are in this case with a difference of six months, these two energy resources present a complete complementarity and the index results equal to 1.

This result should be presented as a function of distance and a very appropriate form for this presentation is shown in Fig. 7.3. There is perfect complementarity between the central cell in the network shown on the left and each of the two cells shown in the network on the right. The distances between the central cell and the other two cells can be considered to be 2 and 4, respectively. Thus, a bar with height 1 appears in abscissa or distance equal to 2 and another also with height 1 appears at distance 4.

If there were power plants in matching cells, complementarity between these cells could be considered to compose maps of complementarity, as discussed above. As power plants do not appear in matched cells in Fig. 7.2, the complementarity indicated in abscissa 0 in Fig. 7.3 equals zero. However, information at other distances could be used to compose complementarity maps corresponding to certain distances between cells or corresponding to intervals of distances between cells.

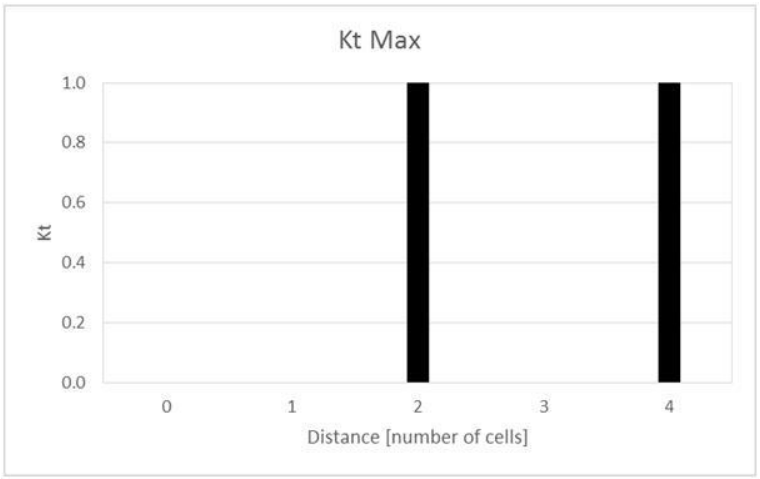

Fig. 7.3. Spatial complementarity for the hypothetic region with power plants indicated in Fig. 7.2, with temporal complementarity indicated as a function of distance.

In the sequence, some other basic cases, for a better understanding, will be presented and discussed. Fig. 7.4 shows a case in which a hydroelectric plant is inserted in a region with wind turbines in all cells of the network, presenting energy availabilities with the same distributions of Fig. 7.2. Fig. 7.5 shows the spatial complementarity for this case, of course with unit values for all distances between cells. If there were different values of complementarity, the maximum values would be shown in the graph.

The situation in Fig. 7.2 sets up a complementarity in time that is total for two of the available distances, while the situation in Fig. 7.4 configures a complementarity that is complete at all distances available in the network of hexagonal cells under analysis. The total complementarity, considering its three components, as presented and discussed by Beluco et al. [7-1], should also take into account the components of energy and amplitude.

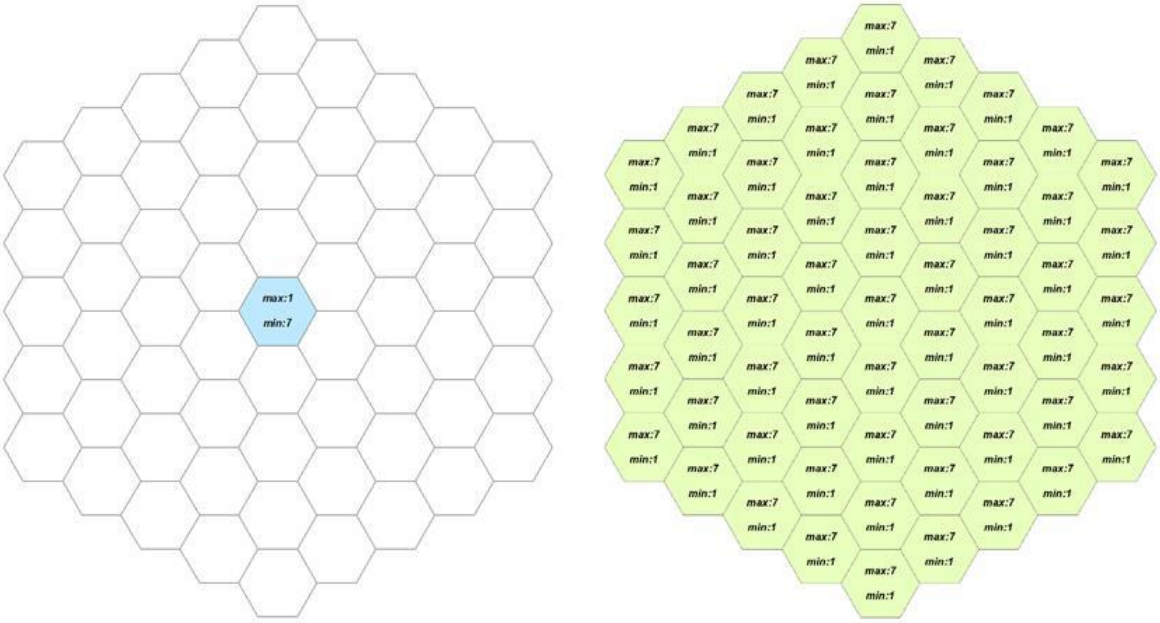

Fig. 7.4. Nets corresponding to a region with one hydroelectric power plant (left) inserted in a region full of wind turbines (right).

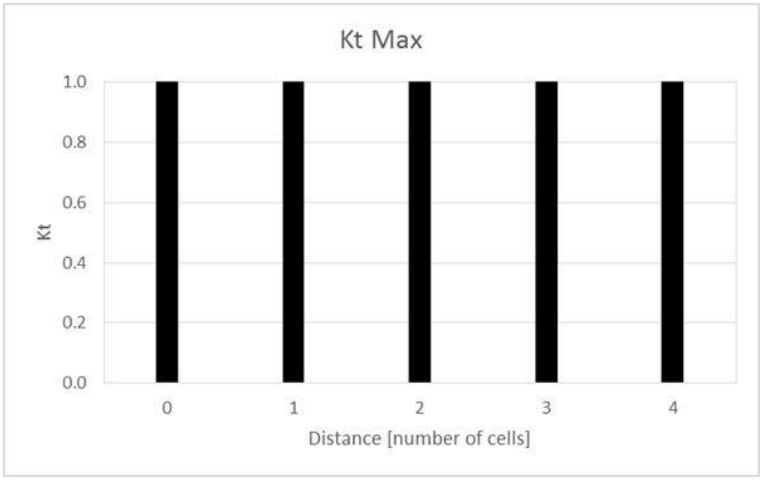

Fig. 7.5. Spatial complementarity for the case of Fig. 7.4.

Fig. 7.6 shows a situation where a hydroelectric plant (left) placed in the central cell has its complementarity established with a distribution (right) of wind turbines in which there is a set of turbines in the central cell and other sets distributed in cells in the periphery of the analyzed region. These cells have the same maximum and minimum energy availability distributions of the previous cases. The comparisons will become more complex as there are more cells in the network on the left, as already appears in the next case.

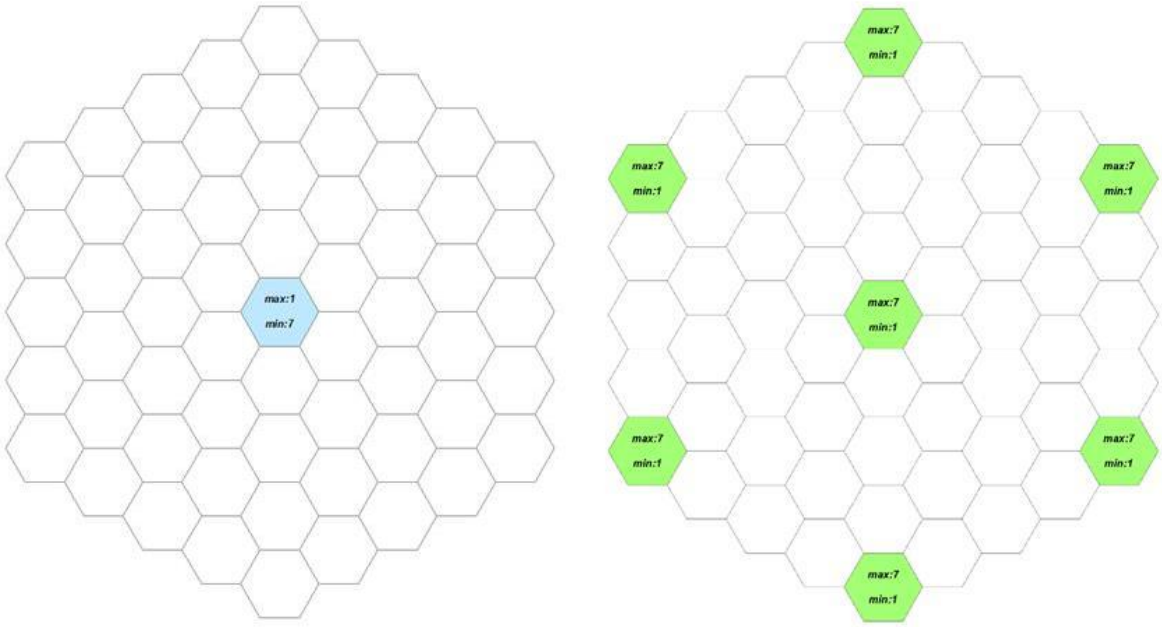

Fig. 7.6. Nets corresponding to a region with one hydroelectric power plant (left) inserted in a region with wind turbines (right) in the center and in some cells of the extremity of the region.

Fig. 7.7 shows the spatial complementarity for the case of Fig. 7.6. The first bar corresponds to the comparison of the central cells and corresponds also to the trivial case discussed above. The other bar corresponds to the comparison of the central cell of the network on the left with the cells on the periphery of the network on the right. As the lags correspond in these cases to six months, the values of complementarity correspond to the complete complementarity.

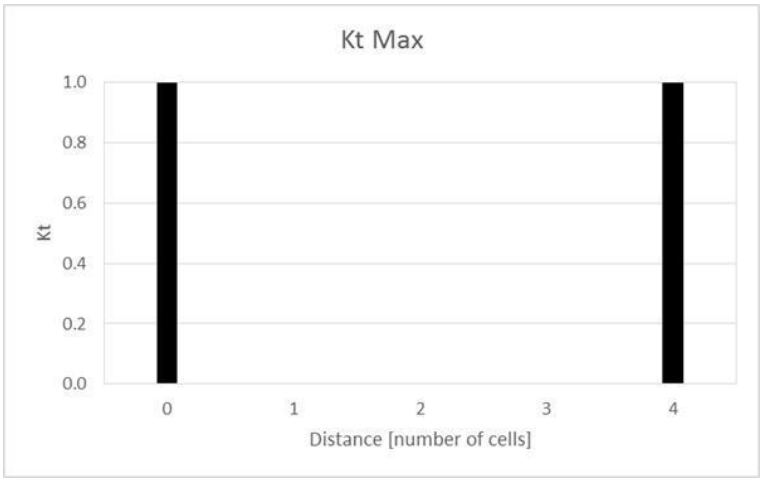

Fig. 7.7. Spatial complementarity for the case of Fig. 7.6.

The cases above, shown in Fig. 7.2, Fig. 7.4 and Fig. 7.6, can be considered simple because the networks on the left always have only one cell with hydroelectric plants. The cases in which the left network presents more than one cell with hydroelectric plants can be solved in the same way, establishing values of temporal complementarity from the comparison of cells in the left and right networks.

Fig. 7.8 shows a distribution of power plants in the networks closest to reality. In the left network there are two cells with hydroelectric plants, while the network on the right presents four cells containing wind turbines. On the right, the cell in darker green is differentiated from the others because it presents a distribution of maximum and minimum energy availability different from those that were being adopted in the previous cases.

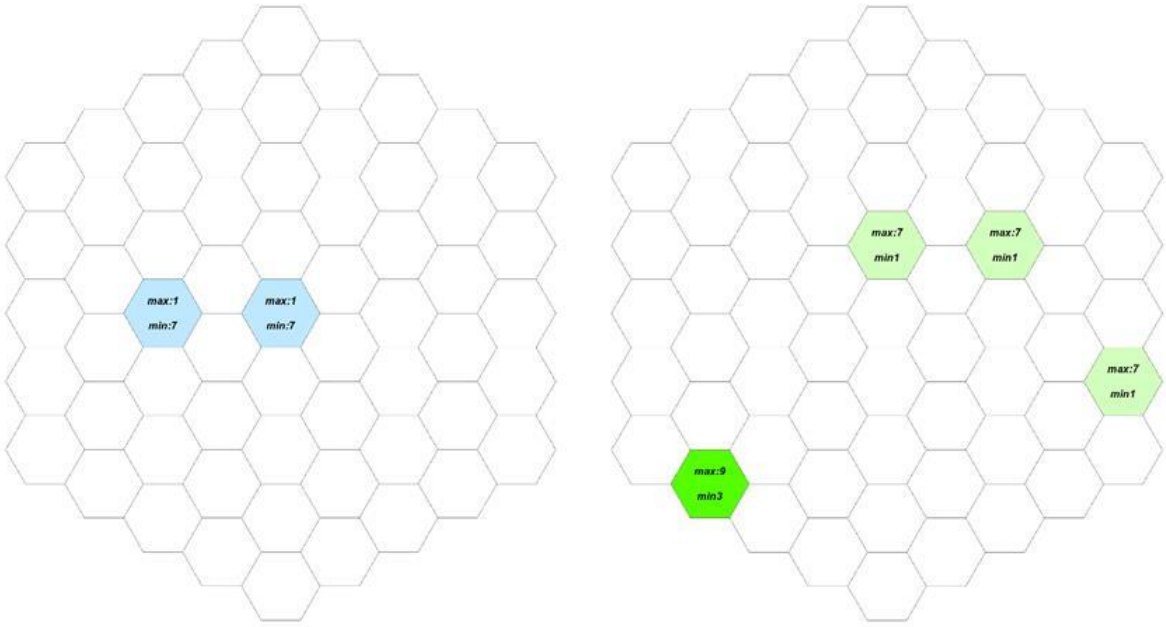

Fig. 7.8. Nets corresponding to a region with two cells containing hydro power plants (left) and four cells containing wind turbines (right).

Fig. 7.9 shows the graph with spatial complementarity as a function of distance for the case of Fig. 7.8. At distances in which complementarities are partial, if they correspond to more than one value of complementarity for the same distance, the larger result is shown in the diagram. It is for the distance d equal to 3 that appears in the diagram a value of complementarity smaller than the unit.

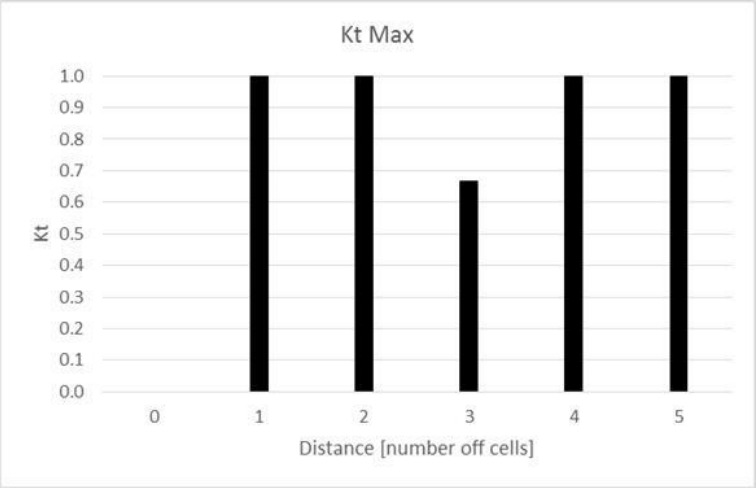

Fig. 7.9. Spatial complementarity for the case of Fig. 7.8.

Fig. 7.10 shows a more complex situation than the previous ones, in which several cells containing plants in the two networks appear. In addition, these plants exploit energy resources with maximum and minimum energy availability in different months throughout the year. In the left network, the cells in dark blue, and in the network of the right the cells in dark green, present distributions of energy availability different from the distributions of the previous cases.

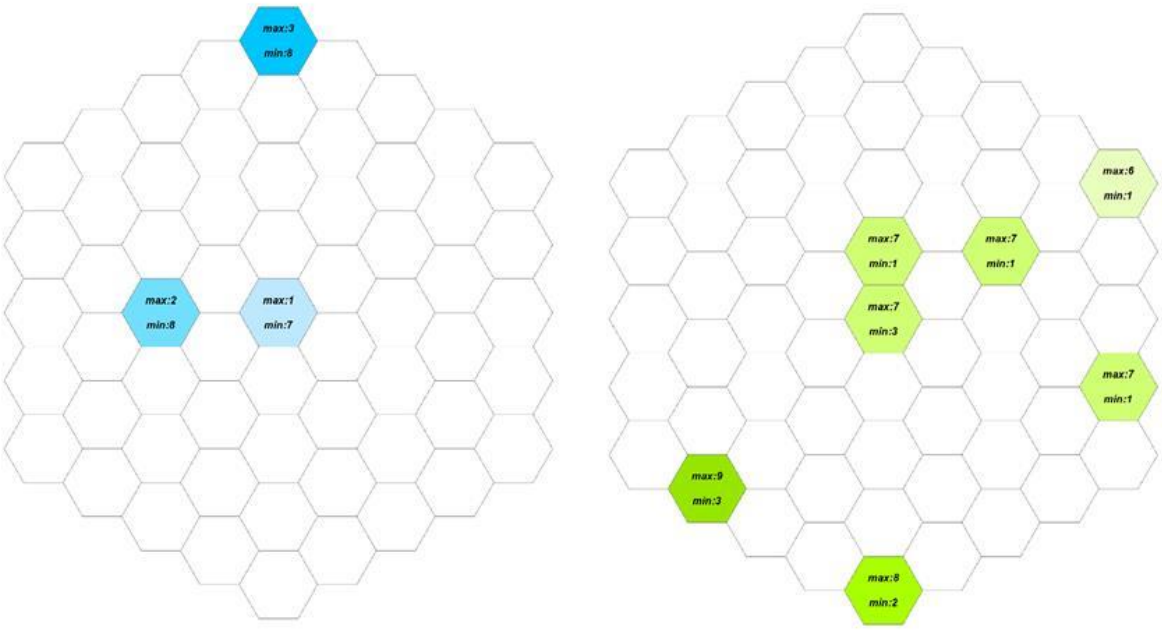

Fig. 7.10. Nets corresponding to a region with three cells containing hydro power plants (left) and seven cells containing wind turbines (right).

Fig. 7.11 shows the spatial complementarity diagram corresponding to this case. This diagram does not show all the distances between cells containing power plants, and furthermore shows many unitary results, which present a kind of "saturation" over possible complementarity results. This is clearly a limitation of the presented method, and may be circumvented possibly with complementarity diagrams that do not show only the maximum values at each distance.

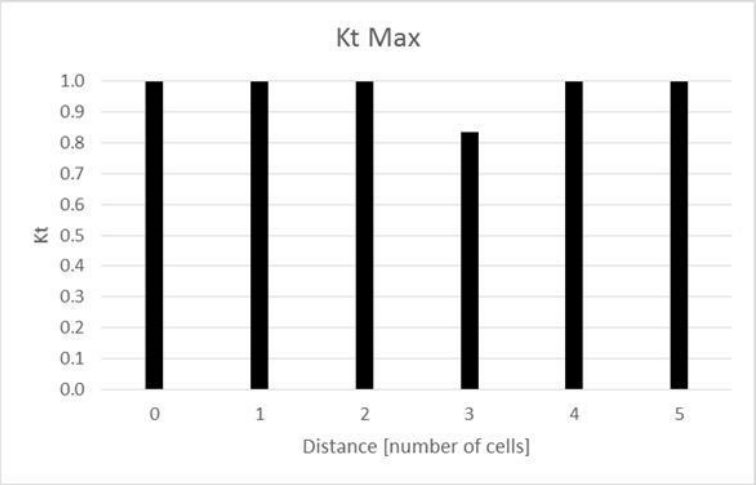

Fig. 7.11. Spatial complementarity for the case of Fig. 7.10.

This process for evaluating the spatial complementarity allows assessment of how power plants located in a given region may present complementary. Before this paper, this would be possible only peer-to-peer and now an evaluation is possible comparing plants at different sites. The survey of full complementarity can be an important tool for planning and management of energy resources.

One limitation is that spatial complementarities across different distances are represented in the same diagram. Another limitation is that different complementarities in the same distance will be shaded by the criterion adopted to define what complementarity will be in this position. In this paper, the graphs were assembled considering the maximum values in each distance, but average values of complementarity could also be adopted.

7.5 An example of application

The region of the north coast of the state of Rio Grande do Sul, in the extreme south of Brazil, will be used for an example of application. This region can be viewed on Google Maps [3.3] and is shown in Fig. 7.12. A 500 square kilometer cell network was set up to allow this assessment. The figure shows this network and shows that there are hydroelectric plants in two cells and that there are wind turbines in three cells.

Fig. 7.13 shows the complementarity diagram for the region shown in Fig. 7.12. The maximum and minimum energy availability distributions for hydroelectric plants and wind turbines in this case have complete complementarity and this is expressed in the diagram. The data for this analysis were obtained with the HidroWeb [7-4] system, available online, and the Wind Atlas 0 of the State of Rio Grande do Sul, having been manipulated as proposed by Beluco et al [7-1].

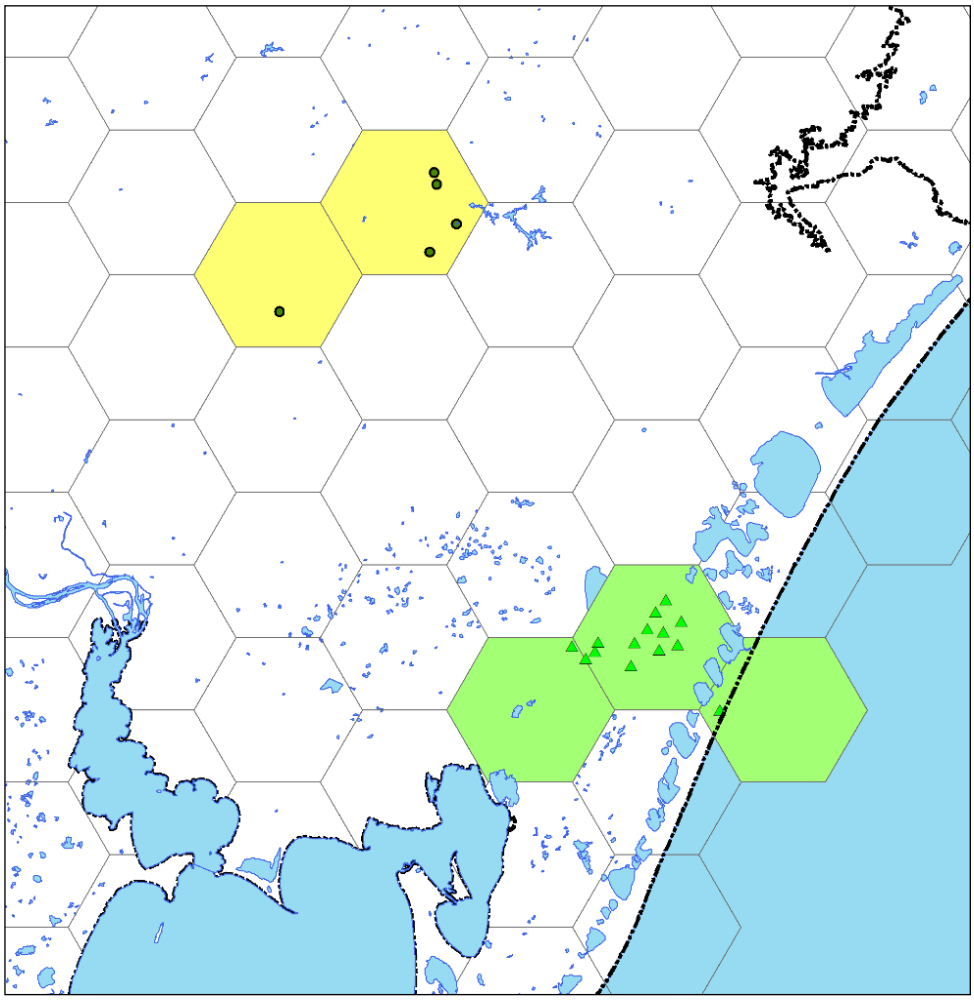

Fig. 7.12. A network with 500 km2 cells assembled to evaluate spatial complementarity in the region of the northern coast of the State of Rio Grande do Sul.

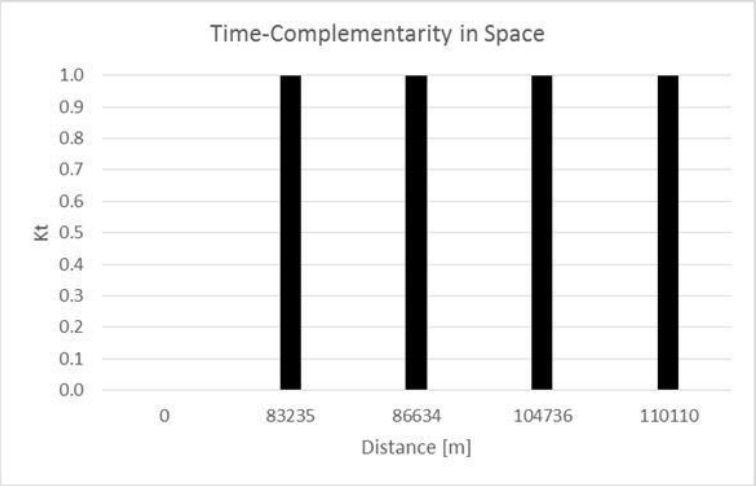

Fig. 7.13. Spatial complementarity for the case of Fig. 7.12.

Fig. 7.13 and Fig. 7.14 respectively show the locations of hydro power plants and wind farms identified in the region shown in Fig. 7.12. Fig. 7.13 identifies the five hydroelectric power plants with numbers from 1 to 5. In 1 the Herval 0 power plant is located, 2 is the Bugres[7-7]0 plant, 3 the Canastra 0 power plant, 4 the Toca 0 plant and in 5 is located the Passo do Inferno0 power plant.

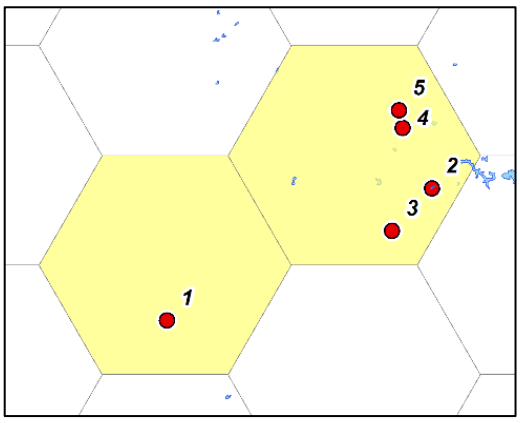

Fig. 7.14. Location of the five hydroelectric power plants identified in two cells of the network shown in Fig. 7.12 and considered for determining complementarity in Fig. 7.13.

Fig. 7.14 identifies the four wind farms with numbers from 1 to 14. In 1 and 8 are located respectively Sangradouro II 0 and Sangradouro I 0; in 2, 6 and 11 are located respectively Lagoa dos Barros III 0, Lagoa dos Barros I 0 and Lagoa dos Barros II 0; in 3, 9 and 12 are located respectively Osório I 0, Osório II 0 and Osório III 0; in 4, 10 and 13 are located respectively Índios III 0, Índios I 0 and Índios II 0; in 5 is located the Chicolomã 0 wind farm and in 7 is located the Cidreira 0 wind farm.

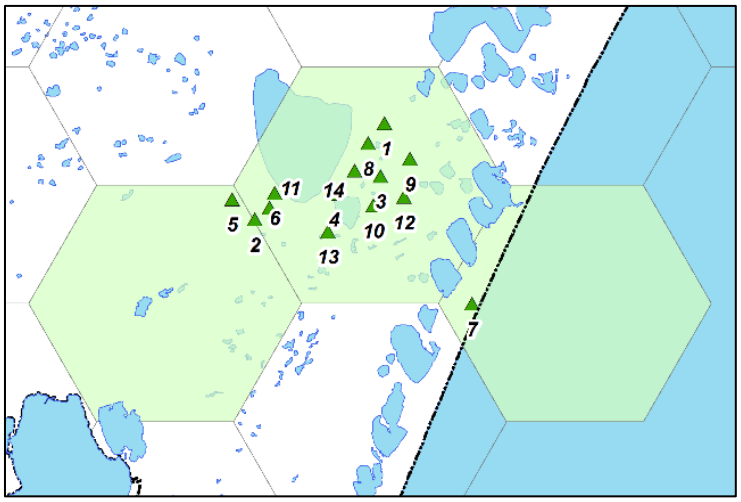

Fig. 7.15. Location of the fourteen wind power plants identified in three cells of the network shown in Fig. 7.12 and considered for determining complementarity in Fig. 7.13.

The analysis undertaken in this paper considers only the months in which the minimum energy availability occurs in the power plants located in these two figures; analyzes considering energy and amplitude complementarity components will be undertaken following following the research work. It is necessary to express in the two dimensions of a map a much larger amount of information and this paper constitutes a first step in the description of spatial complementarity.

Some cells appear in these figures containing several plants, while others contain few or no plants at all. A prior evaluation of the complementarity components will enable assessing whether the hexagonal cell network has been well established. The purpose of the analysis to be undertaken may induce the choice of a network with smaller cells. The dimensions of the cell network to be adopted should be related to the expected results.

The establishment of the network cells may influence the results of the energetic complementarity assessment, if complementary plants appear in the same cell. This internal complementarity to a cell cannot be identified in the data collection that will result in the evaluation of complementarity. An analysis considering the largest power plants should be undertaken and of course the analysis of a region with many power plants may require large computational processing capacities.

7.6 Final remarks

This paper discussed some issues related to energetic complemetarity and presented bases for a methodology allowing the determination of time complementarity through space. The proposal basically suggests the determination of the complementarity in time between different positions and their expression through a chart of complementarity as a function of distance. This paper also presented an application of the proposed methodology to the north coast of the State of Rio Grande do Sul, in southern Brazil.

The method has some limitations. One of them, spatial complementarity in several directions is presented in only one diagram, with superimposition of complementarity values for different directions in only one value. Another limitation, for a same distance, even in different positions, should be adopted only one value of complementarity; in principle, in this article, the maximum value was considered, but an average value could be considered.

7.7 Acknowledgements

This work was developed as a part of research activities on water resources management and renewable energy at the Instituto de Pesquisas Hidráulicas (IPH), Universidade Federal do Rio Grande do Sul (UFRGS). The authors acknowledge the support received by the institution. The second author acknowledges the financial support received from CNPq for his research work (proc. n. 309021/2014-6.).

7.8 References

[7-1] Beluco, A., Kroeff, P.K., Krenzinger, A. (2008) A dimensionless index evaluating the time complementarity between solar and hydraulic energies. Renewable Energy, 33, 10, 2157-2165. http://dx.doi.org/10.1016/j.renene.2008.01.019

[7-2] Beluco, A., Souza, P.K., Livi, F.P., Caux, J. (2015) Energetic complementarity with hydropower and the possibility of storage in batteries and water reservoirs. In: Sørensen, B., Ed., Solar Energy Storage, Academic Press, London, 155-188. http://dx.doi.org/10.1016/B978-0-12-409540-3.00007-4.

[7-3] https://goo.gl/maps/3ezz3m9fm2M2

[7-4] Water Resources National Agency (ANA); HidroWeb, Brazilian Water Resources Database. Available in www.hidroweb.ana.gov.br, accessed on August 22, 2017.

[7-5] Mines and Energy State Secretary, Rio Grande do Sul Wind Atlas.

Available in minasenergia.rs.gov.br/atlas-eolico-2016-03, accaessed on August 22, 2017.

[7-6] https://goo.gl/maps/PBxDo9kEcWB2

[7-7] https://goo.gl/maps/EDKWw5MWBqC2

[7-8] https://goo.gl/maps/6cVRAGuTSaQ2

[7-9] https://goo.gl/maps/KMP31dzwJVR2

[7-10] https://goo.gl/maps/kyzFbHgbLK22

[7-11] https://goo.gl/maps/SmsbLgJwmvK2

[7-12] https://goo.gl/maps/Ex7F6y9gvPG2

[7-13] https://goo.gl/maps/m5ULeACSvDk

[7-14] https://goo.gl/maps/SL4pigs7bJC2

[7-15] https://goo.gl/maps/2hAFUGbdhEw

[7-16] https://goo.gl/maps/APib4Vvdcyu

[7-17] https://goo.gl/maps/df18LiQZL5F2

[7-18] https://goo.gl/maps/oM6iEMDhB6k

[7-19] https://goo.gl/maps/upE7VUgMkL92

[7-20] https://goo.gl/maps/jiGXfV1P4ez

[7-21] https://goo.gl/maps/eGhduuoqAXJ2

[7-22] https://goo.gl/maps/tLi8HmLnN9r

[7-23] https://goo.gl/maps/kdNYG9dtTNP2

[7-24] https://goo.gl/maps/xFjnUWVJBBx

8. "ROSAS DE COMPLEMENTARIDADE" AVALIAÇÃO DA COMPEMENTARIDADE ESPACIAL NO TEMPO ENTRE RECURSOS ENERGÉTICOS

8.1 Apresentação

Este capítulo, apresenta o trabalho *"Complementarity Roses Evaluating Spatial Complementarity in Time between Energy Resources"* publicado no periódico *"Energies"*, em 2018, pela editora *MDPI*, tendo como autores o Prof. Alfonso Risso, o Prof. Alexandre Beluco.e a Profa. Rita de Cássia Marques Alves.

Abstract

Hybrid systems have higher initial costs than systems based on only one renewable resource, but allow the fulfillment of the demands of consumer loads with lower values for the cost of energy. The possible complementarity between the resources used can contribute to a better use of the available energy. On a large scale, complementarity between power plants can serve as a tool for the management of energy resources. A complete evaluation of complementarity needs to consider three components: time complementarity, energy complementarity and complementarity between amplitudes of variation. Complementarity can also be assessed between energy resources in one place (which may be termed temporal complementarity) and between resources at different sites (termed spatial complementarity). This paper proposes a method for quantifying spatial complementarity over time and for its expression through maps. The method suggests the establishment of a hexagonal network of cells and the determination of complementary roses for each cell that contains plants. This article also applies the method proposed to some hydroelectric plants and wind farms in the State of Rio Grande do Sul, in southern Brazil, and presents the map of spatial complementarity obtained.

Keywords

Energetic complementarity; spatial complementarity; complementarity in time; hydro energy; wind energy; southern Brazil.

8.2 Introduction

Hybrid systems in various dimensions and compositions are becoming increasingly common and increasingly the target of research projects related to their design and optimization and related to their proposition as alternatives for a sustainable future. The initial costs of systems based on renewable resources have been showing significant reductions over the last few years, both due to the growth in demand for energy conversion devices and due to ongoing investment in research and development. In this scenario, the possible complementarity between energy resources may be a tool for technology managers to decide on new plants and investments in renewable resources still in the process of maturation.

The subject complementarity has been studied for some years seeking a description that allows exploring all its potential as a design parameter and as a tool for planning and management of renewable energy resources. Ghirardi et al. (1997) [8-8] evaluated the complementarity between water resources along the South American territory and Cantão et al. (2017) [8-6] studied the complementarity between water and wind resources throughout Brazilian territory. The work of Beluco et al (2008) [8-2] proposed a dimensionless index assessing complementarity, with an innovative approach, and Beluco et al. (2012) [8-3] and Kougias et al. (2016) [8-10] proposed methods respectively for analysis and optimization of hybrid systems based on complementary resources.

Energetic complementarity can be understood as a capacity of one, two or even more renewable energy resources to complement each other over time, in one place or at different places. Only complementarity between renewable energy resources makes sense to be evaluated. The different characteristics of intermittency and variability of the various renewable energy alternatives make complementarity difficult to evaluate.

Energetic complementarity is, in a direct sense, an obvious concept, but the work of Beluco et al. (2008) [8-2] was the first to deal with this matter comprehensively. This work discussed the concept of complementarity and proposed a dimensionless index for the quantification of complementarity in time considering resources in a same location. The work of Borba and Brito (2017) [8-5] suggested the evaluation of the complementarity in time by means of a kind of convolution of the energy availability functions.

According to Beluco et al. (2008) [8-2], complementarity in time evaluated in the same place must be divided into three partial complementarities: time-complementarity itself, energy-complementarity and amplitude-complementarity. Beluco et al. (2015) [8-4] also described a situation of complete complementarity. Situations where one or more of these three components appear incomplete match not full complementarities.

Time-complementarity will be complete when availability minima occur six months apart. Energy-complementarity will occur when the average values of the compared energy resources are equal. Amplitude-complementarity will occur when the differences between maximum and minimum energy availability for the compared energy resources are equal. This work will deal only with the determination of the complementarity in time, given by Eq. (1) as presented by Beluco et al. (2008) [8-2], comparing data at different points along spatial coordinates.

Complementarity in one place is easier to represent, since it is enough to associate the final value of complementarity to the place in question. This type of complementarity can be termed as temporal complementarity (having time-complementarity as one of its components). The work of Beluco et al. (2015) [8-4] discusses in more detail some issues related to complementarity and shows a map of temporal complementarity for the State of Rio Grande do Sul.

The energetic complementarity obtained between two different sites is more difficult to represent graphically. This type of complementarity can be called spatial complementarity (also having time-complementarity as one of its components). Additionally, for the same place in space may be assigned different complementarity values associated with the comparison of energy availability of this point with the available energy from several other points.

This article discusses the concept of energetic complementarity focused on the complementarity in time verified between different places along a territory and proposes the use of "roses of complementarity" to graphically express this spatial complementarity. In the end, the spatial complementarity between some hydroelectric power plants and wind farms installed in the State of Rio Grande do Sul, in southern Brazil, is determined and represented by the use of complementarity roses on a map.

The next section discusses the complementarity in time and the complementarity through spatial coordinates and suggests the use of complementary roses for their graphic expression. The two subsequent sections present a method for evaluating spatial complementarity in time by means of complementary roses and an application to the State of Rio Grande do Sul, with the presentation of a map of spatial complementarity in time.

8.3 Spatial complementarity in time and "complementarity roses"

This section is composed of three subsections. The first discusses the determination of complementarity in time between energy resources in the same place, as already presented in the literature. The second section discusses spatial complementarity in time and the third section presents the idea of evaluating spatial complementarity through complementary roses.

8.3.1 Temporal complementarity in time

The term "temporal complementarity" can be used to refer to the energetic complementarity between energy resources in the same place, while the term "spatial complementarity" can be used in the case of complementarity between energy resources in different places. In both cases, complementarity has three components, as presented by Beluco et al. (2008) [8-2], namely time-complementarity, energy-complementarity and amplitude-complementarity.

Fig. 8.1 shows actual energy availability data. The uppermost data, on the left, correspond to typical water availability data in a river section. The lowermost data, on the right, in turn, correspond to the solar radiation incident on a flat horizontal surface. The figure characterizes the mean values of energy and the amplitudes of variation for the two energy resources. The time-complementarity component evaluates the lag between the maximum or minimum values of energy availability of the energy resources considered.

The energy-complementarity component compares average energy values and a maximum value will be obtained if each resource contributes half of the total annual energy. The amplitude-complementarity component compares the amplitudes of variation of each energy resource and, like the energy complementarity component, a maximum value of

complementarity will be obtained if the energy resources compared have the same amplitude variation.

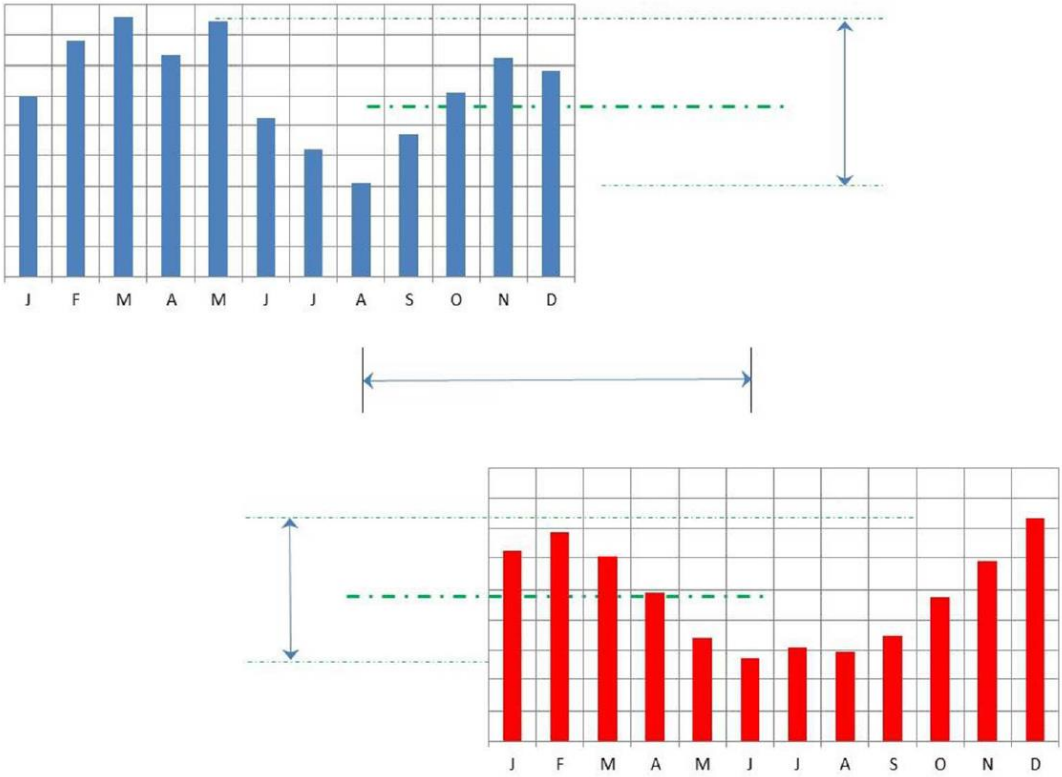

Fig. 8.1. Set of sample data for two renewable energy resources. Adapted from Beluco (2015) [8-1].

This article deals with the time-complementarity component (here called simply as complementarity in time), which is directly related to the time lag between the maximum or minimum values of energy availability of two renewable resources. Eq. (1) presents the complementarity in time as defined by Beluco et al. (2008) [8-2]. This equation assigns a linear characteristic to the complementarity in time and other equations can be proposed.

$$\kappa_t = \frac{|d_1 - d_2|}{\sqrt{|D_1 - d_1||D_2 - d_2|}} \qquad (1)$$

In this equation, D is the number of the day (or month) in which the maximum energy availability occurs and d is the day (or month) in which the minimum value occurs. Subscript 1 indicates one of the energy resources while the number 2 indicates the other. The denominator

assesses whether energy resources have a 180-day (or six-month) interval between maximum and minimum energy availability, which also affects the complementarity in time.

The application of this equation should not be performed from a mathematically more rigid point of view, as discussed by Beluco (2015) [8-1]. Its application must be carried out by a trained human analyst with a good sense of analysis. The evaluation of the energy resources shown in Fig. 8.1, for example, indicates a complementarity equal to 2 over 6, that is, equal to 0.3333. The minimum values of energy availability occur in months apart from each other for 2 months.

8.3.2 Spatial complementarity in time

As discussed above, spatial complementarity is the complementarity between energy resources located at different sites. This concept, duly quantified and mapped, can lead to important tools for managing energy resources. The appropriate exploitation of spatial complementarity can contribute to lower cost of installation of power plants and optimization of operation costs of plants inserted in an interconnected system.

The problem is then the determination of complementarity between operating plants (or sites with energetic potential) in different locations and not in the same place. It is necessary to determine the complementarity in time between energy resources such as those shown in Fig. 8.1, but located at different sites. Such a calculation will generate information on complementarities with different sites, placed at different distances, and in different orientations.

For simplicity, some limitations to this problem will be established, allowing the basic problem of determining spatial complementarity to be solved.

This article will then present only the determination of complementarity in time. In addition, a region under study will be modeled with the application of a network of hexagonal cells. Thus, the energy in each cell will be the sum of the energy generated (or available energy resources) on its surface, according to the analysis being undertaken.

8.3.3 Complementarity roses

The previous work by Risso and Beluco (2017) [8-11] proposed the analysis based on the establishment of a network of hexagonal cells, but suggested the determination of complementarity in a limited way, not relating the spatial complementarity with its angular distribution throughout the territory under analysis.

Fig. 8.2 shows a network of hexagonal cells established on a hypothetical distribution of hydroelectric power plants and wind farms. The cells are differentiated between cells with hydroelectric plants (in blue), cells with wind farms (in yellow), cells with both types of plants (in gray) and cells without plants (without color).

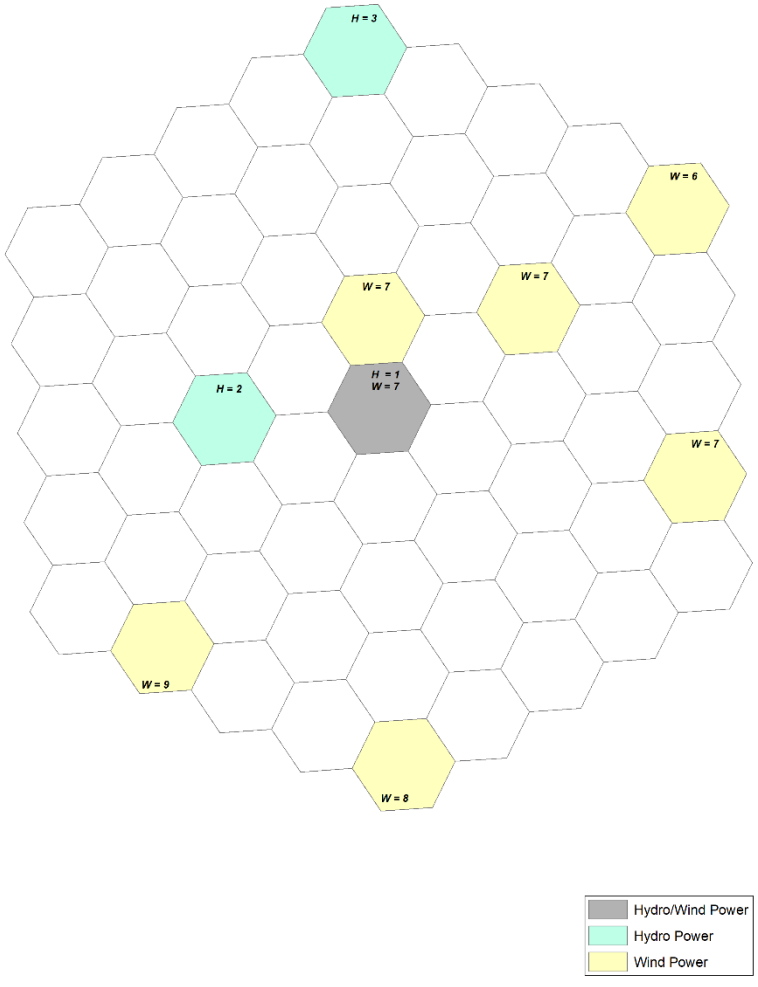

Fig. 8.2. Hexagonal cell network with hypothetical distribution of hydroelectric power plants and wind farms. H and W indicate respectively the months of the year for which there is minimum energy availability for hydroelectric plants and wind farms.

The goal is then to determine the complementarity in time of each cell that contains some power plant with other cells that also contain power plants. There are three parameters to be determined: the complementarity in time with the other grid cells that contain power plants, their respective distances and their respective directions.

In Fig. 8.2, H and W indicate the months in which the minimum energy availability value occurs. These values serve as reference for the determination of complementarity in time. Eq. (1) should be used and in this calculation the interval between the months in which minimum and maximum energy availability values will be considered equal to 6 months.

The first step is to choose one of the cells containing plants and determine their complementarity with the other cells that also contain plants, taking into account in each calculation the respective distance and orientation. Fig. 8.3 shows the cell network of Fig. 8.2 with one identifier per cell. In addition, in this figure appears a cell chosen as reference for the determination of the complementarity that is the cell in blue denominated H-29.

Comparing the hydroelectric plant in cell H-29 with the wind farm in the central cell, W-33, a complementarity equal to 0.83 is obtained. This complementarity is greater than that existing between the hydroelectric plants present in these two cells. So because of this the cell H-33 appears in Fig. 8.3 painted in yellow.

Following the same reasoning, the comparison of the hydroelectric plants in the H-29 cell with the wind farms in the cell W-40 and in the cell W-46 results, respectively, in complementarities equal to 0.83 and 0.67. Consequently, these cells are painted in Fig. 8.3 respectively in yellow and green. Other cells in this figure were painted according to the complementarities determined with the H-29 cell. Complementarity is maximal only with the cell W-15, painted in red.

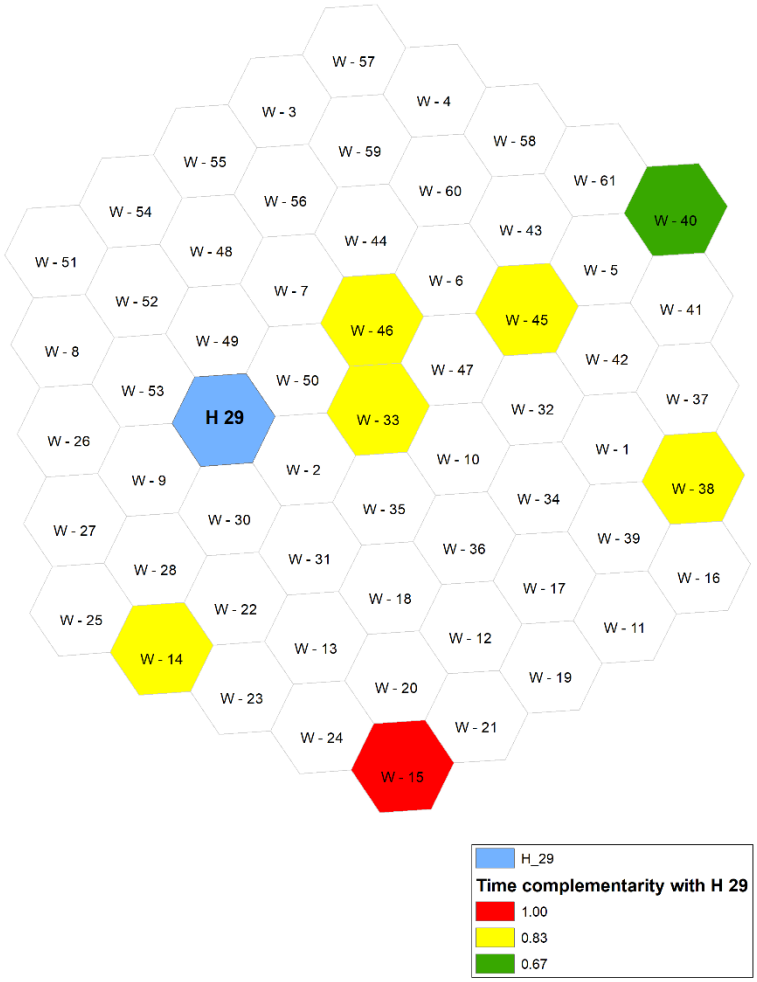

Fig. 8.3. Complementarity in time between the cell marked in blue, containing hydro power plants, and the other cells of the network containing power plants, shown in Fig. 8.2. H and W labeled in each cell, followed by numbers, constitute an identification for each cell.

The next step would be to replicate this process for all cells containing power plants. However, it would also be necessary to represent the results on only one map. One solution to this problem of representation is the use of a complementarity rose, representing in each cell the complementarity identified with all other cells.

Fig. 8.4 (a) shows the complementarity rose for the cell H-29, showing yellow lines pointing to the cells W-33 and W-40 and a green line towards the cell H-46. There is also a red line in the direction of the cell W-15. These lines show their respective distances and their orientations. Fig. 8.4 (b), Fig. 8.4 (b) and Fig. 8.4 (d) respectively present complementarity roses for the cells H-33, H-40 and H-46.

The complementarity rose shown in Fig. 8.4 (b) is different from the other complementary roses since it corresponds to a cell containing hydroelectric power plants and wind farms. The indication of the complementarity between the energetic resources present in this cell occurs with the application of a central circle, filled with the color corresponding to the complementarity. in this case, full complementarity, therefore with a circle painted in red.

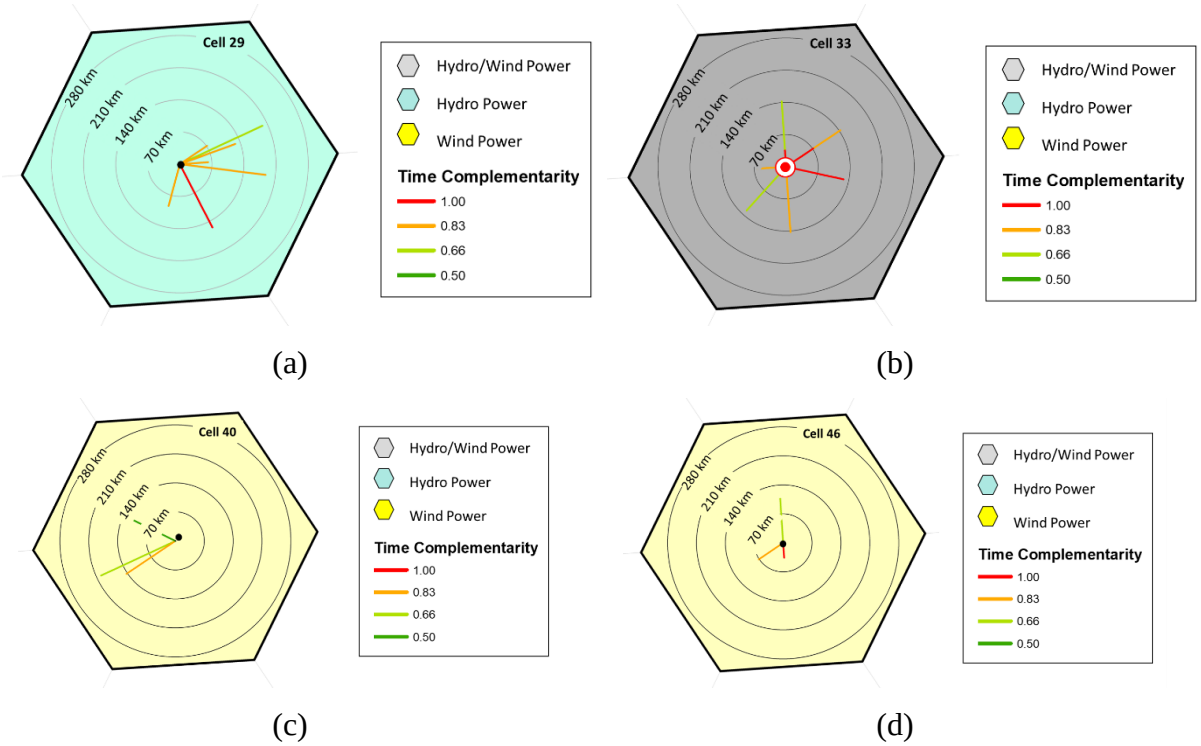

Fig. 8.4. Complementarity roses for the cells (a) H-29, (b) W-33, (c) W-40 and (d) W-46, as identified in Fig. 8.2.

Fig. 8.5 shows models for determining the roses of complementarity. In (a), a model for cells containing only one energetic resource. In (b), a model for cells containing two or more energy resources. Slice directions are matched by the relative positions of the compared cells. The lengths are related to the distances between the cells. The colors are established by the legend, associating a color scale with the different values of complementarity.

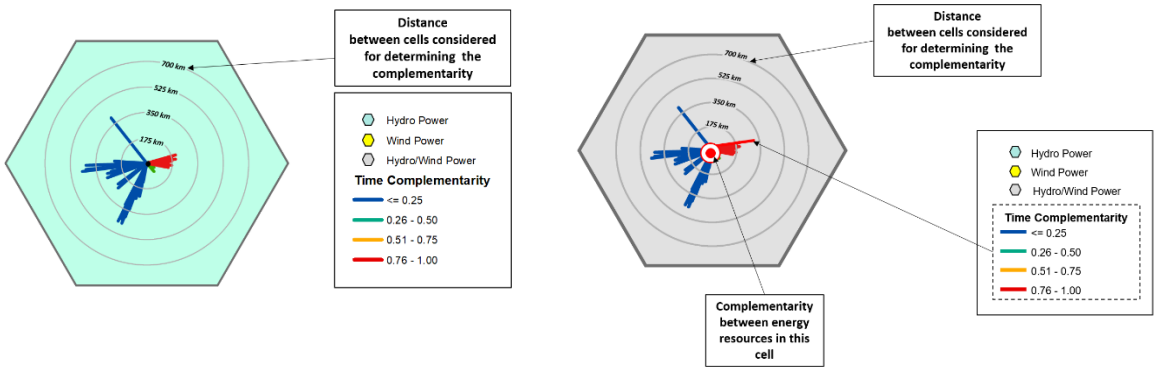

(a) (b)

Fig. 8.5. Models for determining roses of complementarity: (a) with only one energy resource per cell and (b) with two or more energy resources per cell.

Fig. 8.6 shows the map made with the complementarity roses determined for the cells and the hypothetical distribution of power plants proposed in Fig. 8.2. As expected, the lines in a cell always find identical lines in their counterpart. With this idea in mind, it is relatively easy to look at the cells in the hexagonal network shown in Fig. 8.6 and identify which cells have maximum complementarity with each other.

The next section proposes a method for quantifying spatial complementarity in time and its expression through a map containing complementary roses in cells containing power plants.

8.4 A method evaluating spatial complementarity

The method for establishing the spatial complementarity in time (with the use of complementarity roses) over a specified region can be stated in five steps as follows:

[1] To delimit the region for which the spatial complementarity will be determined, identifying the plants in operation and-or the sites with energetic potential that will be considered in the complementarity analysis;

[2] Obtain data of power supplied (for plants in operation)) or energy availability (for sites with energetic potential) that will be considered in the determination of complementarity in time considering different sites;

[3] Establish a network of hexagonal cells over the region chosen for the analysis, identifying the cells containing operating plants and-or sites with energetic potential and recording the distances between these cells;

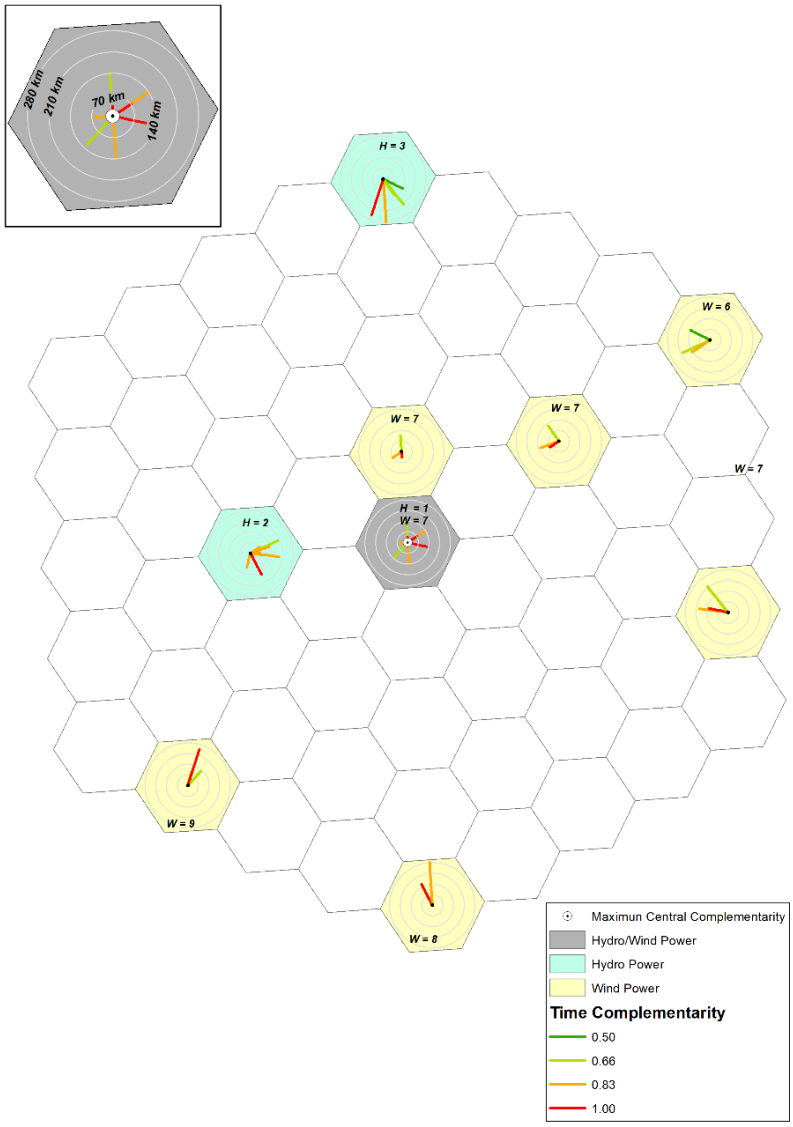

Fig. 8.6. Map of spatial complementarity in time for the network of hexagonal cells of Fig. 8.2.

[4] Determine the complementarity in time for each cell that contains some plant (existing or potential), comparing it with all other cells containing plants, noting in a complementarity rose for this cell the different values of complementarity according to the respective distances;

[5] Finally, evaluate the final result obtained with the superposition of the complementarity roses on the respective hexagonal cells and on the map, possibly suggesting some simplification if the complementarity roses have become too full, making the visual reading of the information along the map difficult.

The next section presents the application of this method to a set of hydroelectric power plants and wind farms in the State of Rio Grande do Sul, in southern Brazil.

8.5 Complementarity in space for some hydropower plants and wind farms along Rio Grande do Sul, in southern Brazil

The State of Rio Grande do Sul is the most southern state in Brazil and can be seen on reference [8-9]. Rio Grande do Sul has a surface area of 281,730.223 square kilometers and an estimated population of 11,286,500 inhabitants. According to ANEEL (2017) [8-7], Rio Grande do Sul has installed capacity of 9,517.817 MW, with a combination of hydroelectric power plants, thermoelectric power plants and wind farms.

In this paper, the determination of spatial complementarity in time between some hydropower plants and some wind farms and its expression through a map with roses of complementarity is the only interest, without the intention of exhausting the subject. The objective is just to demonstrate the potentialities of the method proposed here.

In this sense, some hydroelectric plants and some wind farms were selected along the territory of the State. A network of hexagonal cells was established to group the selected plants. The generation data were obtained in order to determine the complementarity component in time, as defined by Beluco et al. (2008) [8-2].

Fig. 8.7 shows the State of Rio Grande do Sul and the network of hexagonal cells established for this study.The network has 582 hexagonal cells, each with 500 km2. This study selected 431 hydro power plants, marked in blue dots and inserted in 141 cells represented in the map painted with blue. This study also selected 222 wind farms, marked in red spots and inserted in 141 cells painted with yellow.

The region to the north of the State presents greater topographic differences and presents a drainage network more dense and mighty and therefore receive a greater number of hydroelectric plants. The southernmost region of the State has the largest wind potential and therefore concentrates the wind farms.

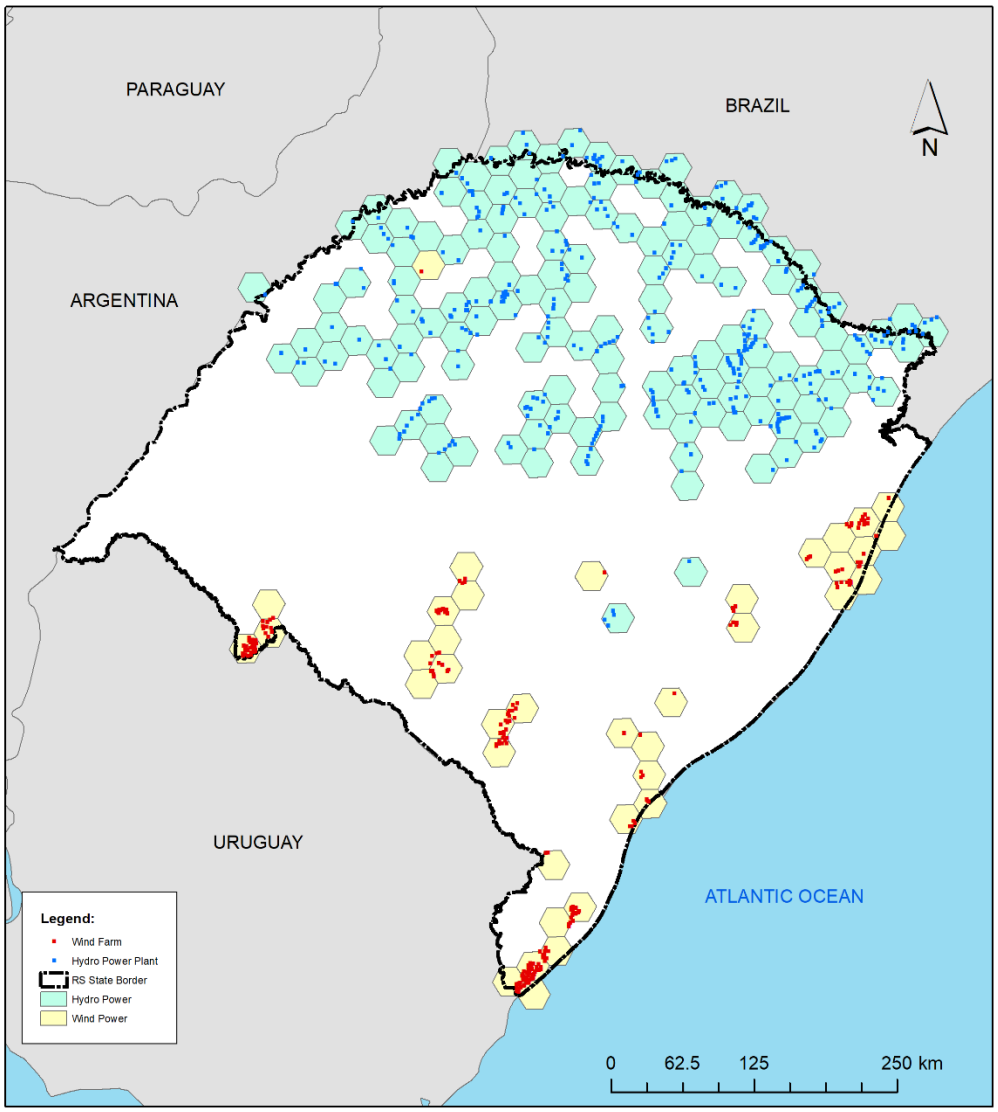

Fig. 8.7. Network with 582 hexagonal cells of 500 km2 each, for analysis of spatial complementarity in the time along the State of Rio Grande do Sul, indicating hydroelectric power plants and wind farms considered in the analysis.

The cells identified in this figure should then have their potentials compared in order to determine complementarity in time. The index proposed by Beluco et al. (2008) [8-2] is here applied to energy resources located in different positions. It is necessary to determine the values of complementarity and the corresponding directions.

Fig. 8.8 shows the map of Rio Grande do Sul with the roses of complementarity indicating spatial complementarity in time. This figure shows the detailing of one of the

complementary roses located in the upper left corner, which contains hydroelectric plants. The map obtained is a complex figure to be analyzed at a first glance.

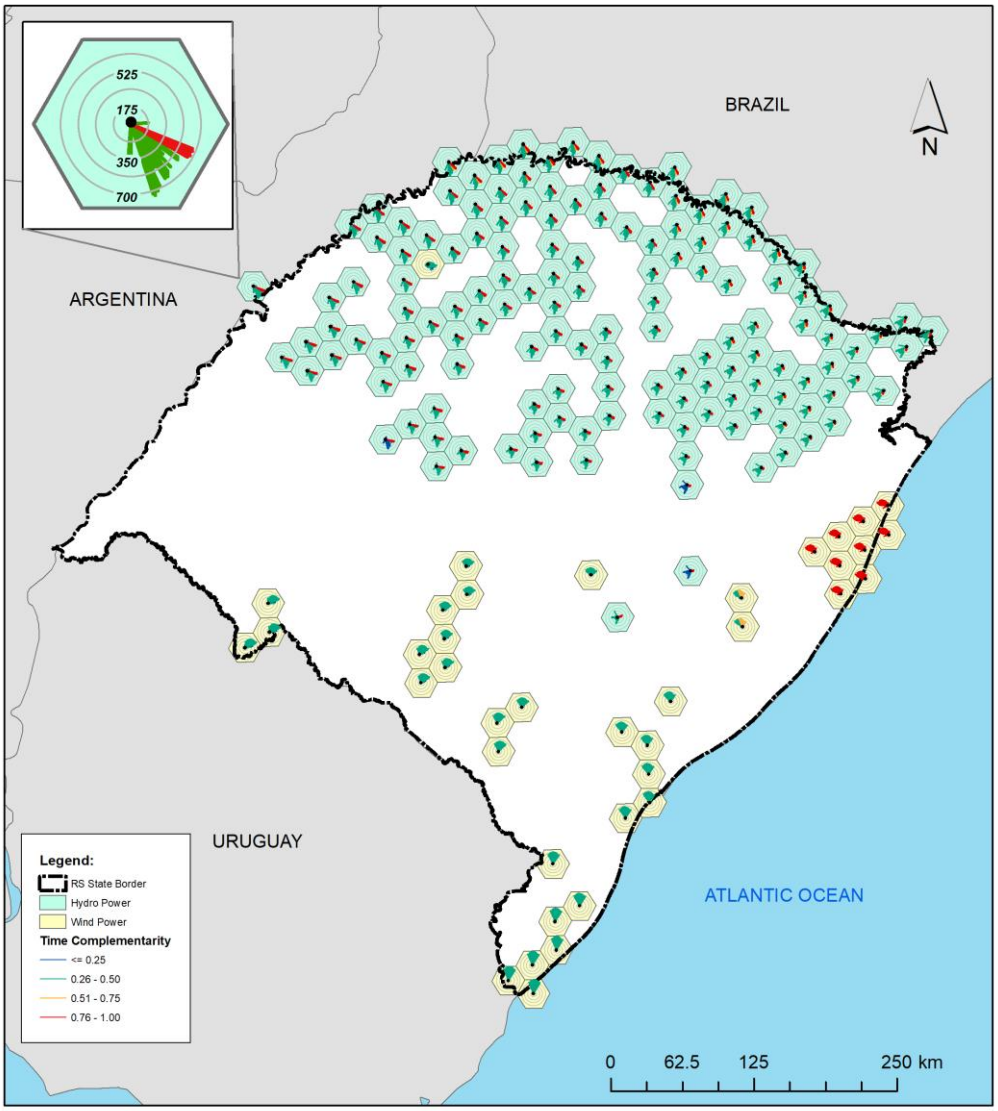

Fig. 8.8. Maps of the State of Rio Grande do Sul with roses of complementarity indicating the spatial complementarity in the time between the plants marked in Fig. 8.7.

Only the hydroelectric cell that had its complementarity rose shown in detail in the upper right corner, and the wind cells located in the northernmost part of the coast, have red lines. These lines in red indicate existence of complementarity in time reaching maximum values. The identification of this maximum complementarity (between a hydroelectric plant in the far west and wind farms in the east) can be considered as the main result of this work.

As can be expected, the cells at the extremities of the studied region will exhibit lines of complementary roses, which could be termed as petals, with longer lengths. Likewise, the cells in the most central parts will present a large number of lines with intermediate lengths. In addition, it can also be expected that the roses will present great variations of intensities of complementarity as the resources analyzed are more intermittent.

Fig. 8.9 shows a detail of the central part of the map shown in Fig. 8.8. This map at a better scale allows a better observation of the roses of complementarity. The complementary roses of the cells of the north coast present more petals with maximum complementarities oriented to the hydroelectric plants of the central north region, besides those already identified in Fig. 8.8.

The cell that appears in detail in the upper left corner is one of these cells. Petals with approximately maximum complementarity at distances of the order of 350 km are complemented with these cells of the north coast. Intermediate complementarities with wind farms to the south and southwest complete the petals of this rose of complementarity.

The wind farms to the southwest of this position, in turn, present intermediate complementarities also with the more distant power plants, located in the region of the cell detailed in the map of Fig. 8.8.

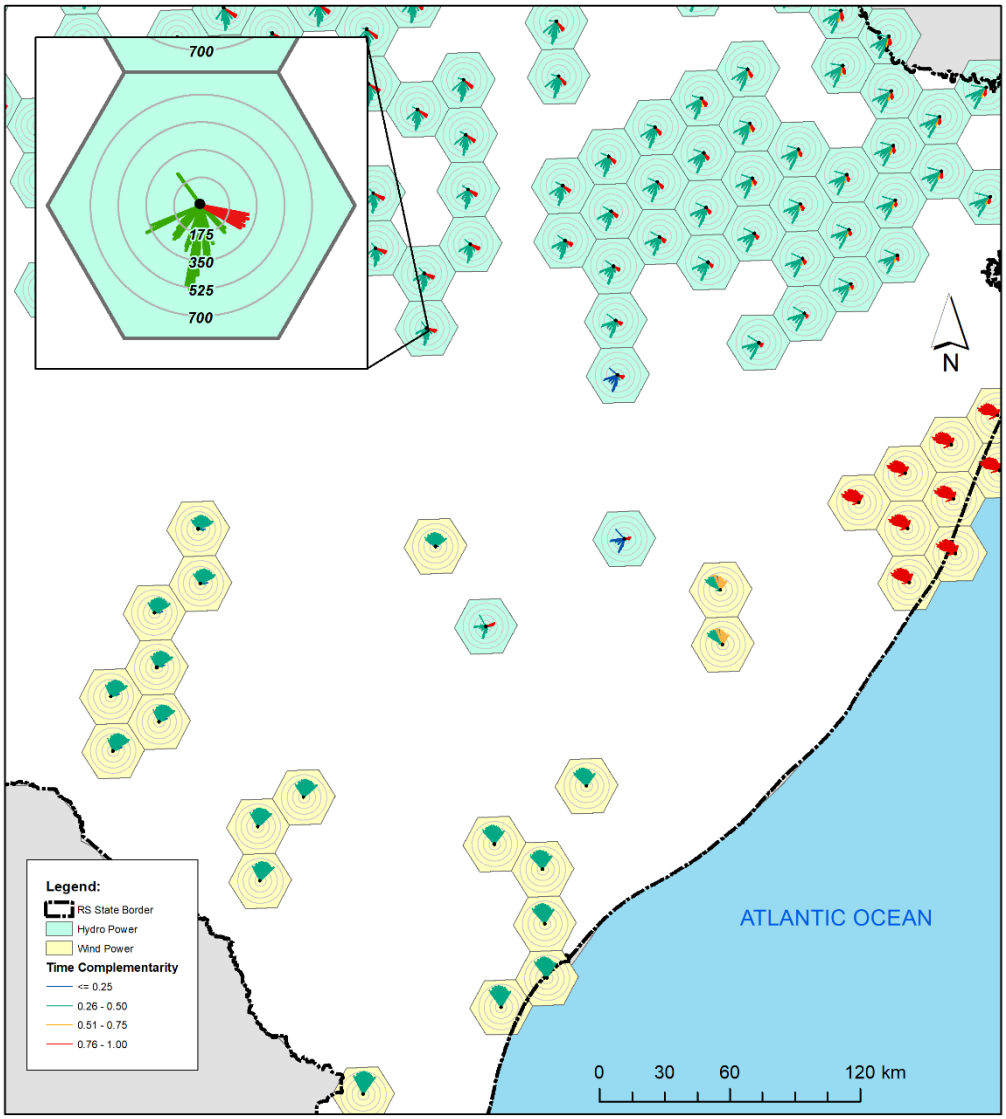

Fig. 8.9. Detail of the eastern center region of the map shown in Fig. 8.8.

8.6 Conclusions

This article discussed the concept of complementarity and contributed to a better understanding of spatial complementarity. This paper proposed a method for determining the spatial complementarity in time and its expression through maps.

The proposed method is based on the determination of complementary roses, whose petals will have length determined by the distance to another cell and their color will indicate the complementarity between these two cells.

This article also shows the application of the proposed method for the determination of spatial complementarity in time between some hydroelectric power plants and wind farms identified along the territory of the State of Rio Grande do Sul, the southernmost State of Brazil, and presents the map prepared with this application.

The possibility of expressing spatial complementarity in time through a map opens the way for a better use of the concept of complementarity as a tool for the management of renewable energy resources and for prioritization of energy generation projects.

A better knowledge of the applicability of the proposed method will come with its application to other case studies and its application also to determine the other components of complementarity, in addition to the complementarity in time. Likewise, the quality of the information on the complementarity map will be better as the data used to determine complementary roses are better.

8.7 Acknowledgements

This work was developed as a part of research activities on renewable energy developed at the Instituto de Pesquisas Hidráulicas, Universidade Federal do Rio Grande do Sul, southern Brazil. The authors acknowledge the support received by the institution. The last author acknowledges the financial support received from CNPq for his research work (proc. n. 309021/2014-6).

8.8 References

[8-1] Beluco, A. (2015) A concept of boundaries of performance for analysis of hybrid systems based on complementary energy resources. In: Prasad, R. Shivakumar, B.G. Sharma, U.C. Energy Management; Energy Science and Technology, Vol.12; Houston, TX, USA, Studium Press LLC, p.459-483.

[8-2] Beluco, A. Souza, P.K. Krenzinger, A. (2008) A dimensionless index evaluating the time complementarity between solar and hydraulic energies. Renewable Energy, v.33, n.10, p.2157-2165.

[8-3] Beluco, A. Souza, P.K. Krenzinger, A. (2012) A method to evaluate the effect of complementarity in time between hydro and solar energy on the performance of hybrid hydro PV generating plants. Renewable Energy, v.45, p.24-30.

[8-4] Beluco, A. Souza, P.K. Livi, F.P. Caux, J. (2015) Energetic complementarity with hydropower and the possibility of storage in batteries and water reservoir. In: Sorensen, B. (org.) Solar Energy Storage, Academic Press, p.155-188.

[8-5] Borba, E.M. Brito, R.M. (2017) An index assessing the energetic complementarity in time between more than two energy resources. Energy and Power Engineering, v.9, n.9, p.505-514.

[8-6] Cantão, M.P. Bessa, M.R. Bettega, R. Detzel, D.H.M. Lima, J.M. (2017) Evaluation of hydro wind complementarity in the Brazilian territory bt means of correlation maps. Renewable Energy, v.101, p.1215-1225.

[8-7] Electric Energy National Agency [Agência Nacional de Energia Elétrica, ANEEL] (2017) Installed power capacity in State of Rio Grande do Sul. Available in www2.aneel.gov.br/aplicacoes/ResumoEstadual/ResumoEstadual.cfm, accessed on August 05, 2017.

[8-8] Ghirardi, A.O. Costa, F.S. Damazio, J.M. (1997) Analysis of hydrological complementarities at continental level in South America [in Portuguese]. Revista Brasileira de Recursos Hídricos, v.2, n.2, p.143-156.

[8-9] Google Maps at https://goo.gl/maps/s9bAbfCEopK2.

[8-10] Kougias, I. Szabo, S. Monforti-Ferrario, F. Huld, T. Bodis, K. (2016) A methodology for optimization of the complementarity between small hydropower plants and solar PV systems. Renewable Energy, v.87, p.2, p.1023-1030.

[8-11] Risso, A. Beluco, A. (2017) Bases for a methodology assessing spatial complementarity in time. Energy and Power Engineering, v.9, n.9, p.527-540.

9. COMPATIBILIZAÇÃO ENTRE O MODELO DE DISPONIBILIDADE HÍDRICA SUPERFICIAL ISLSCP II UNH/GRDC E A BASE MATRICIAL HYDROBASINS PARA ESTIMATIVA DE VAZÕES DE LONGO PERÍODO EM BACIAS HIDROGRÁFICAS DO RIO GRANDE DO SUL

9.1 Apresentação

Este capítulo, apresenta o trabalho "*Compatibilization Between ISLSCP II UNH/GRDC Composite Monthly Runoff Model and HYDROBASINS Base for Long-Term Flow Estimation in Rio Grande do Sul"* submetido ao periódico *"Journal of Hydrology"*, em 2019, pela editora *ELSEVIER* tendo como autores o Prof. Alfonso Risso; Engª Mariana Tosi Corrêa; Prof. Alexandre Beluco, Profª. Rita de Cássia Marques Alves e o Prof. Laurindo Guasselli.

Abstract

The objective of this paper is to evaluate the accuracy of the ISLSCP II UNH / GRDC monthly water availability model coupled to the HydroBASINS georeferenced matrix base to simulate spatially and temporally long-term flow rates. Because they have different resolutions, interpolation operations are necessary for data compatibility. With the monthly surface runoff matrix and the flow directions matrix, the monthly surface runoff sheet generated upstream of each cell is obtained. Multiplying this matrix by the average resolution of cells in the latitudes of the study region gives the average monthly flow in each cell. Summing all monthly weighted cumulative flows over a year results in the long-run average flow. The state of Rio Grande do Sul was used as a study area. The verification of the modeled flows was made through the comparison with flows measured in fluviometric stations, presenting $R^2 = 0.9365$. The areas of the modeled watersheds and the measured areas were analyzed for each river post, resulting in $R^2 = 0.99998$. The high correlation between the modeled and observed values confirms the accuracy of the methodology used.

Keywords: surface runoff model; water availability; long period flows

9.2 Introduction

This paper aims to evaluate the accuracy of an ISLSCP II UNH / GRDC monthly water availability model (Fekete, Vorosmarty & Grabs, 1999 [9-6]; Fekete, Vorosmarty & Grabs, 2002 [9-7]) coupled to the HydroBASINS georeferenced matrix base (Lenhner & Grill, 2013)

[9-10] for simulate spatially and temporally long-term flow rates. Long-run average flow is defined as the average of the series flow rates available at one location (Tucci, 2002) [9-13].

To validate the model, data from the time series of fluviometric stations provided by the National Water Agency (ANA) [9-8], through the HidroWeb portal, were used.

The state of Rio Grande do Sul, the southernmost state in Brazil, was chosen to illustrate the application of the adopted methodology.

9.3 Methodology

The compatibility between the surface runoff model and the watershed database comprises the crossing between the drainage network data, altimetry and water availability. For that, monthly runoff, annual flow and drainage area are modeled. Comparing the results obtained with the flow and area data observed in fluviometric stations, it is possible to verify the accuracy of the model used.

9.3.1 Modeled data

Monthly Runoff: ISLSCP II UNH / GRDC - Composite Monthly Runoff (Fekete, Vorosmarty & Grabs, 1999 [9-6]; Fekete, Vorosmarty & Grabs, 2002 [9-7]). It consists of composite runoff data combining monthly average estimates from a simulated water balance model derived from climate data with monitored river discharge. Such a data assimilation scheme preserves the spatial specificity of water balance calculations, constrained by more accurate flow measurement. The resulting composite flow estimates are useful for numerous applications, from water resource assessments (Vorosmarty 2000 [9-15]; Revenga 2000 [9-11]) to the validation of atmospheric models (Dai and Trenberth, 2002) [9-2].

UNH / GRDC composite runoff data cover the geographical range between 55 ° S and 83 ° N excluding Greenland and the Arctic Archipelago. The spatial resolution is 0.5 ° in latitude and longitude, and the temporal coverage ranges from January 1986 to December 1995.

Altimetry and drainage network: HydroSHEDS SRTM (Lehner, Verdin & Jarvis, 2006) [9-9]. Developed by the Conservation Science Program of the World Wildlife Fund, it is mainly based on elevation data obtained during NASA's Shuttle Radar Topografy Mission (NASA) mission (Farr & Kobrick, 2000) [9-5].

The SRTM digital elevation model allows basin boundaries to be derived from the hydrographic data layers provided by HydroSHEDS. As a result, river basins are consistently delineated at different scales, and a hierarchical sub-basin sub-division was created following the topological concept of the Pfafstetter coding system (Verdin & Verdin 1999) [9-14]. The resulting polygonal layers are called HydroBASINS (Lenhner & Grill, 2013) [9-10] and represent a subset of the HydroSHEDS database with a grid resolution of 15 seconds (approximately 500 m in Ecuador).

9.3.2 Observed data

Fluviometric stations and drainage area: Hidroweb / ANA (http://hidroweb.ana.gov.br/) [9-1]. The National Water Agency (ANA) is responsible for managing and updating the national water resources monitoring system. The Hidroweb portal was created in order to make this information public and allows the user to select and download the stations of interest, whether they are fluviometric or rainfall, and their respective values of rainfall, flow, quota, drainage area, etc.

Long term average flow: Super Data Management - IPH / UFRGS (Fan, 2010) [9-4]. The software was created by the Large-scale Hydrology (HGE) research group of the Institute of Hydraulic Research (IPH) of the Federal University of Rio Grande do Sul (UFRGS), with the purpose of facilitating the manipulation and visualization of a large set of hydrological data. Developed in VB.NET language, its features include visualization of the temporal availability of data and the generation of graphs for comparison of hydrographs and permanence curves of different stations. In addition, it includes the calculation of hydrological statistics for flow data such as long period average, mode, 10% (Q90), 5% (Q95), 50% (Q50), 90% (Q10), among others.

9.3.3 Spatial analysis of modeled data

The monthly runoff data was downscaled to a resolution of 450 x 450 m, the same as the flow direction and accumulated flow matrices available in the HidroBASINS database. For this, the natural neighbor interpolator was used (Sibson, 1981) [9-12]. The new monthly surface runoff matrix then represents the water availability in each cell.

From the HidroBASINS flow direction matrix, it is estimated a new accumulated flow matrix, which is weighted by the monthly surface runoff matrix. Thus, the surface runoff generated upstream of each cell is calculated for each month (Fig. 9.1). By multiplying this value by the model resolution and dividing it by the number of seconds in a month, you get the average monthly cell flow in m^3 / s. Summing up all the weighted monthly accumulated flows over a year results in the long-run average flow (Fig. 9.1).

9.3.4 Spatial analysis of observed data

As previously mentioned, fluviometric stations scattered throughout the state of Rio Grande do Sul were selected to verify the model used. The choice of stations was filtered to choose those with the same temporal window as the surface runoff model, ie from 1984 to 1995. Consideration was also given to stations with different sized drainage areas in order to test the applicability. model for different watershed sizes. In addition, historical series with no or few failures were prioritized, considerably reducing the number of stations suitable for the study. Table 1 shows the 10 selected river stations and, in Figure 3, their locations and respective watersheds.

Tab. 9.1. Fluviometric stations selected to collect flow and drainage area data.

Basin code	Designation of fluviometric station	River
70700000	Passo Socorro	Pelotas
72530000	Passo do Ligeiro	Ligeiro
73480000	Ponte do Rio Passo Fundo	Passo Fundo
74600000	Cascata Buricá	Buricá
75185000	Ponte Nova do Potiribu	Potiribu
76700000	Passo dos Britos	Ibirapuitã
86440000	Passo do Prata	Prata
86470000	Ponte do Rio das Antas	Antas
85900000	Rio Pardo	Jacuí
87905000	Passo do Mendonça	Camaquã

9.4 Results and discussion

The spatial analysis of modeled data had as its product the monthly maps presented in Figure 1, which represent the surface runoff upstream of each cell. By summing all the weighted accumulated flows over a year, we obtain the long-term average flow, represented in Fig. 9.2. Fig. 9.3 shows the location and drainage areas of the selected river stations for the study.

With the values of long-term average flow and delimitation of river basins of fluviometric stations based on the model used, it is possible to compare them with data provided by ANA. Table 2 at first glance shows a considerable approximation between the observed and modeled flow values. For area data, the approximation is even greater for both small (~ 500 km²) and large (~ 40,000 km²) basins. In order to obtain a more accurate comparison between the values, the linear correlation graphs for the flow and area variables were plotted (Fig. 9.4 and Fig. 9.5, respectively). According to Dancey and Reidy (2006) [9-3], values of R^2 up to 0.30 should be considered weak, between 0.40 and 0.60 moderate and, above 0.70, strong.

For flow data, $R^2 = 0.9365$ is observed, ie a high correlation value. The modeled and observed variables are highly dependent on each other, which confirms the good efficiency of the model for the region under study. For area data, the correlation is $R^2 = 0.99998$, an almost perfect correlation. Estimates of the drainage areas modeled at the fluviometric stations are practically identical to those monitored by ANA.

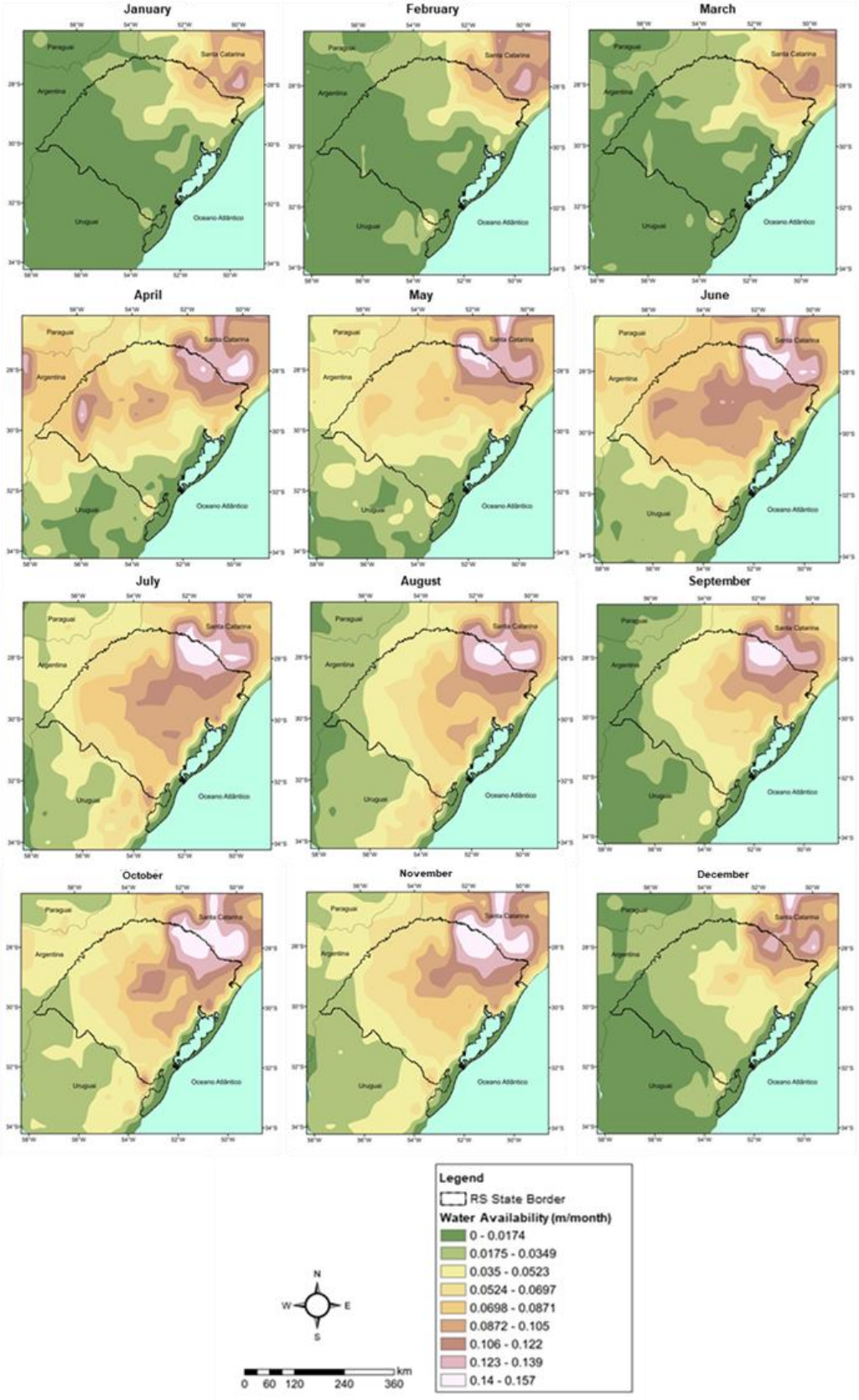

Fig. 9.1. Water availability maps, given in water depth per month, for the 12 months of the year.

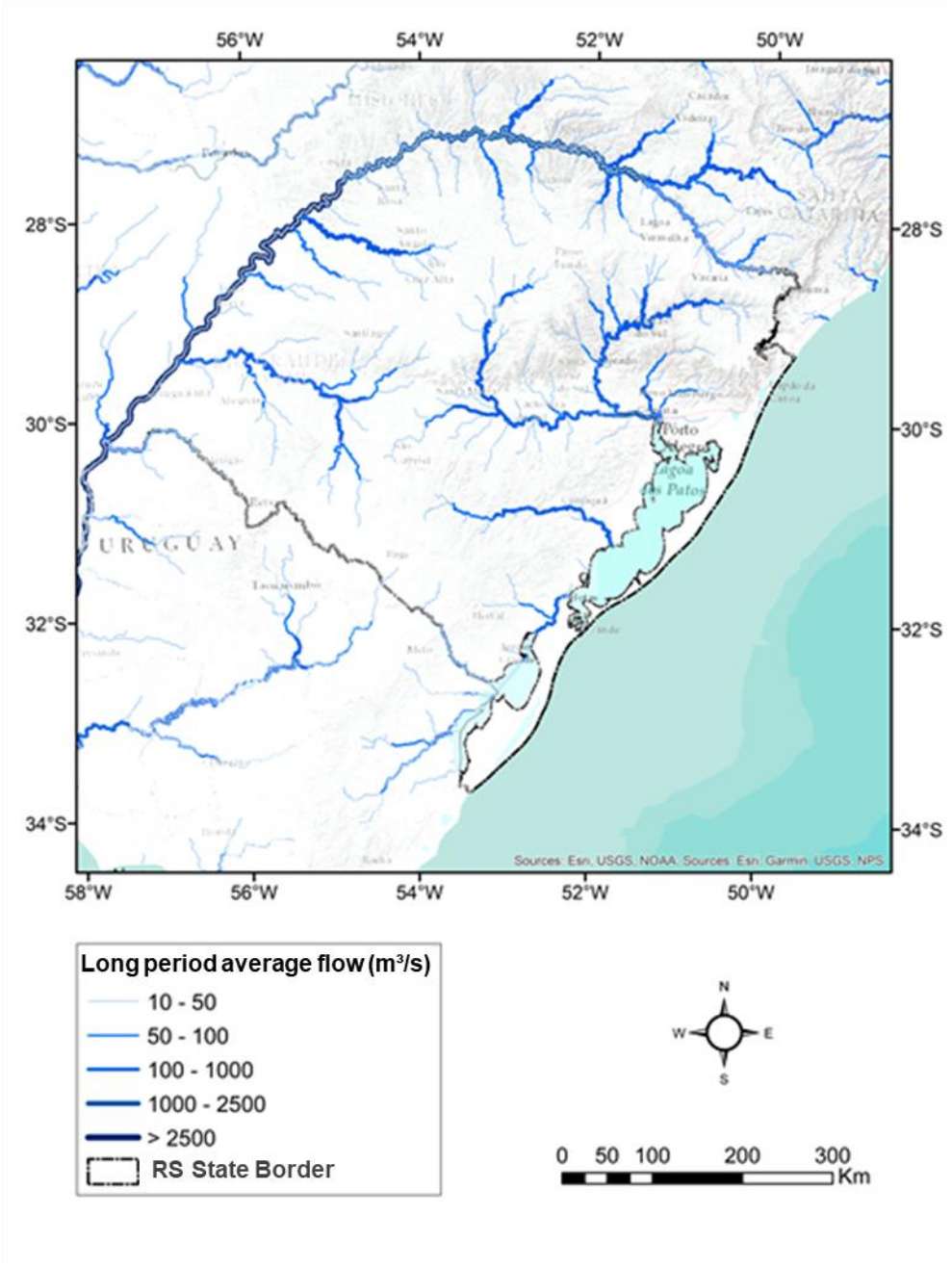

Fig. 9.2. Average long-term flow in water basins in Rio Grande do Sul.

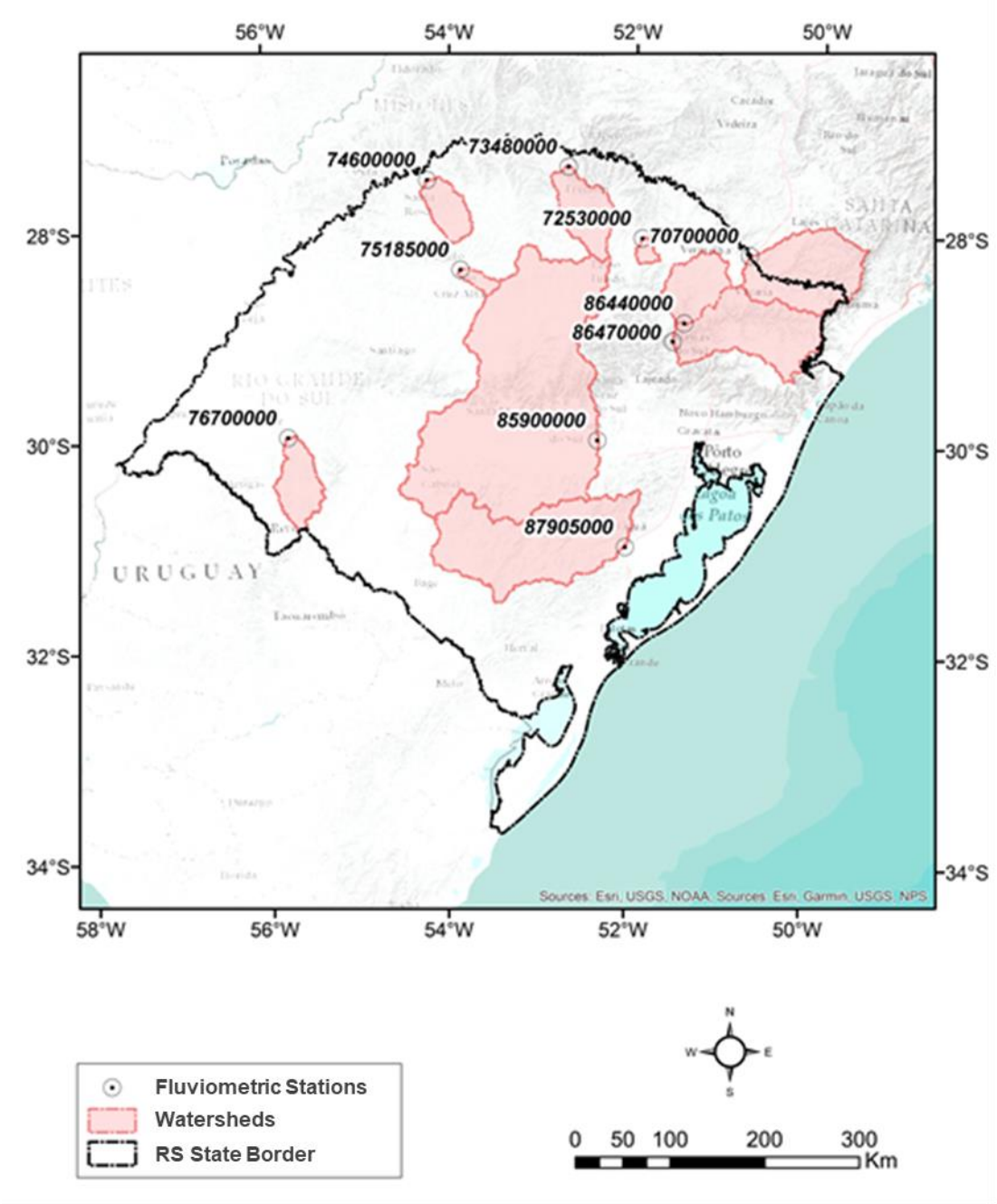

Fig. 9.3. Location and delimitation of the watershed of the 10 chosen river stations, based on the modeled data.

Tab. 9.2. Flow and area data modeled and observed for the 10 river stations distributed throughout the state of Rio Grande do Sul.

Código do posto fluviométrico	Vazão observada (m^3/s)	Vazão modelada (m^3/s)	Área observada (km^2)	Área modelada (km^2)
70700000	201.40	305.29	8400.00	8378.63
72530000	13.50	17.64	460.00	456.14
73480000	102.78	96.93	3710.00	3693.27
74600000	53.98	31.39	2260.00	2258.18
75185000	15.76	12.93	609.00	606.91
76700000	60.72	40.19	3200.00	3173.62
86440000	84.10	128.46	3600.00	3613.89
86470000	321.19	387.99	12500.00	12427.10
85900000	979.86	811.25	38700.00	38840.70
87905000	359.52	235.41	15600.00	15492.00

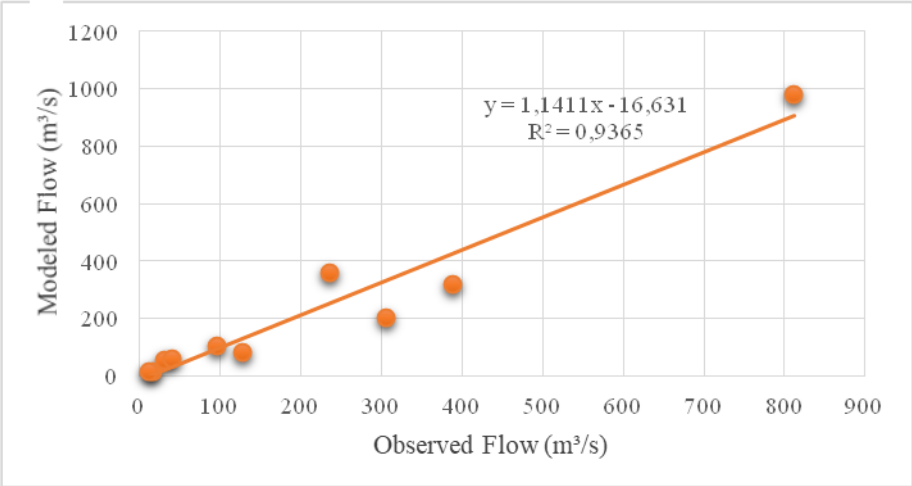

Fig. 9.4. Linear correlation between modeled and observed flow data.

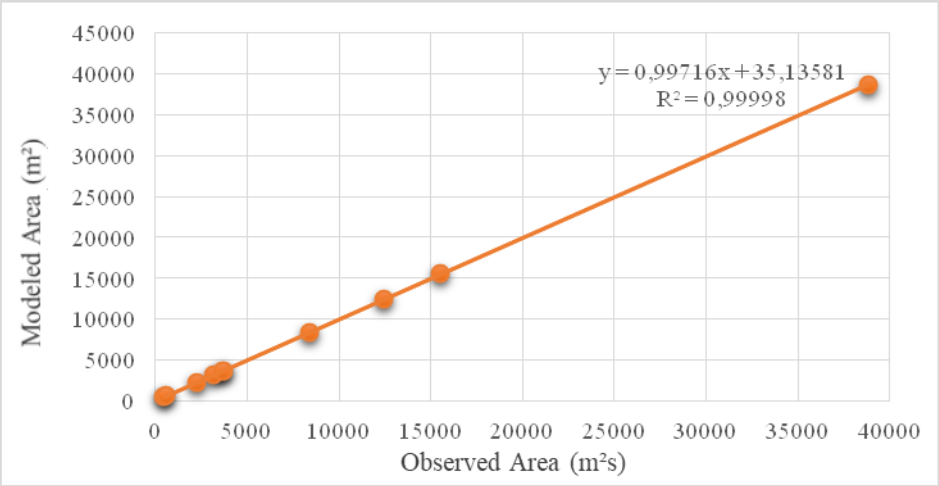

Fig. 9.5. Linear correlation between modeled and observed area data.

For flow data, $R^2 = 0.9365$ is observed, ie a high correlation value. The modeled and observed variables are highly dependent on each other, which confirms the good efficiency of the model for the region under study. For area data, the correlation is $R^2 = 0.99998$, an almost perfect correlation. Estimates of the drainage areas modeled at the fluviometric stations are practically identical to those monitored by ANA.

9.5 Final remarks

The aim of this paper was to verify the accuracy of a global monthly surface runoff model derived from a simulated water balance model. It was based on the comparison between modeled data, developed by the University of New Hampshire, and data inferred by ANA, made available through the HidroWeb portal.

Distinct watershed sizes were tested in order to identify for which situations the global model presents better results. Drawing the dispersion diagram of the flow and area data, a high correlation between them was verified, confirming the accuracy of the model used. The different drainage area sizes were not determinant for the model application. However, it is recommended to use a higher number of river stations in this type of verification. Only 10 were selected for this study, due to the a priori conditions mentioned. The use of this methodology for other places in Brazil is also suggested.

The foundation of the effectiveness of this type of model proved to be very useful to estimate monthly and annual average flows. In addition, it enables the analysis of spatiotemporal variability of water availability and may be useful in different applications of water resources such as hydroelectric potential, zoning of areas at risk of flooding, irrigation and drainage, etc.

Acknowledgements

The authors are grateful for the support of their respective institutions for their research work in the area of renewable energy and geoprocessing, which culminated, among other things, in the preparation of this article. The third author acknowledges CNPq's support for his work as a researcher (Case No. 312941 / 2017-0).

9.6 References

[9-1] ANA – Agência Nacional das Águas. Hidroweb: Sistemas de informações hidrológicas. http://hidroweb.ana.gov.br. 27 jul. 2019.

[9-2] Dai, A. and K. E. Trenberth: Estimates of freshwater discharge form continents: Latitudinal and seasonal variations, *Journal of Hydrometeorology*, submitted, 2002.

[9-3] Dancey, Christine P. & Reidy, John.2006. Estatística Sem Matemática para Psicologia: Usando SPSS para Windows. Porto Alegre, Artmed.

[9-4] Fan, F.M. Manual do programa Manejo de Dados Hidroweb. Projeto Integrado de Cooperação Amazônica e de Modernização do Monitoramento Hidrológico, FINEP/ANA/IPH-UFRGS, Porto Alegre (RS), p. 10, 2010.

[9-5] Farr, T. G., and M. Kobrick (2000), Shuttle Radar Topography Mission produces a wealth of data, *Eos Trans. AGU, 81*(48), 583, 585.

[9-6] Fekete, B. M., Vorosmarty, C. J., and Grabs,W.: Global, Composite Runoff Fields Based on Observed River Discharge and Simulated Water Balances, GRDC Report 22, Global Runoff Data Center, Koblenz, Germany, 1999.

[9-7] Fekete, B. M., Vorosmarty, C. J., and Grabs, W.: High resolution fields of global runoff combining observed river discharge and simulated water balances, Global Biogeochem. Cyc., 16(3), doi:10.1029/1999GB001254, 2002.

[9-8] Inventário das estações fluviométricas/Agência Nacional de Águas. – 2 ed. - Brasília: ANA; SGH, 2009.

[9-9] Lehner, B., K. Verdin, and A. Jarvis (2006), HydroSHEDS technical documentation, World Wildlife Fund, Washington, D. C. Available at http://hydrosheds.cr.usgs.gov.

[9-10] Lehner, B., Grill G. (2013): Global river hydrography and network routing: baseline data and new approaches to study the world's large river systems. Hydrological Processes, 27(15): 2171–2186. Available at www.hydrosheds.org.

[9-11] Revenga, C., J. Brunner, N. Henninger, K. Kassem & S. Murray: Global Freshwater Ecosystem Assessment, World Resources Institute, Washington, DC, 2000.

[9-12] Sibson, R. A Brief Description of Natural Neighbor Interpolation, chapter 2 in Interpolating Multivariate Data. New York: John Wiley & Sons, 1981. 21–36.

[9-13] Tucci, C. E. M. Hidrologia: Ciência e Aplicação. 3º edição. (2002) Porto Alegre: Editora da UFRGS/ ABRH. Cap 2, p. 40-42.

[9-14] Verdin, K.L., Verdin, J.P. (1999): A topological system for delineation and codification of the Earth's river basins. Journal of Hydrology 218 (1-2): 1-12.

[9-15] Vorosmarty, C. J., P. Green, J. Salisbury and Lammers, R. B.: Global water resources: Vulnerability from climate change and population growth, *Science*, 289, 284-288, 2000.

10. AVALIAÇÃO QUALITATIVA DA COMPLEMENTARIDADE ESPACIAL ENTRE RECURSOS DE ENERGIA RENOVÁVEL E ROSAS DE COMPLEMENTARIDADE

10.1 Apresentação

Este capítulo, apresenta o trabalho "*Qualitative evaluation of spatial complementarity between renewable energy resources with complementarity roses"* publicado no periódico *"MethodsX"*, em 2019, pela editora *ELSEVIER* tendo como autores o Prof. Alfonso Risso; Prof. Alexandre Beluco e Profª. Rita de Cássia Marques Alves.

Abstract

Energetic complementarity is a subject that has been concentrating more and more attention of the researchers around the world in the last years, a concept that can be applied both in energy planning and in operation of energy systems based on renewable energy resources. Spatial complementarity is the energetic complementarity evaluated between two renewable resources in different locations and, as well as the complementarity evaluated between resources in the same location, has three components: time-complementarity, energy-complementarity and amplitude-complementarity. At the same site, however, complementarity assessment can involve multiple resources simultaneously, and the study of these circumstances requires appropriate tools to handle such information.This method paper describes a method to build complementarity roses expressing the spatial complementarity between two or more renewable energy resources throughout a region, appropriate for the expression of this complementarity through maps.

Keywords:

Renewable energy, Energetic complementarity, Hybrid energy systems, Spatial complementarity, Complementarity roses, Maps of complementarity.

- The method allows the graphic characterization of the spatial complementarity along a region with the use of maps.
- The complementarity rose, inspired by the compass-rose, expresses a reasonable amount of information in one graphic symbol.
- A complementarity rose can be built with components or with total complementarity, determined with different methods.

Specifications Table

- Subject Area: Energy
- More specific subject area: Renewable Energy
- Hybrid Energy Systems Method name: Method for qualitative evaluation of spatial complementarity between renewable energy resources with complementarity roses
- Name and reference of original method: Complementarity roses evaluating spatial complementarity in time between energy resources. Risso et al. [10-3]. Energies (2018), v.11, n.7, #1918.
- Resource availability: N/A

Method details

Background

The subject of the complementarity between renewable energy resources has been attracting the attention of a growing number of researchers around the world in recent years. The work of Beluco et al. [10-1] suggested a dimensionless index for the evaluation of the complementarity between two or more renewable resources in the same place. One of the challenges is the evaluation of the complementarity between renewable resources in different places and the work of Risso et al. [10-3] proposes a qualitative evaluation of this type of complementarity, denominated as spatial, with the use of complementary roses. Ref. [10-4] presents a more extensive discussion on the subject, also advancing on issues related to the performance of hybrid systems based on complementary resources. Ref. [10-5] relates the reliability of a hybrid system with the complementarity between energy resources and Refs. [10-2] - [10-6] present practical situations related to complementarity. This method article summarizes a method for the qualitative evaluation of spatial complementarity by means of complementarity roses.

Method

The method for qualitative evaluation of spatial complementarity between renewable energy resources with complementarity roses consists of the following steps:

1. Establish the extension of the study to be performed with the application of complementary roses to evaluate spatial complementarity, specifically determining the region to be covered by the study and the type of complementarity that will be determined (total complementarity or some of its components, complementarity between energy supplies provided by power plants or complemen-tarity between energy potentials).

2. Select the power plants or energy potentials that will be included in the determination

of complementarity within the region already delimited for the study. Obtain data series of power supplied (for plants in operation) or energy availability (for sites with energetic potential) that will be considered in the determination of complementarity. Select coincident time periods in these data series and build monthly average data series. Note. This step suggests the use of monthly data, for the practicality of working with smaller amounts of data, since the evaluation of complementarity itself will require a great amount of information. Clearly, the analysis can be performed with daily data and with hourly data and even with studies differentiating results by seasons, if convenient. Probably the more detailed resolutions will be more convenient for more detailed studies, closer to the definition of energy resource management plans.

3. Establish a network of hexagonal cells over the region chosen for the study, identifying cells containing power plants in operation or sites with energetic potential and recording the distances between these cells. For cells with more than one plant or one energy potential, the data series must be summed resulting in one data series per cell per resource.The distances between cells must be measured between the center points of each hexagonal cell.

   Note. The size of the hexagonal cells must be established from the full extent of the network used for the analysis and the individual size of the cells so that the complementary roses have dimensions that allow their correct visibility and a comprehensive analysis of spatial complementarity. Ref. [10-3] shows an example of a hexagonal network determination.

4. Determine the complementarity (as established in step # 1) for each cell containing some existing or potential plant, comparing it with all other cells containing plants, recording in a complementarity rose for this cell the different values of complementarity obtained as a function of the direction and the distance between the compared cells.Complementary roses must be determined according to the next two steps, as the cell under analysis contains only one or more than one renewable resource.

   Note. Complementarity can be determined in different ways, including with the method described in Ref. [10-2]. This reference describes a simplified method for determining the total complementarity and its components from monthly average data series.

5. If the cell under analysis contains only one renewable resource, the type of this resource must be indicated with the color assigned to that cell. From their central point, lines should be drawn in the respective directions to the other cells containing plants, with the respective colors defined by the complementarity intensities and with the respective lengths indicating the distances to those cells. The center of the cell should be marked with a single dot. Note. Fig. 10.1 shows an example of a cell containing only one energy resource. The caption indicates the color of the feature present in that cell. The circles indicate the distances and the colors of the lines indicate (according to the corresponding legend) the intensities of complementarity in each direction. Fig. 10.1 and Fig. 10.2

together can clarify the construction of these cells.

6. If the cell under analysis contains more than one renewable resource, the cell should be filled with gray and the center point should be thicker than a single point and its color should indicate the intensity of temporal complementarity between the energy resources present in this cell. As in the previous step, from their central point, the lines should be drawn in the respective directions to the other cells containing plants, with the respective colors defined by the complementarity intensities and with the respective lengths indicating the distances for those cells.

   Note. Fig. 10.2 shows an example of a cell containing more than one energy resource. The central point indicates the intensity of complementarity between the energy resources present in this cell. The circles indicate the distances and the colors of the lines indicate (according to the corresponding legend) the intensities of complementarity in each direction. Fig. 10.1 and Fig. 10.2 together can clarify the construction of these cells.

7. Superpose the hexagonal network with the cells indicating their complementary roses on the map of the region under analysis to give a graphic expression of spatial complementarity (Fig. 10.3). Evaluate if the final result allows a good expression of the complementarity, eventually eliminating some cells from the analysis to compose an easy-to-read map.

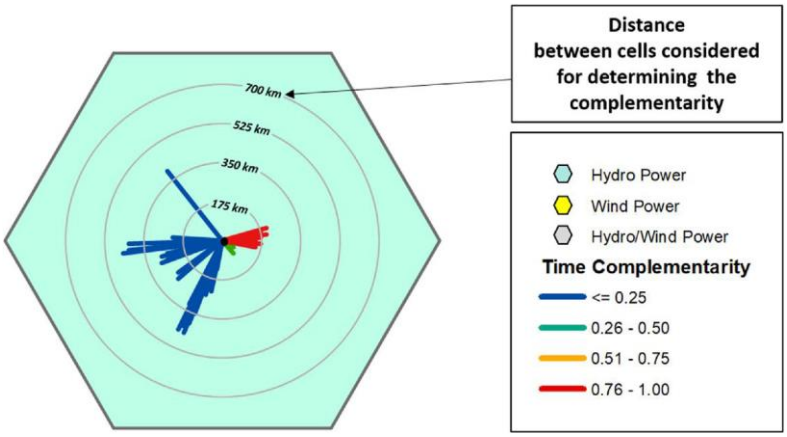

Fig. 10.1. Model for determining complementarity rose for a hexagonal cell with only one renewable energy resource. (Figure reproduced from Ref. [10-3]).

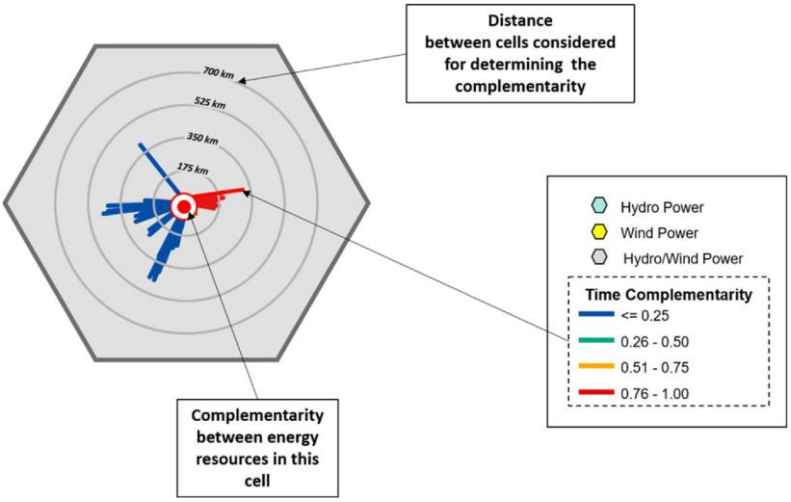

Fig. 10.2. Model for determining complementarity rose for a hexagonal cell with more than one renewable energy resource. (Figure reproduced from Ref. [10-3]).

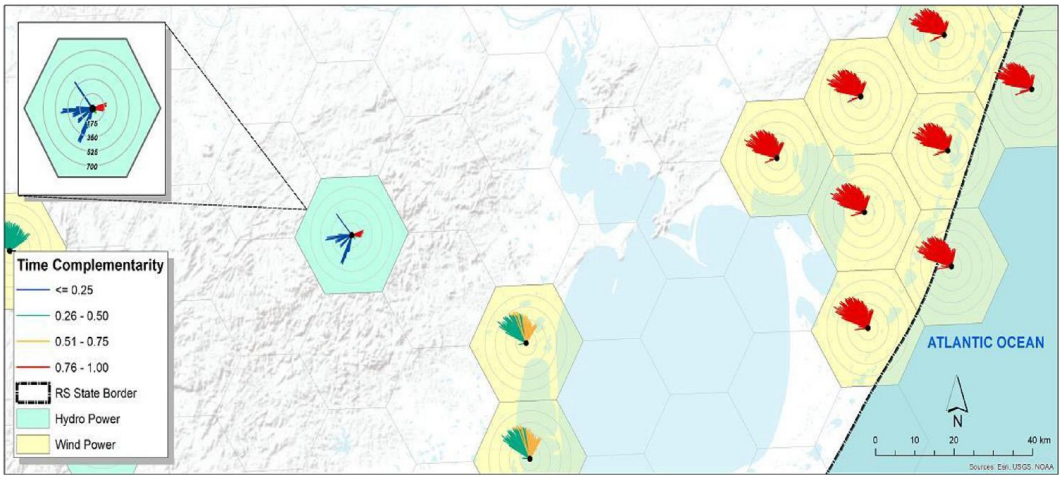

Fig. 10.3. Map of spatial complementarity.

Acknowledgements

The authors are grateful for the support received by their institutions for the research work that led to this article. The second author acknowledges the financial support received from CNPq for his research work (proc. n. 312941/2017-0).

10.2 References

[10-1] A. Beluco, P.K. Souza, A. Krenzinger, A dimensionless index evaluating the time complementarity between solar and hydraulic energies, Renew. Energy 33 (10) (2008) 2157–2165.

[10-2] A. Beluco, A. Risso, F.A. Canales, Simplified Evaluation of Energetic Complementarity Based on Monthly Average Data Submitted for publication by MethodsX, (2019)

[10-3] A. Risso, A. Beluco, R.C.M. Alves, Complementarity roses evaluating spatial complementarity in time between energy resources, Energies 11 (7) (2018) 1918.

[10-4] A. Beluco, P.K. Souza, F.P. Livi, J. Caux, Chapter 7 – energetic complementarity with hydropower and the possibility of storage in batteries and water reservoirs, in: B. Sorensen (Ed.), Solar Energy Storage, Academic Press, 2015, pp. 155–188.

[10-5] J. Jurasz, A. Beluco, F.A. Canales, The impact of complementarity on power supply reliability of small scale hybrid energy systems, Energy 161 (2018) 737–743.

[10-6]] J. Jurasz, P.B. Dabek, B. Kazmierczak, A. Kies, M. Wdowikowski, Large scale complementarity solar and wind energy sources coupled with pumped storage hydroelectricity for Lower Silesia (Poland), Energy 161 (2018) 183–192.

[10-7] A. Naeem, N. Ul Hassan, C. Yuen, S.M. Muyeen, Maximizing the economic benefits of a grid-tied microgridusing solar-wind complementarity, Energies 12 (3) (2019) 395.

[10-8] Y. Liu, C. Yuen, N. Ul Hassan, S. Huang, R. Yu, S. Xie, Electricity cost minimization for a microgridwith distributed energy resource under different information availability, IEEE Trans. Ind. Electron. 62 (4) (2015) 2571–2583.

[10-9] W. Tushar, C. Yuen, H. Mohsenian-Rad, T. Saha, H.V. Poor, H.L. Wood, Transforming energy networks via peer-to-peer energy trading: the potential of game-theoretic approaches, IEEE Signal Process. Mag. 35 (4) (2018) 90–111.

11. PONDERADORES DE DISTÂNCIA PARA PARÂMETROS DE COMPLEMENTARIDADE ESPACIAL ENTRE RECURSOS ENERGÉTICOS RENOVÁVEIS NO ESTADO DO RIO GRANDE DO SUL

11.1 Apresentação

Este capítulo, apresenta o artigo *"Ponderadores de Distância para Parâmetros de Complementaridade Espacial entre Recursos Energéticos Renováveis no Estado do Rio Grande Do Sul"*, aceito para publicar no *Anuário do Instituto de Geociências (2019).* Editor: Instituto de Geociências da Universidade Federal do Rio de Janeiro. Autores: Alfonso Risso; Mariana Tosi Corrêa; Alexandre Beluco e Rita de Cássia Marques Alves.

Resumo

Sistemas híbridos de energia têm custos iniciais mais altos do que os sistemas baseados em apenas um recurso renovável, no entanto, apresentam melhor desempenho e um menor custo para a energia fornecida aos consumidores. A possível complementaridade entre os recursos energéticos utilizados pode contribuir para um melhor aproveitamento da energia disponível. Em larga escala, a complementaridade entre usinas de conversão de energia pode servir como ferramenta para a gestão de recursos energéticos. A complementaridade energética pode se manifestar entre recursos ou usinas em um mesmo local e/ou entre locais diferentes. Este trabalho faz o uso do estabelecimento de rede de células hexagonais e da elaboração de rosas de complementaridade para quantificar a complementaridade espacial no tempo, expressando seu resultado através de mapas. Essa técnica é aplicada para usinas hidrelétricas e parques eólicos no Estado do Rio Grande do Sul, no sul do Brasil, e apresenta, como resultado, seu mapa de complementaridade espacial no tempo. Entre os resultados, a complementaridade espacial no tempo entre as centrais hidrelétricas situadas na fronteira norte do Estado do Rio Grande do Sul e os parques eólicos que se encontram na costa leste apresentaram máxima complementaridade. Também são avaliados ponderadores capazes de descrever o grau de decaimento da complementaridade em relação à distância, como forma de estimar a área na qual a os efeitos de complementaridade energética podem ser aproveitados de modo mais eficaz.

Palavras-chave: Geoprocessamento; Complementaridade; Energia

Abstract

Hybrid energy systems have higher start-up costs than systems based on just one renewable

resource, however, they deliver better performance and a lower cost for energy supplied to consumers. The possible complementarity between the energy resources used can contribute to a better use of the available energy. On a large scale, complementarity between power conversion plants can serve as a tool for the management of energy resources. Energy complementarity can be verified between resources or plants in the same place and - or between different sites. This work makes use of the hexagonal cell network establishment and the elaboration of complementary roses to quantify the spatial complementarity in time, expressing its result through maps. This technique is applied to hydroelectric plants and wind farms in the state of Rio Grande do Sul, southern Brazil, and presents, as a result, its spatial complementarity map in time. Among the results, the spatial complementarity in time between the hydroelectric power plants located on the northern border of the state of Rio Grande do Sul and the wind farms on the east coast showed maximum complementarity. Weights are also evaluated capable of describing the degree of decay of the complementarity with respect to the distance, as a way of estimating the area in which the effects of energy complementarity can be used more effectively.
Keywords: Geoprocessing; Complementarity; Energy

11.2 Introdução

Com a crescente demanda por energia em todo o mundo, estimula-se cada vez mais o uso e desenvolvimento de energias que produzam o menor impacto ambiental possível. Acordos de redução da emissão de gases de efeito estufa vêm mudando o cenário energético mundial, incentivando o interesse em encontrar maneiras de assegurar o fornecimento de energia de forma sustentável.

Embora o desempenho técnico de recursos renováveis possa ser equiparado aos meios mais hegemônicos de obtenção de energia, ainda há ressalvas quanto a sua aprovação, dada a necessidade de se levar em consideração uma maior quantidade de variáveis durante os processos de implantação e geração de energia nos mais diversos tipos de aproveitamentos para conversão de energia.

Segundo Beluco (2003) [11-2], “a palavra complementaridade pode ser interpretada como capacidade para servir de complemento. A expressão complementaridade energética refere-se então à capacidade de uma ou mais fontes apresentarem disponibilidades energéticas complementares no tempo, no espaço ou em ambos. A complementaridade no espaço pode existir quando as disponibilidades energéticas de uma ou mais fontes se complementam ao

longo de uma região. A complementaridade no tempo pode existir quando as disponibilidades apresentam períodos que se complementam ao longo do tempo em uma mesma região. ”

Para ambos os casos, a complementaridade só será completa se abranger os componentes tempo, energia e amplitude. A complementaridade no tempo será completa quando a disponibilidade mínima ocorrer no período de defasagem de seis meses. A complementaridade energética ocorrerá quando os valores médios dos recursos energéticos comparados forem iguais. A complementaridade da amplitude ocorrerá quando as diferenças entre a disponibilidade energética máxima e mínima, para a energia comparada, forem iguais. Além disso, é necessário estabelecer se a complementaridade está sendo avaliada em um mesmo local ou em locais diferentes.

O termo “complementaridade temporal” pode ser usado para se referir a complementaridade energética entre recursos situados em um mesmo local. A Fig. 11.1 mostra dados reais de disponibilidade de energia. Os dados mais altos, à esquerda, correspondem a dados típicos da disponibilidade da água em uma seção de rio. Os dados mais baixos, à direita, correspondem à radiação solar incidente em uma superfície plana horizontal. A figura caracteriza os valores médios de energia e as amplitudes de variação para os dois recursos energéticos. A componente de complementaridade do tempo avalia a defasagem entre os valores máximos ou mínimos de disponibilidade de energia para os recursos energéticos considerados. A componente de complementaridade compara os valores médios de energia, e um máximo valor será obtido se cada recurso contribuir com metade da energia anual total. A componente de complementaridade da amplitude compara as amplitudes de variação de cada recurso energético e, como a componente de complementaridade energética, será obtido um valor máximo de complementaridade se os recursos energéticos comparados têm a mesma variação de amplitude.

A complementaridade entre recursos energéticos situados em locais diferentes pode ser denominada como "complementaridade espacial", complementando a denominação de "complementaridade temporal" discutida no parágrafo anterior, para a complementaridade entre recursos energéticos situados em um mesmo local. Essa diferenciação foi proposta no artigo de Risso et al. (2018) [11-10], um dos primeiros trabalhos dedicados ao estudo da complementaridade espacial. É importante ressaltar, entretanto que tanto a complementaridade temporal quanto a complementaridade espacial ainda terão as três componentes descritas acima: a complementaridade no tempo, a complementaridade de energia e a complementaridade entre amplitudes. Uma abordagem equivalente a essa que divide a complementaridade em três componentes foi proposta por Borba & Brito (2017) [11-5], que avaliam a complementaridade

entre dois ou mais recursos energéticos por meio de uma expressão matemática semelhante a uma convolução entre funções matemáticas.

Este artigo versa sobre a componente de complementaridade no tempo, que é diretamente associada ao tempo de defasagem entre os valores máximos e mínimos da disponibilidade de energia de dois recursos renováveis. O índice de complementaridade no tempo k_t, proposto por Beluco et al. (2008) [11-4], é definido conforme a Equação (1) e avalia o intervalo de tempo entre os valores mínimos (ou máximos) das disponibilidades de duas fontes de energia. Se esse intervalo corresponde à metade do período, o índice resultará na unidade. Se corresponder à zero, ou seja, se os valores mínimos coincidirem no tempo, o índice resultará nulo. Os valores intermediários guardam uma relação linear entre si.

$$k_t = \frac{|d_h - d_e|}{|D_h - d_h||D_e - d_e|} \quad (1)$$

Nessa equação, D_h é o dia (ou mês) correspondente ao valor máximo de disponibilidade hídrica, d_h é o dia (ou mês) correspondente ao valor mínimo de disponibilidade hídrica, D_e é o dia (ou mês) correspondente ao valor máximo de disponibilidade eólica, d_e é o dia (ou mês) correspondente ao valor mínimo de disponibilidade eólica. O denominador avalia se os recursos energéticos possuem um intervalo de 180 dias (ou seis meses) entre as disponibilidades de energia máxima e a mínima.

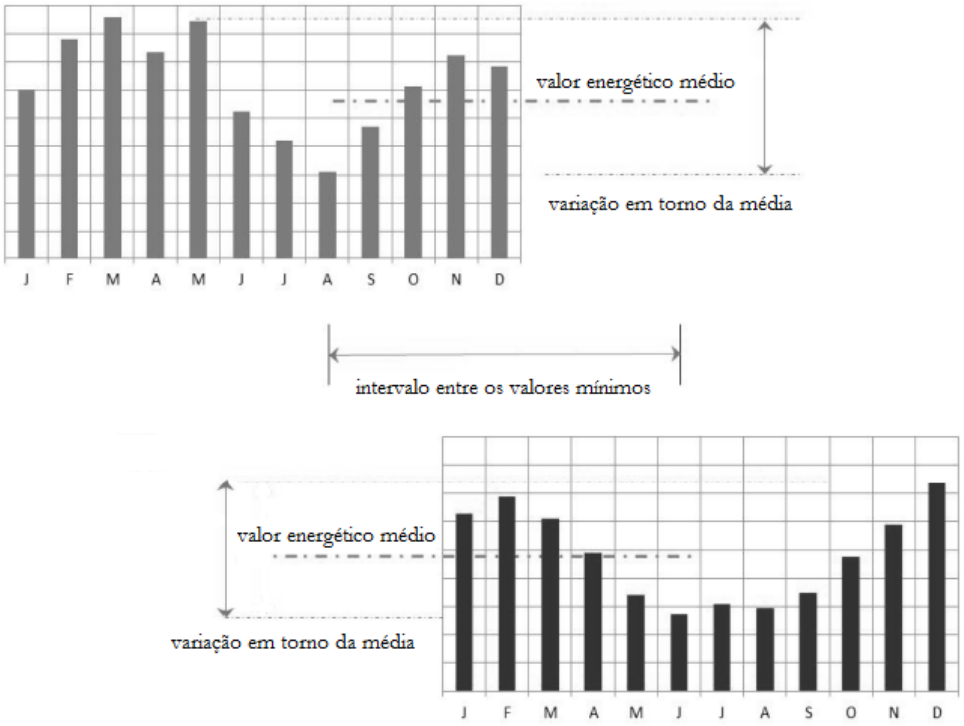

Fig. 11.1. Conjunto de dados para dois recursos renováveis (adaptado de Beluco, 2015).

O estudo da complementaridade, em suas várias formas, visa contribuir para a consolidação de uma nova ferramenta para gestores de recursos renováveis e de recursos energéticos e um modo mais amplo. O Brasil é privilegiado com uma grande disponibilidade de recursos energéticos renováveis e sua matriz energética apresenta uma crescente diversidade de suprimentos de energia, obtidos de diferentes recursos. Entretanto, o cenário persistente de crises políticas e econômicas faz com que a oferta de novos suprimentos de energia não aconteça com a celeridade necessária. O conceito de complementaridade contribui para um melhor planejamento da expansão do sistema elétrico e do aproveitamento dos recursos disponíveis.

Este artigo então é composto de cinco seções além desta introdução, que apresentou brevemente os temas a serem tratados ao longo das próximas seções. As próximas duas detalham o conceito de complementaridade espacial e o uso de rosas de complementaridade. A seção seguinte introduz o estudo de caso abordado neste artigo, centrado na complementaridade espacial entre usinas hidrelétricas e fazendas eólicas ao longo do território do Estado do Rio grande do Sul. A quinta seção discute a inserção de ponderadores de distância para uma melhor expressão da complementaridade espacial com rosas de complementaridade. A última seção reúne s resultados do trabalho e conclui o artigo.

11.3 Complementaridade espacial no tempo

Como discutido previamente, a complementaridade espacial é aquela que ocorre quando os recursos energéticos estão localizados em locais diferentes. Quando devidamente quantificado e mapeado, esse conceito pode servir como importante ferramenta para gestão de recursos energéticos. O estudo adequado da complementaridade espacial pode contribuir na minimização de custos de instalação de usinas de energia, otimizar os custos de operação para sistemas interligados, além de tornar o abastecimento energético mais equilibrado e eficiente.

Caso fosse necessário determinar a complementaridade espacial no tempo entre recursos energéticos mostrados na Fig. 11.1, eles deveriam estar, necessariamente, localizados em diferentes lugares, com distâncias e orientações distintas. Este artigo, apresentará o estudo da complementaridade no tempo e será efetuada a modelagem de uma dada região através do método da rede de células hexagonais, conforme elucidado por Risso & Beluco (2017) [11-9]. O estudo de caso será centrado na complementaridade entre usinas hidrelétricas e fazendas eólicas no Estado do Rio Grande do Sul.

A metodologia apresentada por Risso & Beluco (2017) [11-9] consiste na utilização de uma malha de hexágonos para representar uma dada região. A escolha do formato hexagonal

foi feita devido ao fato de que a distância do centro de cada hexágono é a mesma para todos hexágonos diretamente vizinhos. A energia de cada célula hexagonal será a soma dos recursos energéticos disponíveis em sua superfície.

A Fig. 11.2 mostra uma rede de células hexagonais estabelecidas em uma distribuição hipotética de usinas hidrelétricas e parques eólicos. As células azuis contêm usinas hidrelétricas, as células amarelas contêm parques eólicos. Células com ambos os tipos de recurso estão sinalizadas em cinza e células sem recursos não possuem cor.

A partir da identificação das células que apresentam recursos energéticos, é então necessário determinar a complementaridade entre elas. Três parâmetros devem ser estabelecidos: a complementaridade no tempo com as outras células da malha hexagonal que possuem centrais elétricas, as respectivas distâncias e as respectivas direções.

Para isso, a Equação (1) deve ser utilizada, sendo que as diferenças entre os valores de máxima e mínima disponibilidade energética que aparecem no denominador serão considerados com o intervalo entre eles for igual a seis meses. Desse modo, a determinação da complementaridade no tempo é simplificada.

Primeiramente, deve-se escolher uma célula que contenha algum recurso e determinar sua complementaridade com outras células que também contenham recursos, levando em consideração suas respectivas distâncias e orientação.

A Fig. 11.3 exibe modelos para determinar as rosas de complementaridade. Nessa figura, à esquerda (A), há um modelo para células contendo apenas um recurso energético. Já na figura á direita (B) há um modelo para células contendo dois ou mais recursos energéticos. As direções das linhas correspondem às posições relativas das células comparadas e seus comprimentos estão relacionados com as distâncias entre as células. A escala de cores, estabelecida pela legenda, indica os diferentes valores de complementaridade.

A Figura 4 mostra o mapa elaborado com as rosas de complementaridade determinadas para as células de distribuição hipotética de usinas proposta na Fig. 11.2. Como esperado, as linhas em uma célula sempre encontram linhas idênticas em suas complementares equivalentes. Baseado nisso, é bastante intuitiva a identificação, na Fig. 11.4, das células da rede hexagonal que possuem máxima complementaridade entre si.

Em suma, o método proposto por Risso et al. (2018) [11-10], que estabelece a complementaridade espacial no tempo a partir das rosas de complementaridade para uma dada região, pode ser apontado em 5 etapas: [1] Delimitar a região para a qual será determinada a complementaridade espacial, identificando as usinas em operação e/ou os locais com potencial energético; [2] Obter dados de energia (para usinas em operação) ou disponibilidade de energia

(para potencial energético) que será considerado na determinação da complementaridade no tempo, considerando lugares diferentes; [3] Estabelecer uma rede de células hexagonais sobre a região escolhida para a análise, identificando as células que contêm usinas em operação e/ou locais com potencial energético e registrar as distâncias entre elas; [4] Determinar a complementaridade no tempo de cada célula que contém algum recurso existente ou potencial e, ao compará-lo com as outras células que contêm algum recurso energético, observar a variação no grau de complementaridade de acordo com as distâncias; [5] Por fim, avaliar o resultado final obtido com a superposição das rosas de complementaridade nas respectivas células hexagonais e no mapa e, se necessário, sugerir alguma simplificação na representação, caso as rosas de complementaridade se tornem muito cheias e dificultem a leitura visual das informações ao longo do mapa.

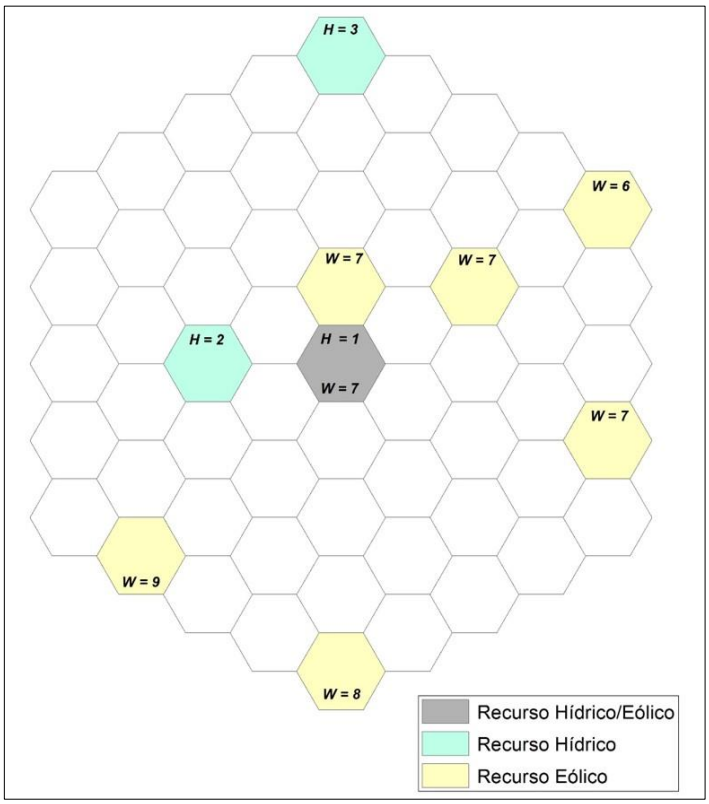

Fig. 11.2. Malha hipotética de células hexagonais com usinas hidrelétricas (H) e parques eólicos (W), com indicação dos meses do ano com menor disponibilidade energética segundo Risso *et al.*(2018) [11-10].

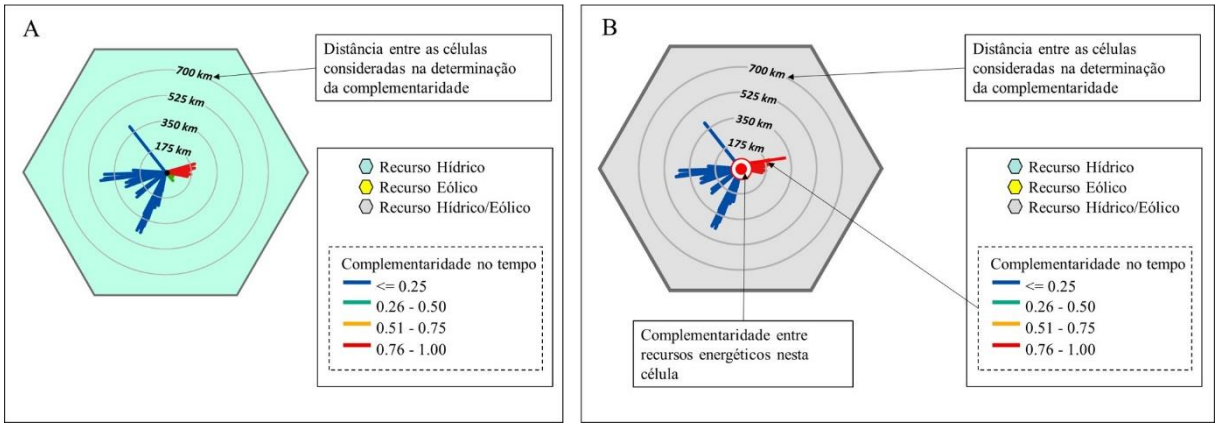

Fig. 11.3. Modelos para as rosas de complementaridade: (A) com apenas um recurso energético por célula e (B) com dois ou mais recursos por célula, segundo Risso *et al.* (2018) [11-10].

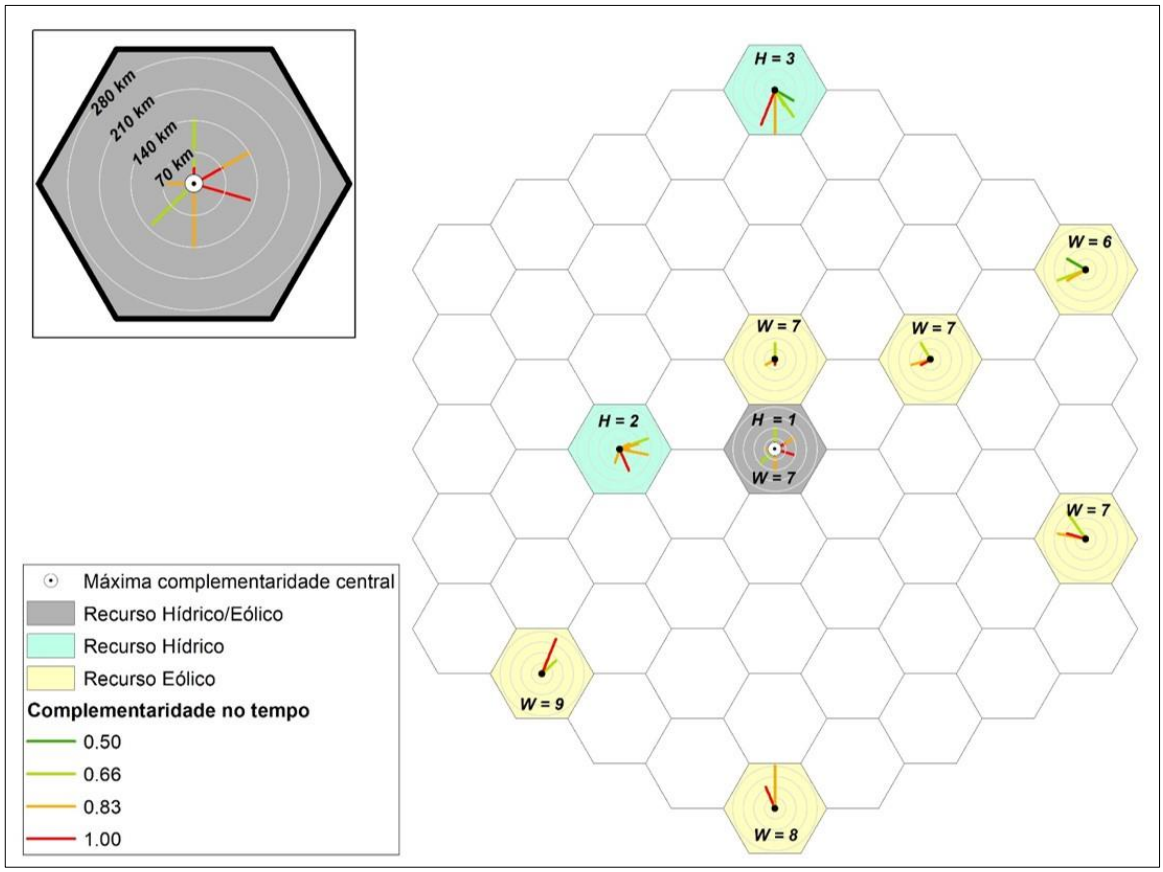

Fig. 11.4. Mapa da complementaridade espacial no tempo para a rede de células hexagonais da Figura 3, segundo Risso et al. (2018) [11-10].

11.4 Dados espaciais

Nesse artigo, três bases de dados georreferenciados contendo informações de infraestrutura, recursos hídricos e eólicos foram utilizados para implementação das ferramentas para estimativa da complementaridade espacial no tempo.

Quanto à infraestrutura nacional de geração de energia elétrica, foram utilizadas Camadas Shapefile (ESRI) disponibilizadas pelo Sistema de Informações Geográficas do Setor Elétrico (SIGEL – ANEEL) [11-11]. Os planos de informações são referentes a Aproveitamentos Hidrelétricos e Aerogeradores.

A disponibilidade de recursos hídricos superficiais para geração de energia foi identificada através de dados da base georreferenciada do International Satellite Land Surface Climatology Project (ISLSCP II) – University of New Hampshire [11-8]. Os planos de informação utilizados são pertencentes ao módulo Hidrologia e Solos ISLSCP II UNH/GRDC Composite Monthly Runoff. Esses dados de escoamento composto combinam estimativas médias mensais de escoamento de um modelo de balanço hídrico simulado, derivado de dados climáticos com descarga fluvial monitorada. Os dados possuem resolução espacial de 0,5 grau em latitude e longitude. A extensão temporal vai de 1986 a 1995. As cores e valores (1 a 12) representados na legenda associada a base de células hexagonais na Figura 5 indicam os meses de máxima e mínima disponibilidade hídrica, para posterior estimativa da complementaridade temporal.

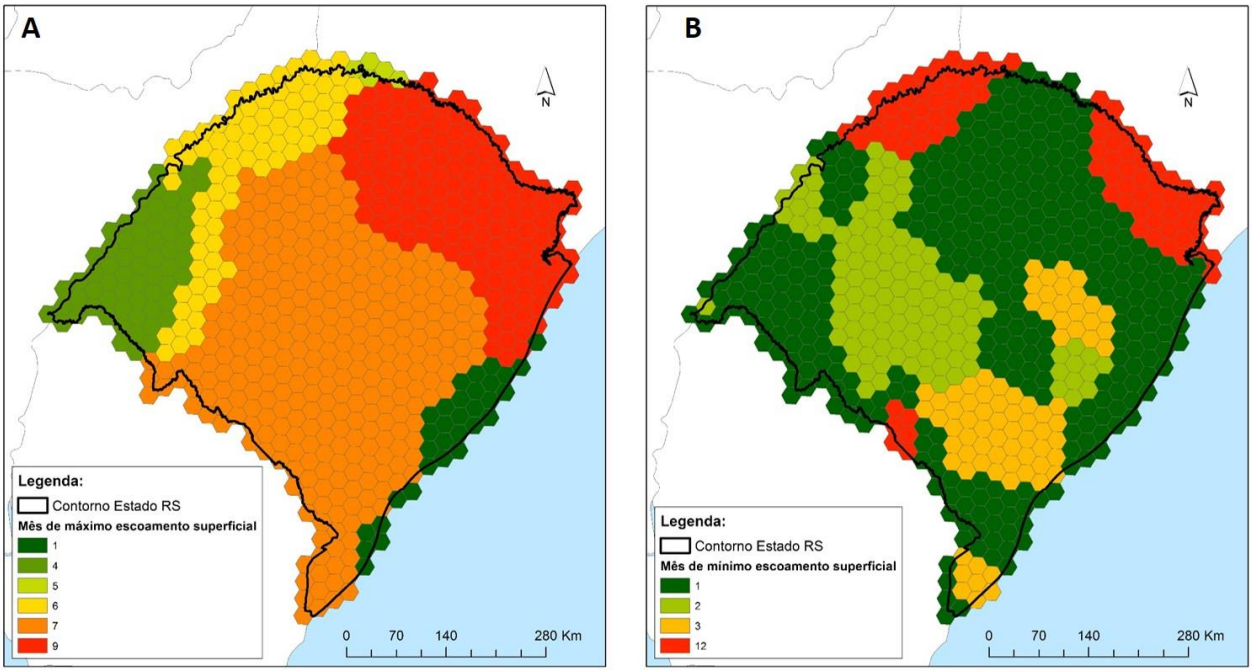

Fig. 11.5. Meses de máxima (A) e mínima (B) disponibilidade hídrica.

A disponibilidade de energia eólica foi identificada através da base de dados georreferenciados do Climatic Research Unit (University of East Anglia [11-6]), apresentados na forma de grades regulares de alta resolução. Os dados possuem resolução espacial de 10 minutos de latitude de longitude. A extensão temporal vai de 1961 a 1990. Da mesma forma que na Fig. 11.5 (disponibilidade hídrica), a Fig. 11.6 apresenta os meses de máxima e mínima disponibilidade eólica, integrados à base de células hexagonais.

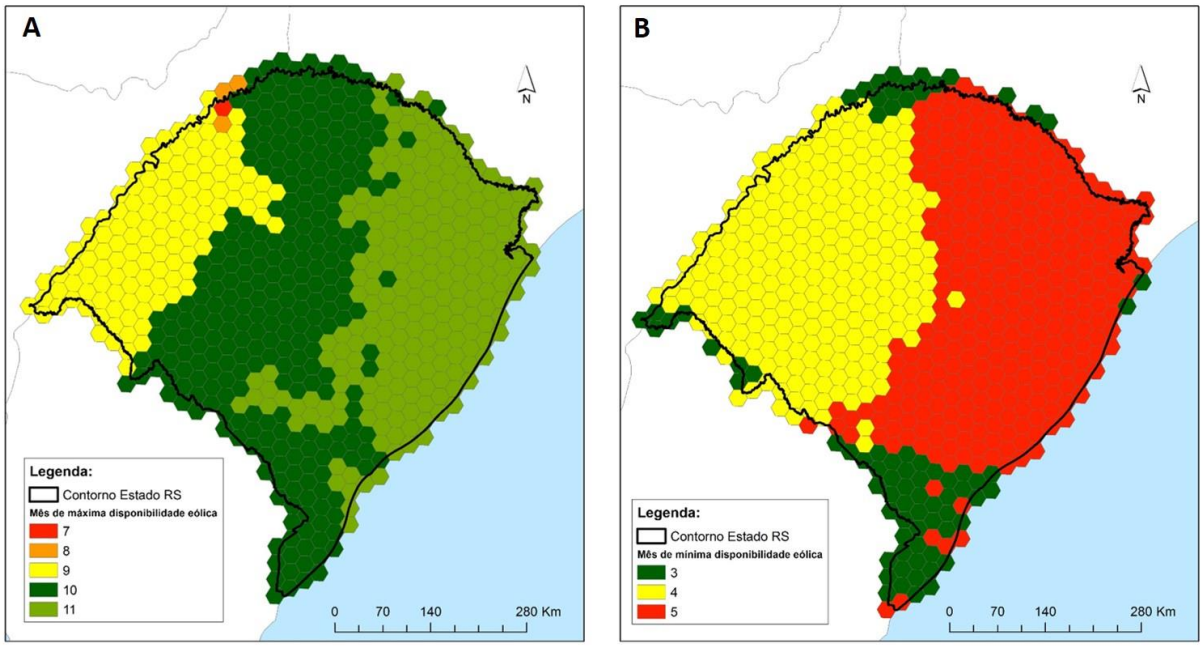

Fig. 11.6. Meses de máxima (à esquerda) e mínima (à direita) disponibilidade eólica.

11.5 Complementaridade entre usinas hidrelétricas e parques eólicos ao longo do RS

O Rio Grande do Sul é o estado mais meridional do Brasil, possui uma área de 281.737,888 km² (IBGE, 2018) e população de 11.329.605 habitantes (IBGE, 2017 [11-7]). A capacidade instalada é de 9.101,0 MW (ANEEL, 2018 [11-1]), sendo uma combinação de usinas hidrelétricas, termelétricas e parques eólicos. Inicialmente, esse trabalho visava auferir a complementaridade de todas as células que compreendem o estado, independentemente de possuírem recurso energético ou não. Os valores do índice de complementaridade, calculados conforme a Equação (1), distância e direção de cada célula podem ser visualizados na Fig. 11.7.

A Fig. 11.8 mostra o cálculo da direção da complementaridade, obtido através do azimute do alinhamento. O elevado número de atributos, próximo a 400.000, tornou as operações bastante penosas de serem feitas, demandando considerável tempo. Em vista disso,

foi necessário diminuir o número de células que seriam empregadas no cálculo da complementaridade. Optou-se, assim, por utilizar apenas as células que contêm recursos energéticos, tanto hídricos como eólicos. A Fig. 11.9 mostra o Estado do Rio Grande do Sul e a rede de 632 células hexagonais que foi estabelecida para este estudo. Cada célula hexagonal possui 500 km². Foram identificados 399 aproveitamentos hidrelétricos, marcados em pontos azuis, inseridos em 136 células representadas pela cor azul. Os pontos vermelhos representam os 186 parques eólicos encontrados, inseridos em 41 células de cor amarela.

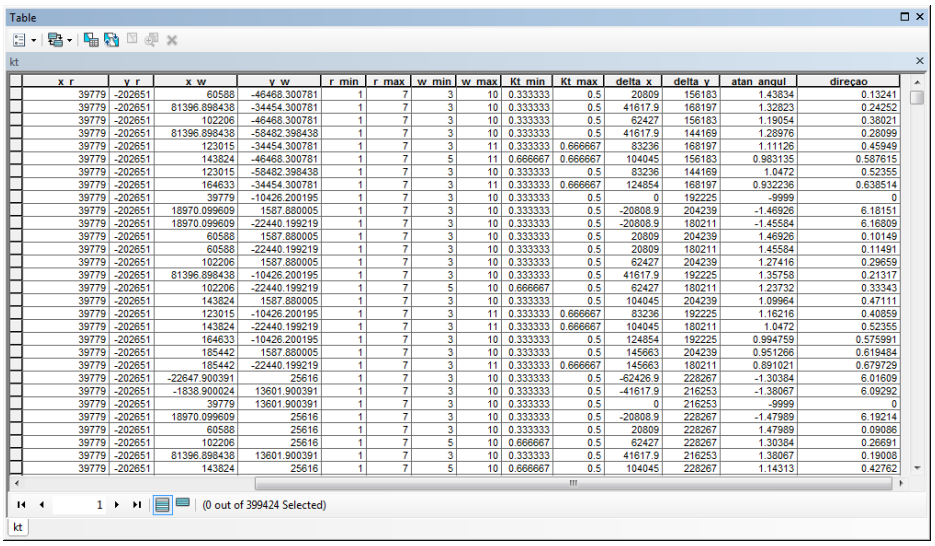

Fig. 11.7. Tabela de atributos com os índices de complementaridade da malha que compreende o Estado do Rio Grande do Sul.

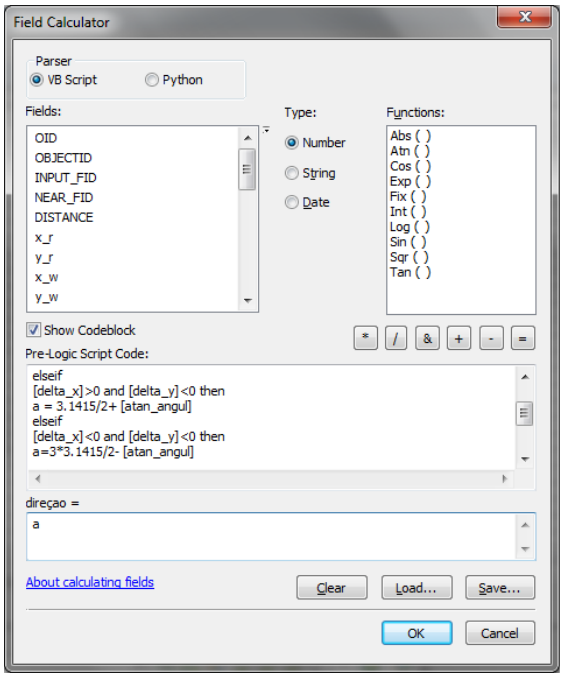

Fig. 11.8. Operação condicional para o cálculo da direção da complementaridade.

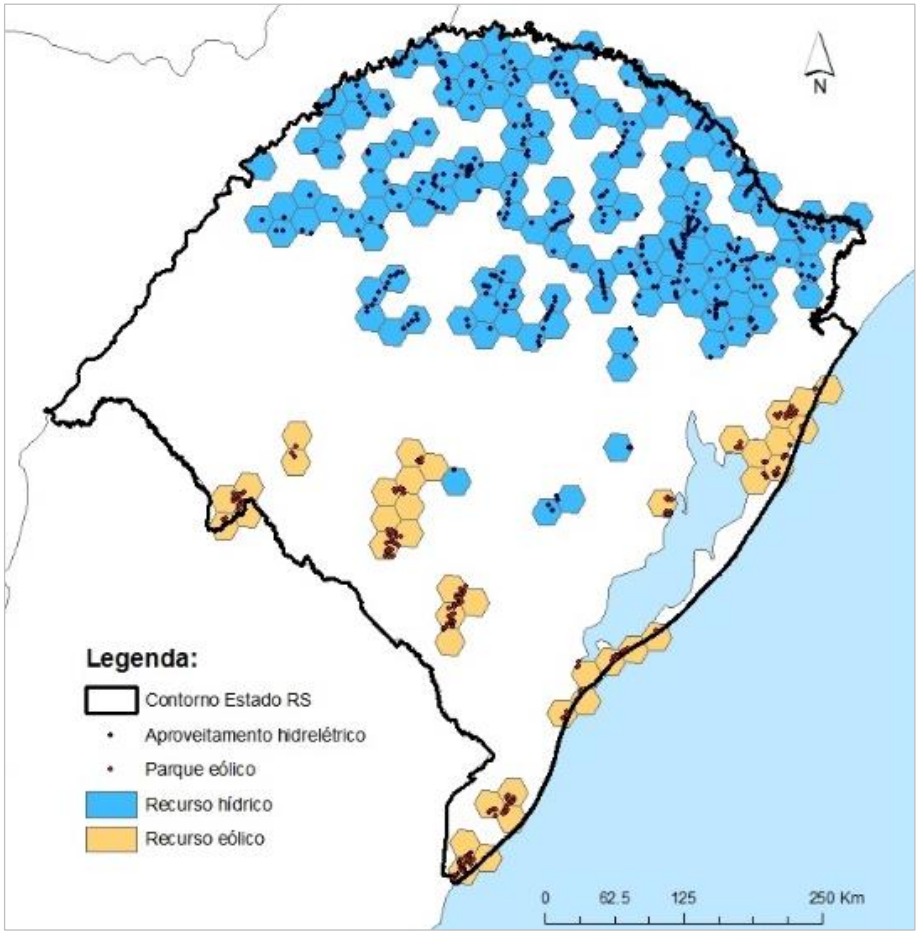

Fig. 11.9. Rede de células hexagonais, indicando aproveitamentos hidrelétricos e parques eólicos no Estado do Rio Grande do Sul.

O norte do estado apresenta maior desnível topográfico, além de possuir uma rede de drenagem mais densa e caudalosa, o que justifica o elevado número de hidrelétricas nessa área. A região mais ao sul do estado possui maior potencial eólico e, portanto, concentram-se ali a maior parte de parques eólicos. Os mapas indicando as complementaridades máximas e mínimas no tempo, são mostrados nas Fig. **11.10** e 11.11. Ao analisar a complementaridade máxima para as células de recursos hídricos, as linhas vermelhas - indicativas de complementaridade máxima - estão presentes próximas à divisa norte do estado. Suas células complementares correspondentes, ou seja, células que contém parques eólicos, situam-se na costa leste, além de poucas células ao sul do estado. A complementaridade mínima é verificada nas mesmas localidades da complementaridade máxima, sendo incluídas algumas células contendo recursos hídricos ao norte do Rio Grande do Sul e células contendo recursos eólicos ao sudeste do estado.

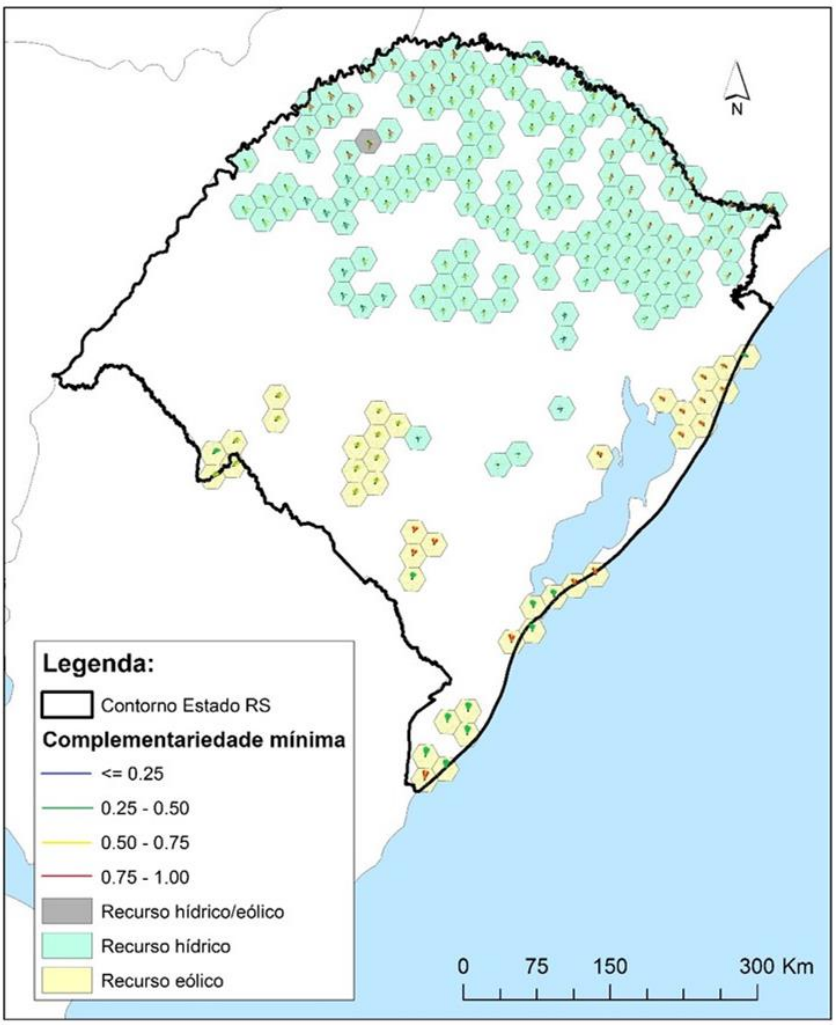

Fig. 11.10. Mapa com as rosas de complementaridade mínima.

Como já era esperado, as células nas extremidades da região estudada exibem linhas de complementaridade, chamadas de pétalas, de comprimentos mais longos. Da mesma forma, as células centrais apresentam pétalas de comprimento intermediário. Ademais, grandes variações na intensidade da complementaridade são justificadas pelo fato de que os recursos analisados tendem a apresentar regimes intermitentes.

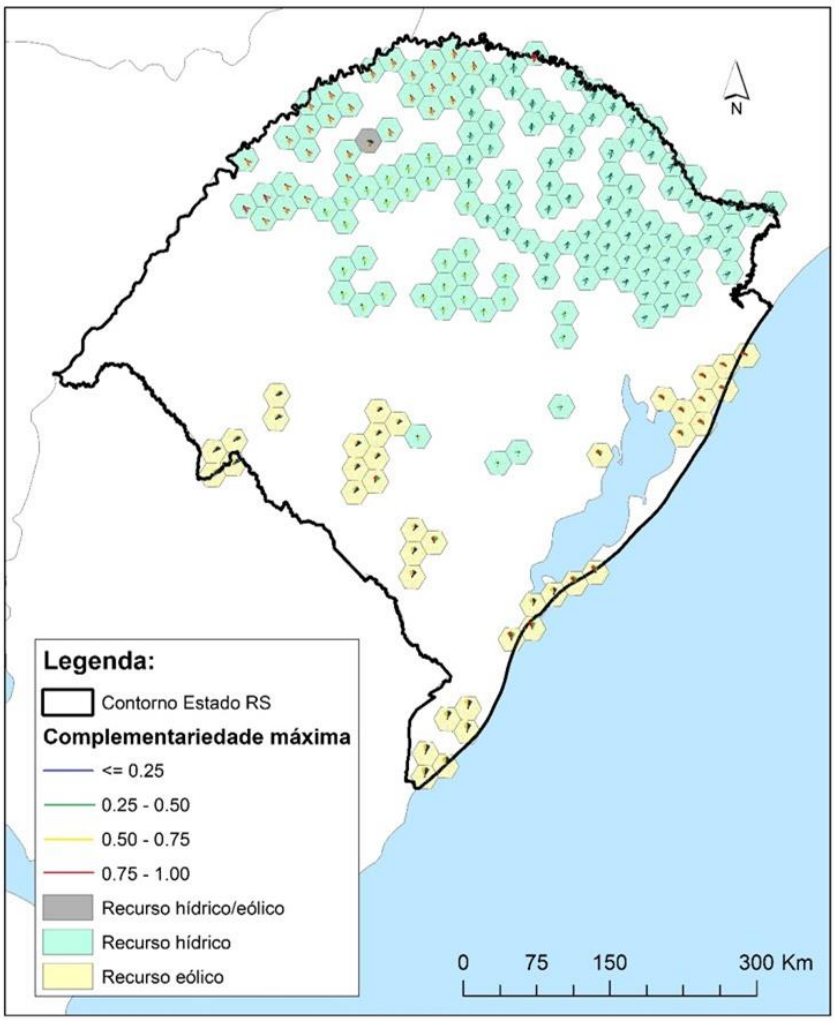

Fig. 11.11. Mapa com as rosas de complementaridade máxima.

A Fig. 11.12 mostra em detalhe a parte central do mapa de complementaridade mínima (Fig. 11.10). Por possuir uma escala maior, permite uma melhor observação das rosas de complementaridade. A célula que aparece em detalhe no canto superior direito, contendo recursos hídricos, apresenta pétalas de máxima complementaridade com distâncias na ordem de 400 a 700 km. Suas complementaridades correspondentes estão nas células eólicas localizadas na costa leste e no extremo sul do estado. Complementaridades intermediárias com parques eólicos ao sul e sudoeste completam as pétalas dessa rosa de complementaridade.

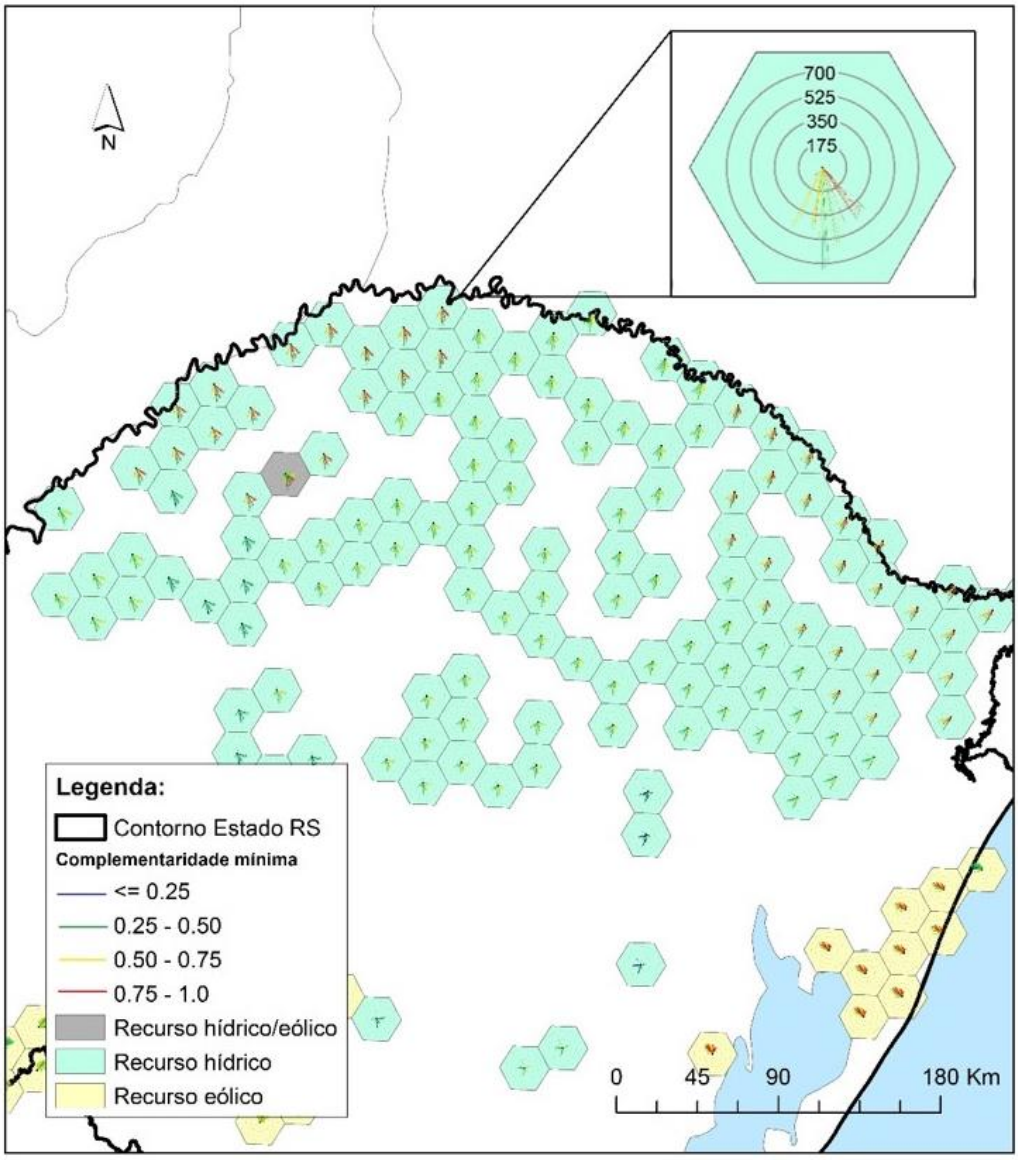

Fig. 11.12. Detalhe da região central do mapa mostrado na Fig. 11.10.

11.6 Ponderadores de distância

Através da interpolação, é possível estimar valores de pontos desconhecidos através de valores de pontos conhecidos. De posse das distâncias máxima e mínima referentes ao cálculo da complementaridade, é aproximada uma função que seja capaz de descrever o comportamento das variáveis analisadas. O coeficiente de ponderação, obtido através da função de aproximação, controla como o efeito da complementaridade será atenuado a medida que a distância a partir do ponto conhecido aumenta.

As Figuras Fig**. 11.13** e Fig**. 11.14** apresentam funções linear e polinomial, respectivamente, que melhor descrevem o grau de decaimento da complementaridade em relação à distância. A Fig. 11.15 mostra as rosas de complementaridade aplicadas para as

funções linear e polinomial, respectivamente. Como era esperado, o grau de complementaridade máxima diminui para ambos os casos, quando relacionados com a distância, já que se trata de funções de decaimento.

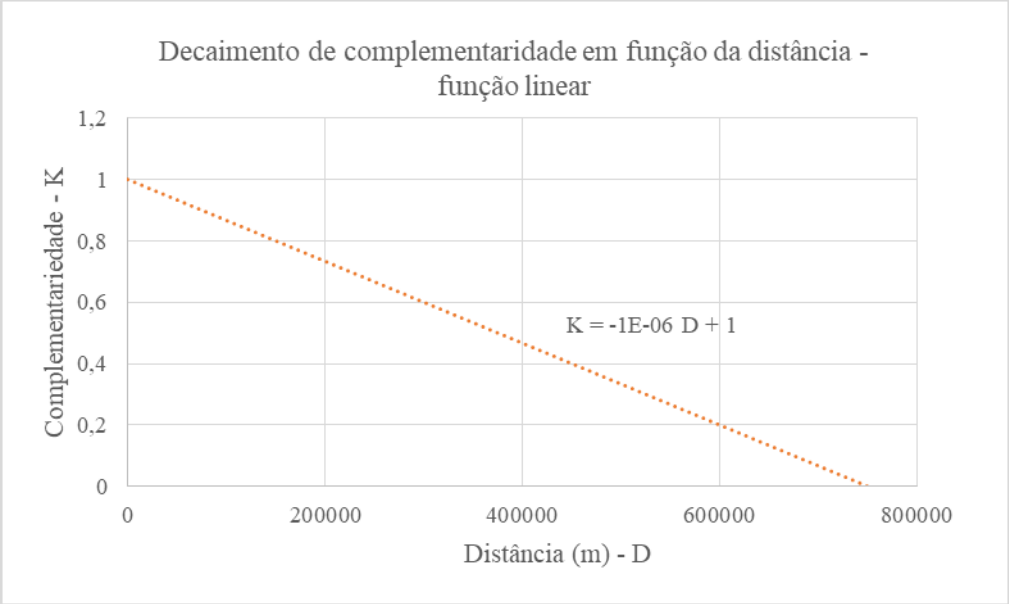

Fig. 11.13. Função linear que descreve o decaimento da complementaridade.

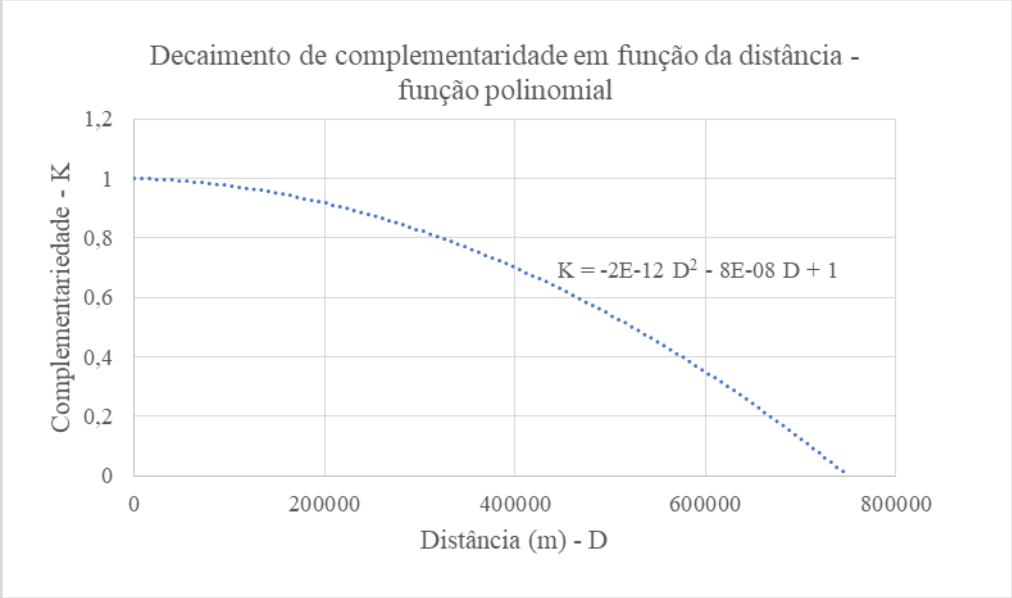

Fig. 11.14. Função polinomial que descreve o decaimento da complementaridade.

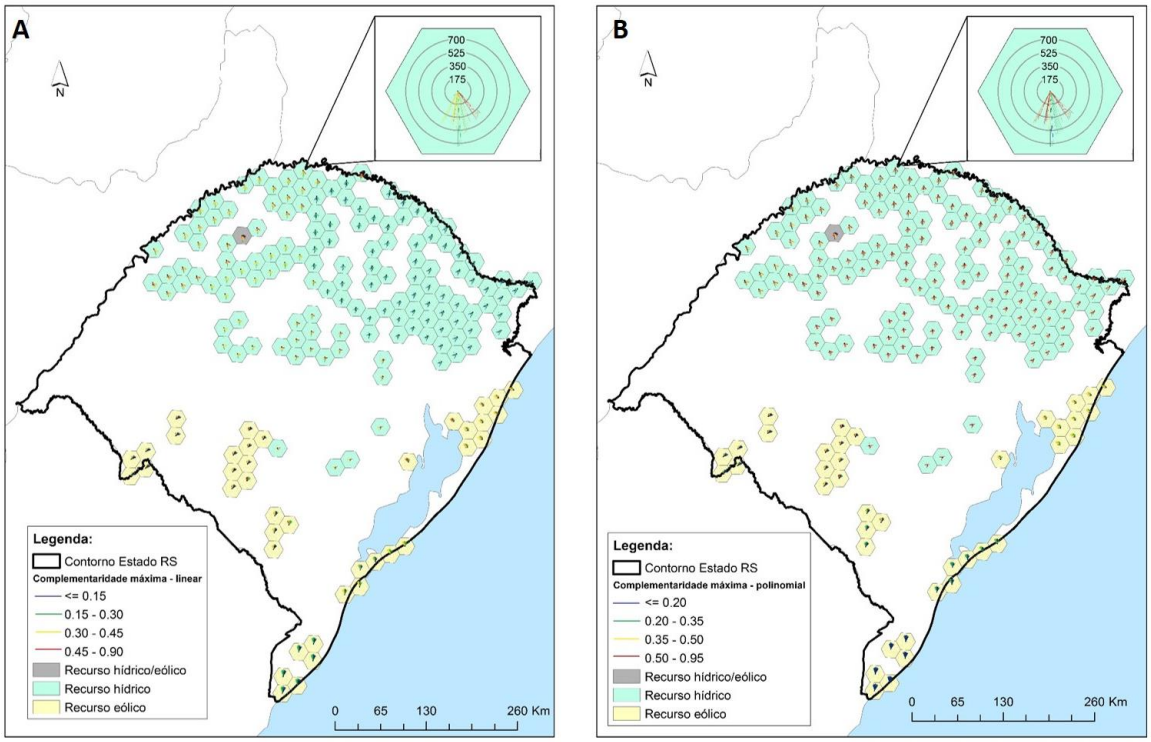

Fig. 11.15. Ponderadores de distância linear (A), e polinomial (B).

Seu estudo faz-se importante quando avaliado juntamente com outro componente da complementaridade espacial, a saber, a complementaridade de energia. A partir de funções ponderadoras, dados de carga energética envolvida e fatores de dimensionamento de redes elétricas, torna-se possível o mapeamento dos locais com maior potencial energético em uma dada região.

11.7 Conclusões

O presente artigo discutiu o conceito de complementaridade e contribuiu para o melhor entendimento de complementaridade espacial, utilizando um método que expressa a complementaridade espacial no tempo através de mapas. O método proposto baseia-se na determinação de rosas de complementaridade, cujas pétalas tem comprimento determinado pela distância com a célula complementar, orientação de acordo com a direção da complementaridade e cor indicando o grau de complementaridade entre as células.

A região escolhida para exemplificação do método foi o Estado do Rio Grande do Sul, no Brasil. Após a coleta de dados de centrais hidrelétricas e parques eólicos, foi possível estimar a complementaridade espacial no tempo entre recursos hídricos e eólicos. Como resultado principal, verificou-se que a complementaridade espacial no tempo atinge valor máximo entre

as centrais hidrelétricas situadas na fronteira norte do estado e os parques eólicos que se encontram na costa leste.

A possibilidade de expressar a complementaridade espacial no tempo através de mapas abre caminho para uma melhor utilização do conceito de complementaridade como ferramenta para a gestão das energias renováveis e para critérios de escolha na priorização de projetos de geração de energia. Um maior conhecimento da utilidade do método proposto virá com a sua aplicação a outros estudos de caso que abranjam a determinação das demais componentes da complementaridade, além da complementaridade no tempo.

A viabilidade de aplicação de ponderadores de distância na análise permite escolher funções matemáticas que melhor representem o grau de decaimento da complementaridade em função da distância. Sua utilidade, quando atrelada a complementaridade de energia, permite a avaliação e identificação de locais que possuam melhor desempenho energético a ponto de serem capazes de atenuar os impactos ambientais causados por tais empreendimentos.

11.8 Agradecimentos

Os autores agradecem o apoio de suas respectivas instituições ao trabalho de pesquisa desenvolvido na párea de energias renováveis e de geoprocessamento e que culminou entre outras coisas, na elaboração deste artigo. O terceiro autor agradece o apoio do CNPq ao seu trabalho como pesquisador (processo n. 312941/2017-0).

11.9 Referências

[11-1] ANEEL, 2018. Agência Nacional de Energia Elétrica. Disponível em: <http://www2.aneel. gov.br/aplicacoes/ResumoEstadual/ResumoEstadual.cfm>. Acesso em: 10. nov. 2018.

[11-2] Beluco, A.; Souza, P.K. & Krenzinger, A. 2003. A complementariedade no tempo entre as energias hidrelétricas e fotovoltaica. *Revista Brasileira de Recursos Hídricos, 8*(1): 99-109.

[11-3] Beluco, A. 2015. A concept of boundary of performance for analysis of hybrid systems based on complementary energy resources. *In:* Prasad, R.; Shivakumar, B.G. & Sharma, U.C. (org.). *Energy Science and Technology Series, vol.12: Energy Management,* Studium Press, p.459–483.

[11-4] Beluco, A.; Souza, P.K. & Krenzinger, A. 2008. A dimensionless index evaluating the time complementarity between solar and hydraulic energies. *Renewable Energy, 33*: 2157–2165.

[11-5] Borba, E.M. & Brito, R.M. 2017. An index assessing the energetic complementarity in time between more than two energy resources. *Energy and Power Engineering, 9*(9): 505-514.

[11-6] CRU, 2018. Climatic Research Unit, da Universidade de East Anglia. Disponível em: <https://crudata.uea.ac.uk/cru/data/hrg/>. Acesso em: 18. set. 2018.

[11-7] IBGE, 2018. Instituto Brasileiro de Geografia e Estatística. Disponível em: <https://cidades. ibge.gov.br/brasil/rs/panorama>. Acesso em: 10 nov. 2018.

[11-8] ISLSCP II, 2018. International Satellite Land Surface Climatology Project, da Universidade de New Hampshire. Disponível em: <https://daac.ornl.gov/ISLSCP_II/guides/comp_ runoff_monthly_xdeg.html>. Acesso em: 18. set. 2018.

[11-9] Risso, A. & Beluco, A. 2017. Bases for a methodology assessing spatial complementarity in time. *Energy and Power Engineering, 9*: 527–540.

[11-10] Risso, A.; Beluco, A. & Alves, R.C.M. 2018. Complementarity roses evaluating spatial complementarity in time between energy resources. *Energies, 11*(7): 1918.

[11-11] SIGEL-ANNEL, 2018. Sistema de Informações Geográficas do Setor Elétrico, da Agência Nacional de Energia Elétrica. Disponível em: <https://sigel.aneel.gov.br/Down/>. Acesso em: 18. set. 2018.

12. UM SISTEMA HÍBRIDO FOTOVOLTÁICO-EÓLICO-HÍDRICO COM CAPACIDADE DE ARMAZENAMENTO POR BOMBEAMENTO INSTALADO EM LINHA SETE, APARADOS DA SERRA, SUL DO BRASIL

12.1 Apresentação

Este capítulo, apresenta o trabalho *"A PV Wind Hydro Hybrid System with Pumped Storage Capacity Installed in Linha Sete, Aparados da Serra, Southern Brazil"*, capítulo 10 do livro *"Modeling and Dynamic Behaviour of Hydropower Plants"* publicado em 2016 pelo *"The Institution of Engeneering and Technology"*, tendo como autores Alfonso Risso, Fausto A. Canales, Alexandre Beluco e Elton G. Rossini.

Abstract

The intermittency and variability of various renewable energy resources, such as wind power and photovoltaic solar energy, can be overcome with the use of these resources in conjunction with energy storage devices. The energy storage as hydraulic power, so before energy conversion, can guarantee high efficiency to the storage process. This study aims to identify the technical and economic feasibility of using wind power and PV modules in conjunction with a reversible hydroelectric power plant installed in Aparados da Serra, in the south of the Serra Geral, a geological structure in southern Brazil that allows topographical height differences of approximately 600 meters. In this work, specifically, a hydro power plant installed at Linha Sete with 610 kW and 400 meters height. This study explores the feasibility of this pumped storage plant operating in conjunction with existing wind turbines and PV modules installed on the surface of reservoirs. The work is based on simulations and optimization performed with well-known software Homer. The results indicate that a group of 10 to 502 MW wind turbines may have capacity factor increased from usual 0.34 to values between 0.50 and 0.60. The results also relate the power capacity and costs per kW installed for PV modules to be feasible. This work also indicates useful conclusions in the design process and implementation of the hybrid system under study.

Keywords

Wind energy, wind diesel hybrid systems, Weibull shape parameter, southern Brazil, computational simulation, software Homer.

12.2 Introduction

Brazil is blessed with one of the largest water resource systems and one of the largest hydroelectric potential in the world. Thus, Brazil has in its territory some of the largest hydroelectric power plants and a lot of water reservoirs with large bodies of water artificially formed. As a result, Brazil is one of the few countries worldwide that have an energy system which is largely based on hydropower. As it is a non-intermittent source of energy, a wide base made with hydropower favors the use of renewables.

The current time of crisis in the global scenario, for various reasons, contributes to the increasing encouragement of the use of renewable energy. Among the different alternatives, recent years have seen a considerable increase in the use of wind turbines and photovoltaic modules. Both for wind energy and photovoltaics, as for other alternatives for power generation, a greater number of new plants will result in higher production of equipment and a trend of reduction in installation costs as well as in operation and maintenance costs.

In this scenario, it is almost obvious consider installing photovoltaic modules on the water surface of reservoirs formed by hydroelectric plants. The PV modules will not shadow useful areas and, covering the surface flooded by the reservoirs, they will contribute to the reduction of water loss by evaporation. Thus, it will be possible to generate photovoltaic energy and to have a larger amount of water to hydroelectric power generation. The panels can be installed on floating structures modulated with a given power, possibly produced in series.

The association between hydroelectric power plants and photovoltaic power plants might seem strange in the past when photovoltaic plants with reasonable values of power did not exist. But hydropower is "constant" and “more available” while photovoltaics is "intermittent" by weather issues and "less available" by its own characteristics. It is precisely the constancy of hydroelectric power plants (and notoriously large hydropower with large storage capacity) that enables greater investment in photovoltaic farms.

A prime example is the hydroelectric power plant in Longyangxia Dam, on the Yellow River, in northwest China. The hydro power plant was installed in 1992, with 1,280 MW of installed capacity and four machines with 320 MW each. A few years ago a project for a PV hydro hybrid system was started culminating in the installation of 320 MW in 2013, a first phase covering 9 km^2, and a further 530 MW in 2015, covering another 15 km^2. The PV hydro hybrid system and the photovoltaic power plant now constitute the world's largest.

The design operation of photovoltaic hydro hybrid systems of this kind can also be decisively influenced by the possible energetic complementarity between hydro and solar energy availability.[12-1], [12-2] and [12-3]. The greater availability of solar energy can occur in periods of low water availability as well as less availability of solar energy can coincide with increased water availability. The use of stored water in the reservoir can be managed in order to increase this effect of energetic complementary.

This chapter presents a feasibility study for implementation of a pumped storage hydroelectric power plant (or reversible hydroelectric power plant) operating with wind turbines and photovoltaic modules. The study is based on results obtained with the well-known software Homer. The next section describes the reversible power plant planned at a place called “Linha Sete”, in southern Brazil, and also describes how this plant will be simulated with Homer. Subsequent sections describe the components of the hybrid system under study, the results and discussions and finally the conclusions.

This chapter presents the results of an exploratory study related to a study of the operation of a pumped storage plant with a set of wind turbines in operation in southern Brazil, in the city of Osório, in a place with wind potential known and currently being explored. The project that resulted in this chapter have also resulted in a paper [12-4] reporting conclusions already obtained on the operation of this pumped storage plant.

12.3 The Linha Sete pumped storage power plant

The hydraulic system considered in this work was identified in an earlier work of the research group [12-5]. It is a set of areas and storage volumes that allow the implementation of two reservoirs in a region in southern Brazil where there are strong topographical height differences. Fig. 12.1 shows the upper and lower reservoirs and their watersheds. The content of Fig. 12.1 was prepared from a region that appears on Google Maps and is located according to Ref. [12-6].

Fig. 12.1. Upper and lower reservoirs in “Linha Sete” and their watersheds.

The reservoirs have been sized for a storage volume of 1,510,000 cubic meters. The lower reservoir has a maximum quota at 290 meters and the upper reservoir at 840 meters. The total height is 655 meters, whereas the machine room is placed 105 meters below the maximum level of the lower reservoir. Simulations have limited accuracy, since the variations in height resulting from operation of the pumped storage system are not simulated by Homer, as discussed below and presented by Canales and Beluco [12-7].

The natural flow available to the lower reservoir was determined by Canales et al. [12-4] and is equal to 0.539 m3/s. This flow will be available for generation in addition to the flow rates obtained with the management of reversible plant, starting from the moment that the lower reservoir is full. Based on the Tennant method describer by Benetti et al. [12-8], 10% of the

annual average flow was adopted as residual flow. Fig. 12.2 shows the stream flow rate available to turbine each month, already considering the residual flow.

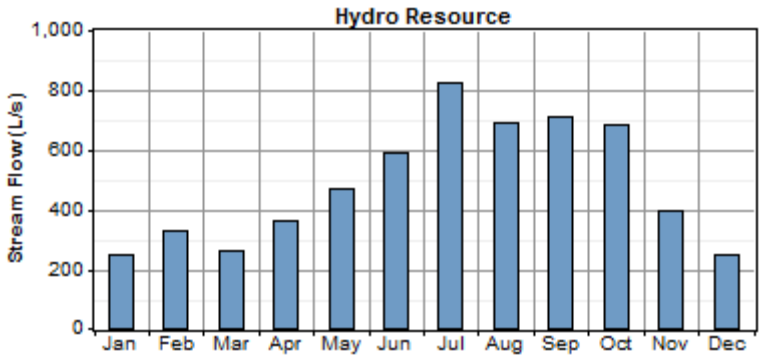

Fig. 12.2. Monthly average stream flow rate available to the turbine at power house, already considering the residual flow.

12.4 Components of the PV Wind Hydro hybrid system

The hybrid system will consist of the pumped storage hydro power plant described in the previous section, operating in conjunction with wind turbines and photovoltaic modules with diesel generators support. The operation of the pumped hydro and wind turbines has been the subject of a recent article [12-4] pointing that the operation of the two reservoirs, even demanding higher initial costs, leads to lower environmental impacts.

Wind farms in Osório, in southern Brazil, were considered in this study. The three wind farms contain 75 turbines model Enercon E-70 E4, providing a total power of 75 MW operated at a capacity factor of about 34%. Based on Braciani [12-9], the average cost per installed kilowatt in wind farms in Brazil is around USD$ 2,156.50/kW. By using this value, the initial cost of each E-70 turbine was set at USD$ 4,313,000 in Homer.

Fig. 12.3 shows the wind data used for simulations with Homer. The monthly average wind speed in Osório at 100m above ground was extracted from Silva [12-10]. These data were used to obtain a synthetic series of hourly wind speed data to the operation site of the wind turbines of the wind parks at Osório. Fig. 12.3 shows two graphs. At first, the average wind speed for each month, the deviations around these averages and maximum and minimum values are shown. This graph shows the typical variability of the wind. The second graph, with strong variation in color, enhances the variability of the wind over days and months.

The photovoltaic modules will be installed on floating structures, as recently proposed by Ferrer-Gisbert et al. [12-11] and Redon-Santafé et al. [12-12]. The basic model for the floating structure considered in this study has dimensions suitable for 50 kW of PV modules. The total area of the water surfaces formed with the two dams is small but sufficient for several tens of structures having these dimensions. Fig. 12.4 shows the incident solar radiation data used in the simulations and obtained automatically by Homer in a NASA database.

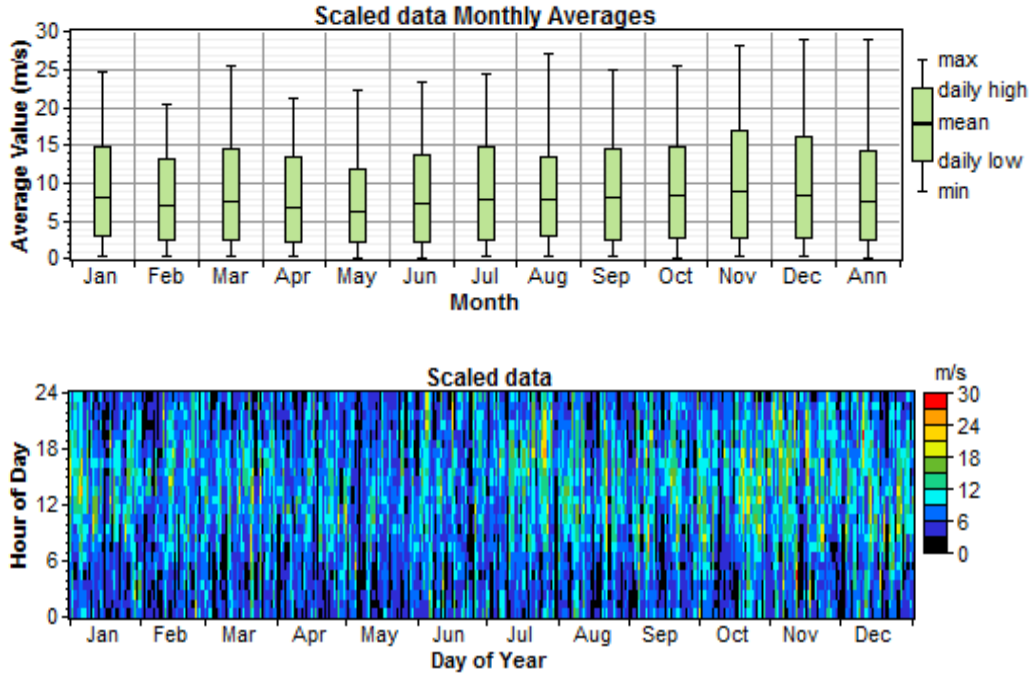

Fig. 12.3. Wind resource input for the case study.

Fig. 12.4 also shows two graphs. At first, the average incident solar radiation on a horizontal plane for each month, the deviations around these averages and maximum and minimum values are shown. The maximum insolation occurs in January, while the minimum occurs in June. In the second graph, it is evident the variation of sunlight available throughout the hours of the day, with the lowest values available in the first and the last hour of the day, and the available peak near midday. Also evident is the change in hours of the day throughout the year.

The cost of the PV modules was considered as USD$ 4,380 per kW and it is compatible with usual costs found for example by Feldman et al. [12-13]. The installation of floating structures, as suggested by Ferrer-Gisbert et al [12-11] and Redon-Santafé et al.[12-12], raise the cost by 30%. The lifetime of the PV system is considered to be 12.5 years, the replacement cost of the PV system at the end of the useful life is 80% of the initial cost and annual cost of

operation and maintenance is 5% of the installation cost. The reflectance of the water surface was considered to be 10% at the installation site. Fig. 12.5 shows parameters of the PV modules.

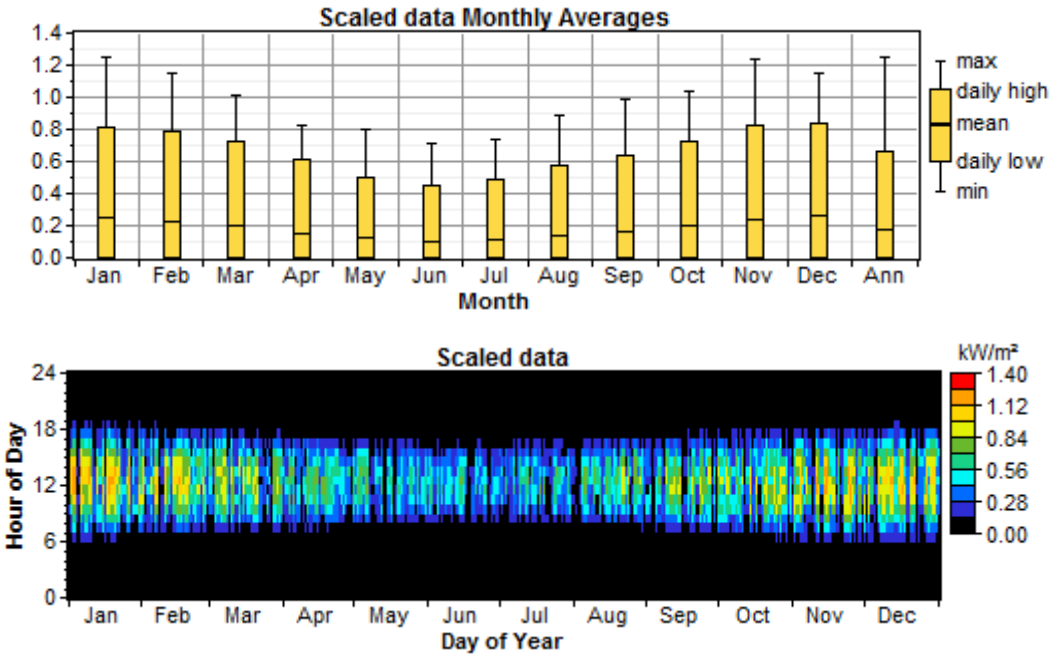

Fig. 12.4. Incident solar radiation on a horizontal plane for the reservoirs location, obtained with software Homer, considered in this study.

Diesel generator sets were considered as support in the simulations, for the times when the availability of renewable energy is not enough to meet the energy demand. The average cost per installed kilowatt for a thermoelectric plant in Brazil was set at USD$ 1,073.50/kW, according to Braciani [12-9]. Several generator sizes were considered, with the technical minimum load ratio set at 30%, according to Kaldellis et al. for heavy oil and diesel engines.

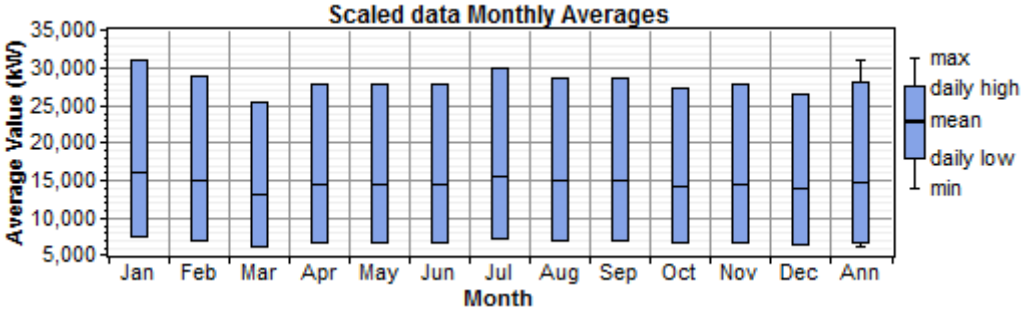

Fig. 12.5. Scaled monthly averages of load profile considered in this study.

A connection to the grid was included, allowing the purchase of energy when there is not enough energy production to meet the consumers, and the sale of energy, when there is excess energy. The connection to the grid considered in the simulations has dimensions comparable to the possible installed powers of the diesel generator sets, allowing eventually the optimization process chooses one over the other.

12.5 Simulations with homer

Homer [12-15] is a software for optimization of hybrid energy systems. It was originally developed by National Renewable Energy Laboratory (NREL) and a version called "Legacy" is now available for universal access. Homer simulates a system for power generation over the time period of 25 years at standard intervals of 60 minutes. [12-16]-[12-17] The Homer software performs simulations of hybrid systems aiming to build optimization spaces according to different sensitivity variables, allowing a complete characterization of performance.

The Homer software simulates hydroelectric power plants operating as "run of the river" power plants. The simulation of hydroelectric power plant with storage capacity and hydroelectric for operation as a reversible plant can be performed as explained by Canales and Beluco [12-7]. The dc bus must contain only the hydroelectric power plant and a battery, adjusted to simulate a pumped storage power plant. The operation of the two reservoirs is simulated with the battery, while the supply of electricity to be transferred to the hybrid system is simulated by the hydroelectric plant. The converter has a single direction of operation.

Simulations with the system of Fig. 12.6 were performed. The optimization variables considered were the following: 0, 10, 20, 25, 30, 35, 40, 45, 50, 55, 60, 65, 70, 75, 80, 85 and 90 wind turbines; 0 MW, 10 MW, 20 MW, 30 MW, 40 MW, 50 MW and 60 MW for the installed power of the diesel gen set; 0 and 1 battery modeled as pumped storage plant; 0 and 722 kW for the converter capacity. The sensitivity inputs were the following: 100 MWh/d, 200 MWh/d, 300 MWh/d, 400 MWh/d and 500 MWh/d for AC load; USD$ 1/L, USD$ 2/L, USD$ 3/L, USD$ 4/L and USD$ 5/L for the cost of diesel oil; 6 m/s, 8 m/s, 10 m/s and 12 m/s for the wind speed. Simulations with the system of Fig. 12.6 were repeated with all these variables and a fixed value of 10 MW for the installed capacity of photovoltaic plant.

Simulations with the system of Fig. 12.7, with the PV modules assembled on floating structures installed over the flooded surface of the reservoir, were performed. The optimization variables considered were the following: 0, 10, 20, 25, 30, 35, 40, 45, 50, 55, 60, 65, 70, 75, 80, 85 and 90 wind turbines; 0 MW, 1,200 MW, 2,400 MW, 4,800 MW, 9,600 MW and 19,200 MW for the installed power of the diesel gen set; 0 kW, 100 kW, 200 kW, 400 kW and 800 kW for the capacity of PV modules; 0 and 1 battery modeled as pumped storage plant; 0 and 722 kW for the converter capacity. The sensitivity inputs were the following: 100 MWh/d, 200 MWh/d, 300 MWh/d, 400 MWh/d and 500 MWh/d for AC load; USD$ 0.50/L, USD$ 0.70/L, USD$ 0.90/L and USD$ 1.10/L for the cost of diesel oil; 6 m/s, 8 m/s, 10 m/s and 12 m/s for the wind speed; 0.0%, 2.5%, 5.0% and 10.0% for the maximum capacity shortage.

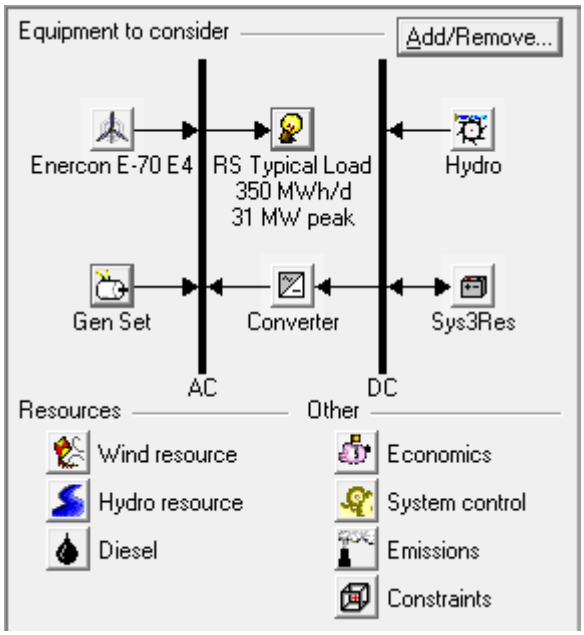

Fig. 12.6. Wind hydro hybrid system with water storage capacity.

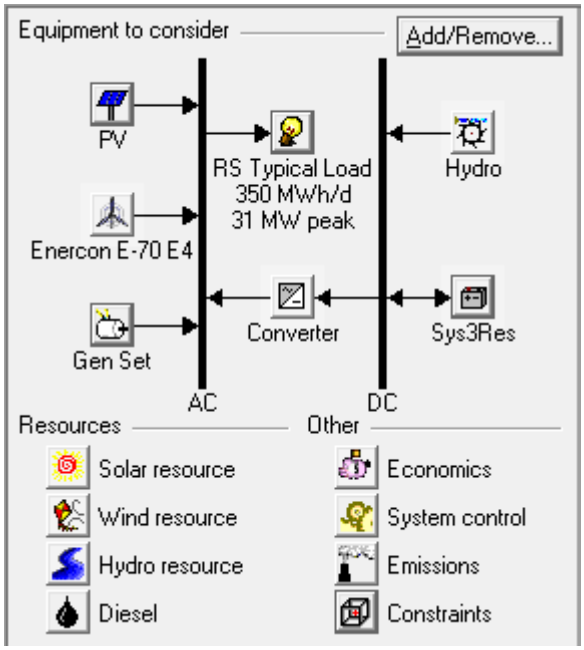

Fig. 12.7. PV wind hydro hybrid system with water storage capacity considered in this study.

A constraint of 95% of energy supplies must be obtained from renewable resources limits the grid purchases. The values for AC load are adopted to determine the dimensions of the main components of the hybrid system. PV costs multipliers were chosen to assess the impact of floating structures, adding 30% to the costs, and to evaluate possible cost reductions obtained through some kind of financial or economic incentives on the price of PV modules.

12.6 Results and discussion

Fig. 12.8 to Fig. 12.11 show the results obtained with the first stage of the simulation, while Fig. 12.12 to Fig. 12.15 show the results obtained with the second phase. A very important result is that Homer did not indicate any optimal solutions in the different optimization spaces shown in these figures (and even others not shown) that contained PV modules. However, in several cases, as discussed below, some combinations containing photovoltaic modules were discarded by very small differences in relation to optimal solutions.

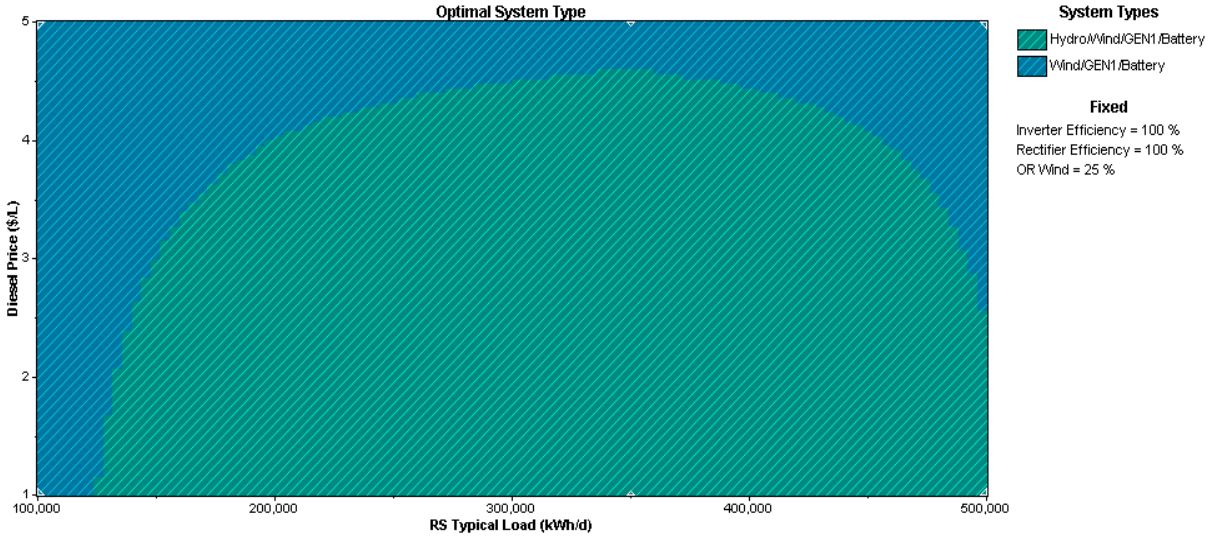

Fig. 12.8. Results for the optimization space obtained for diesel price as a function of local typical load for the system of Fig. 12.6.

Fig. 12.8 and Fig. 12.9 show the optimization space obtained for the system of Fig. 12.6, respectively showing diesel price as a function of the local typical load and showing diesel price as a function of wind speed. The value currently practiced for diesel oil and the average wind speed for the area indicate that the optimal solution includes wind turbines and the pumped storage plant, in addition to supporting diesel generators. This system, considered as a starting point for this study was the subject of a recent article [12-4].

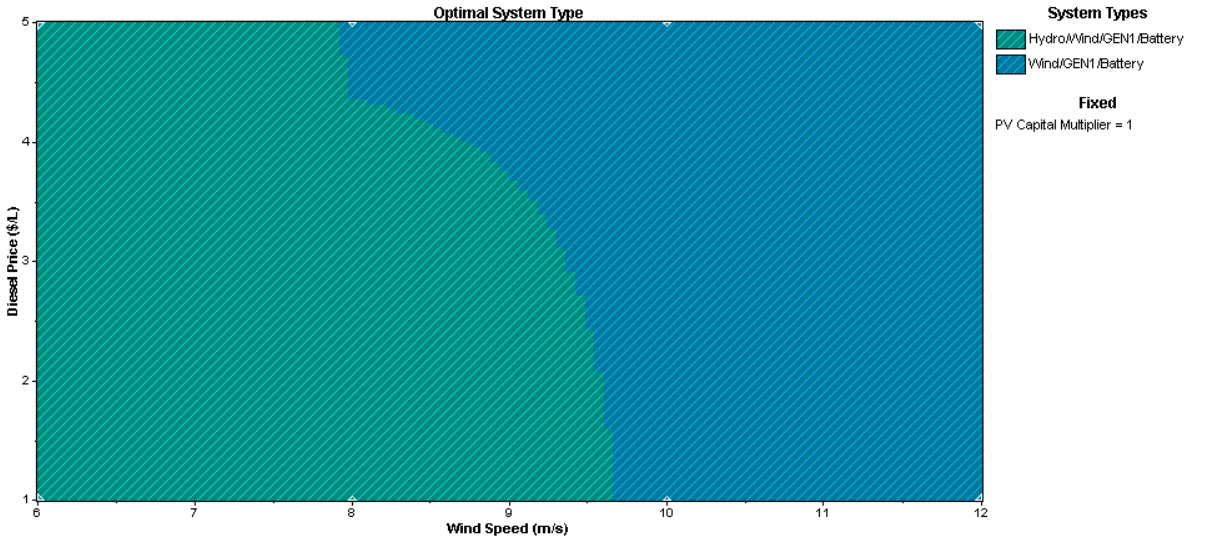

Fig. 12.9. Results for the optimization space obtained for diesel price as a function of wind speed for the system of Fig. 12.6.

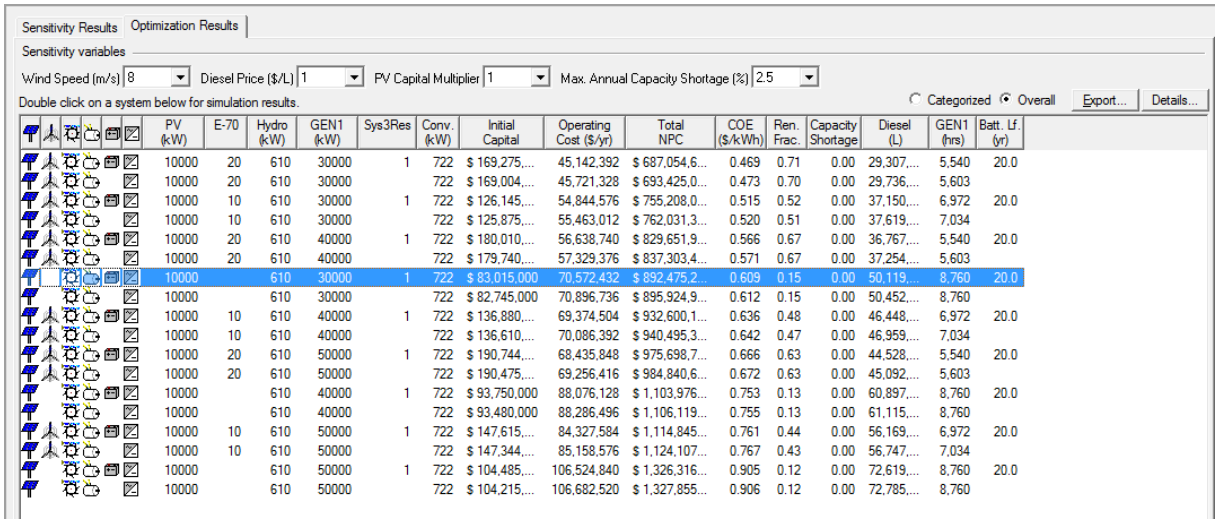

	PV (kW)	E-70	Hydro (kW)	GEN1 (kW)	Sys3Res	Conv. (kW)	Initial Capital	Operating Cost ($/yr)	Total NPC	COE ($/kWh)	Ren. Frac.	Capacity Shortage	Diesel (L)	GEN1 (hrs)	Batt. Lf. (yr)
	10000	20	610	30000	1	722	$ 169,275,...	45,142,392	$ 687,054,6...	0.469	0.71	0.00	29,307,...	5,540	20.0
	10000	20	610	30000		722	$ 169,004,...	45,721,328	$ 693,425,0...	0.473	0.70	0.00	29,736,...	5,603	
	10000	10	610	30000	1	722	$ 126,145,...	54,844,576	$ 755,208,0...	0.515	0.52	0.00	37,150,...	6,972	20.0
	10000	10	610	30000		722	$ 125,875,...	55,463,012	$ 762,031,3...	0.520	0.51	0.00	37,619,...	7,034	
	10000	20	610	40000	1	722	$ 180,010,...	56,638,740	$ 829,651,9...	0.566	0.67	0.00	36,767,...	5,540	20.0
	10000	20	610	40000		722	$ 179,740,...	57,329,376	$ 837,303,4...	0.571	0.67	0.00	37,254,...	5,603	
	10000		610	30000	1	722	$ 83,015,000	70,572,432	$ 892,475,2...	0.609	0.15	0.00	50,119,...	8,760	20.0
	10000		610	30000		722	$ 82,745,000	70,896,736	$ 895,924,9...	0.612	0.15	0.00	50,452,...	8,760	
	10000	10	610	40000	1	722	$ 136,880,...	69,374,504	$ 932,600,1...	0.636	0.48	0.00	46,448,...	6,972	20.0
	10000	10	610	40000		722	$ 136,610,...	70,086,392	$ 940,495,3...	0.642	0.47	0.00	46,959,...	7,034	
	10000	20	610	50000	1	722	$ 190,744,...	68,435,848	$ 975,698,7...	0.666	0.63	0.00	44,528,...	5,540	20.0
	10000	20	610	50000		722	$ 190,475,...	69,256,416	$ 984,840,6...	0.672	0.63	0.00	45,092,...	5,603	
	10000		610	40000	1	722	$ 93,750,000	88,076,128	$ 1,103,976...	0.753	0.13	0.00	60,897,...	8,760	20.0
	10000		610	40000		722	$ 93,480,000	88,286,496	$ 1,106,119...	0.755	0.13	0.00	61,115,...	8,760	
	10000	10	610	50000	1	722	$ 147,615,...	84,327,584	$ 1,114,845...	0.761	0.44	0.00	56,169,...	6,972	20.0
	10000	10	610	50000		722	$ 147,344,...	85,158,576	$ 1,124,107...	0.767	0.43	0.00	56,747,...	7,034	
	10000		610	50000	1	722	$ 104,485,...	106,524,840	$ 1,326,316...	0.905	0.12	0.00	72,619,...	8,760	20.0
	10000		610	50000		722	$ 104,215,...	106,682,520	$ 1,327,855...	0.906	0.12	0.00	72,785,...	8,760	

Fig. 12.10. Optimization results constituting the optimization space shown in Fig. 12.12.

Fig. 12.10 shows the simulation results of this system with a photovoltaic plant with capacity of 10 MW. The optimal result indicates an energy cost of USD$ 0.469 per kWh operating with 20 wind turbines and diesel support system with 30 MW. The seventh system in this list operate without wind turbines and a higher cost, equal to USD$ 0.609 per kWh, with a variation of the charge state of the reservoirs shown in Fig. 12.11. The behavior of the curve, with energy at the beginning of the period identical to the energy in the end, indicates an acceptable performance.

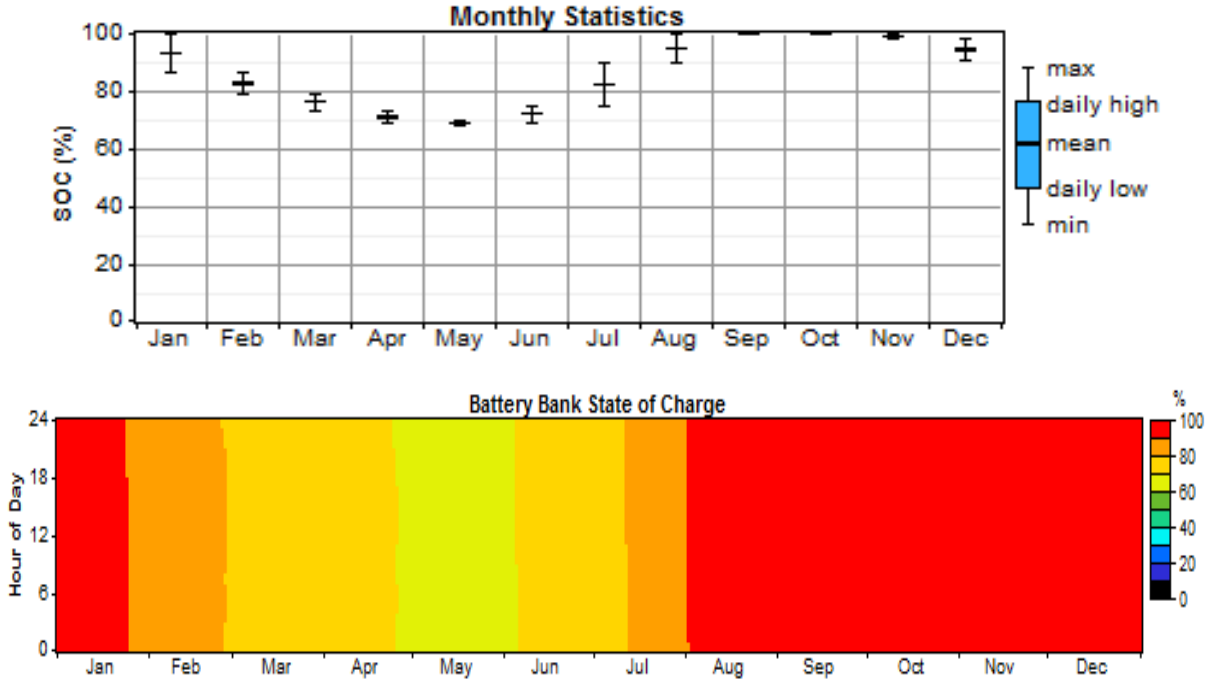

Fig. 12.11. Annual change in state of charge of the reservoirs for a hybrid system shown in Fig. 12.10 with COE equal to USD$ 0.609 per kWh.

Fig. 12.12 and Fig. 12.13 show the optimization space obtained for the system of Fig. 12.6, respectively showing diesel price as a function of the local typical load and showing diesel price as a function of wind speed. The lower load consumers, compared with the preceding figures, have given rise to areas on the bottom left of these optimization spaces, corresponding to combinations not including wind turbines. A lot of points of these optimization spaces show optimal results that led to discard the combinations including PV modules for very small differences.

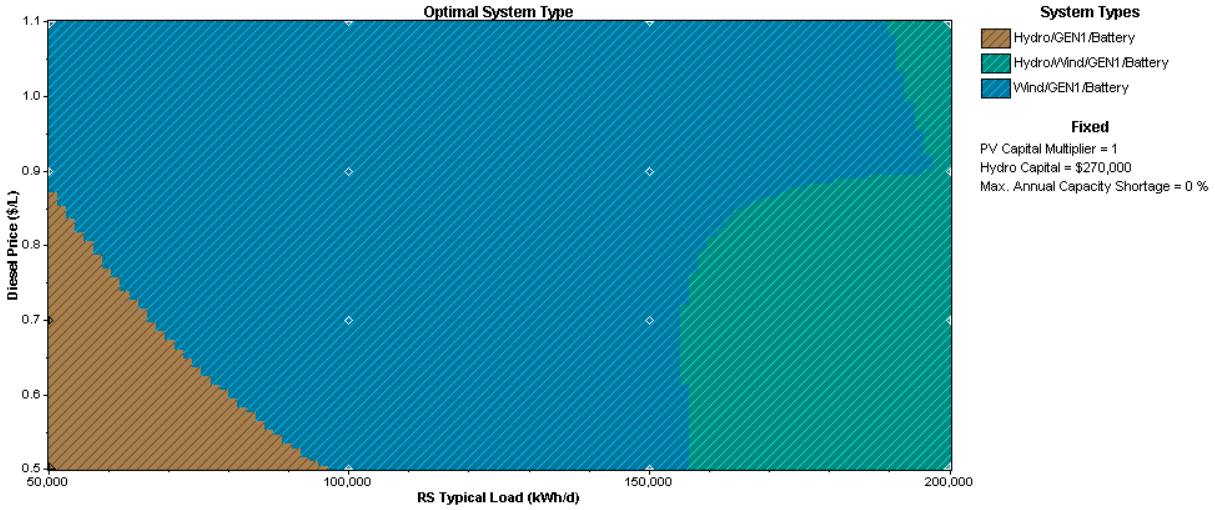

Fig. 12.12. Results for the optimization space obtained for diesel price as a function of local typical load, for the system of Fig. 12.7 with different values for diesel price and consumers load.

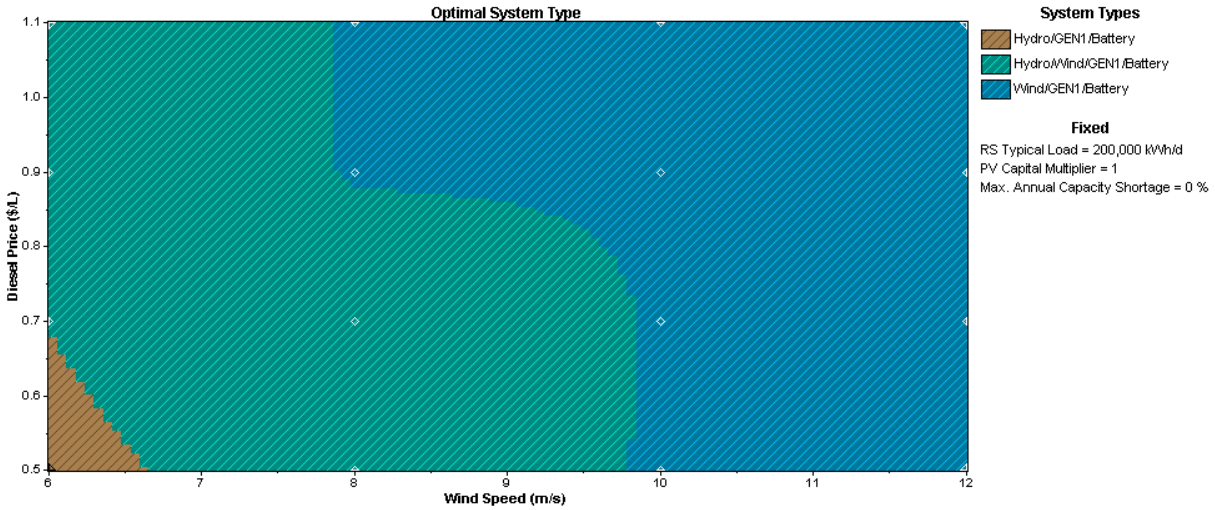

Fig. 12.13. Results for the optimization space obtained for diesel price as a function of wind speed, for the system of Fig. 12.7 with different values for diesel price and consumers load.

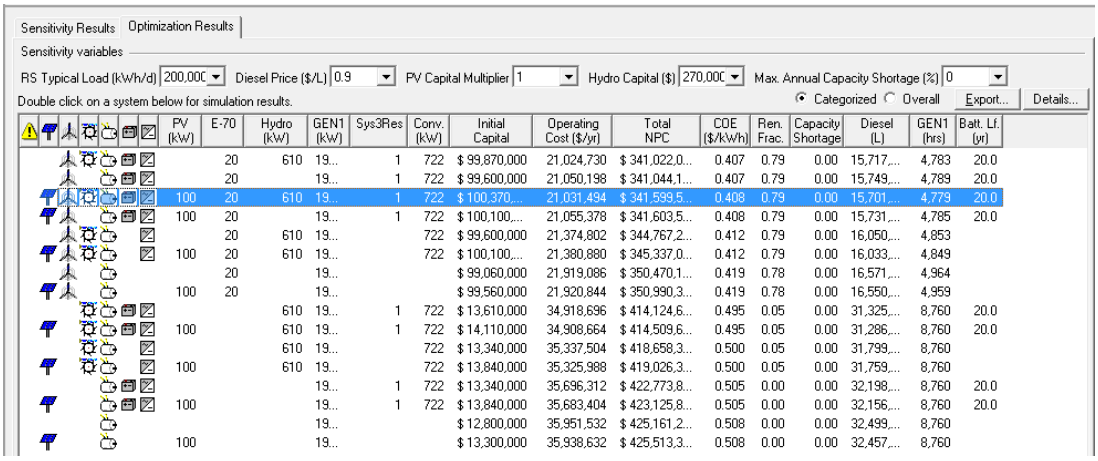

Fig. 12.14. Optimization results constituting the optimization space shown in Fig. 12.12.

The complete output provided by Homer for each feasible option allows estimating and optimizing the capacity of pumped storage system for recovering rejected renewable energy. This can also be used for calculating the effective capacity factor of the wind farm with and without the pumped storage capacity. According to the simulation results and based on the wind resource inputs of this case study, the maximum capacity factor of the wind turbines reported by Homer is 35.6%, including excess electricity. The Osório Wind Park, used as model for creating the wind turbines of this work, reports on its website a capacity factor equal to 32.3%. These values are within the range of values reported by Boccard [12-19], who gathered global results reported by transmission system operators or available in academic literature related to wind farm capacity factors.

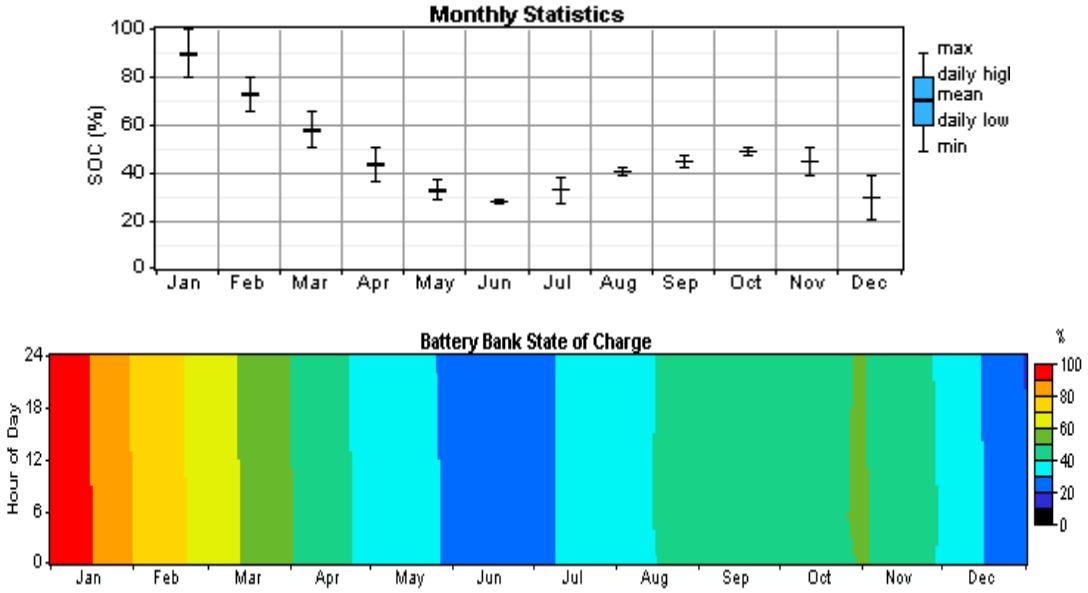

Fig. 12.15. Annual change in state of charge of the reservoirs for a hybrid system shown in **Fig. 12.12** with COE equal to USD$ 0.495 per kWh.

Based on the results simulations, Fig. 12.16 presents the estimated duration curves for rejected power. As explained by Kaldellis et al. [12-20], large amounts of rejected energy also mean severe financial losses that discourage future investments in renewable energy projects. Without the pumped storage plant, the extremely variable wind profile would require more turbines at the wind farm along with a diesel generator of greater capacity, thus increasing the generation cost. As shown in Fig. 12.16 a, a system without storage capacity would reject power about 80% of the time, with 25% of the time rejecting more than 50MW. Conversely, with pumped storage capacity and using the same 50% of the wind farm capacity as benchmark, Fig. 12.16 b and Fig. 12.16 c show that this energy storage technology improves the wind energy absorption, limiting the occurrence of this value to less than 10% of the time and reducing the cost of energy for the system. In Homer, the cost of energy is the average cost per kWh of useful electrical energy produced by the system, which in this case is just the energy used to serve the primary AC Load (no grid sales, DC or deferrable loads are considered in the example).

Fig. 12.14 shows results presented in Fig. 12.12 and corresponding to the consumer load equal to 200 kWh per day and diesel sold at USD$ 0.90 per liter. The first system of this list is what defines the green color at the corresponding point in the optimization space shown in Fig. 12.12. This first system presents cost of energy equal to USD$ 0.407 per kWh, very close to the third system in the list that includes PV modules and provides energy at cost of USD$ 0.408 per kWh. This system includes 100 kW in PV modules, the pumped storage plant, twenty wind turbines and diesel support system with 19.2 MW.

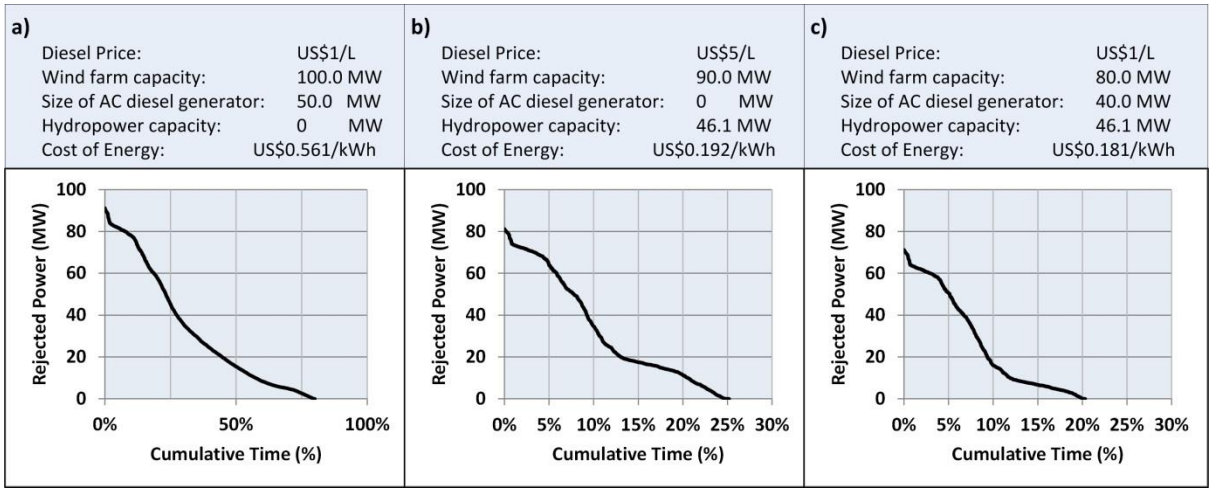

Fig. 12.16. Rejected power duration curves for an average daily load = 500MWh/d for three different conditions.

Most systems in this list have small monthly variations of the state of charge of the reservoirs over a year. The tenth system, however, in the list shown in Fig. 12.14, presents a more pronounced change in the state of charge of the reservoirs. This system includes 100 kW in PV modules, the pumped storage plant and diesel support system without wind turbines. Fig. 12.15 details this change in the state of charge, indicating minimum values during the month of June. A further reduction in the past few months show that the energy available at the end of the year will be less than the energy in the beginning of the year, indicating an unsustainable situation.

12.7 Final remarks

This chapter presented the results of an exploratory study to design a photovoltaic wind hydro hybrid system with storage capacity. The optimal combinations obtained from the simulations did not suggest the inclusion of PV modules, mainly due to its high initial cost and the high cost of energy. Among the non-optimal solutions, it is possible to find solutions including PV modules and that show performance comparable to optimal solutions. Thus, this study suggested a hybrid system constituted by 100 kW in photovoltaic modules, 20 wind turbines and a diesel support system with 19,200 kW, also with the pumped storage plant, providing energy at a cost of USD$ 0.408 per kWh. This study also suggested a system with 10,000 kW in photovoltaic modules and a diesel support system with 30,000 kW, without wind turbines and with the pumped storage plant, providing energy at a cost of USD$ 0.609 per kWh.

12.8 Acknowledgements

This work was developed as a part of research activities on renewable energy developed at the Instituto de Pesquisas Hidráulicas, at Universidade Federal do Rio Grande do Sul, and Universidade Estadual do Rio Grande do Sul. The authors acknowledge the support received by the institutions. The third author also acknowledges the financial support received from CNPq for his research work.

12.9 References

[12-1] Beluco A., Souza P.K., Livi F.P., Caux J., Energetic complementarity with hydropower and the possibility of storage in batteries and water reservoirs, Chapter 7, In: B. Sørensen, Solar Energy Storage, Amsterdan, Netherlands: Academic Press, (2012).

[12-2] Beluco, A. Kroeff, P.K. Krenzinger, A. (2012) A method to evaluate the effect of complementarity in time between hydro and solar energy on the performance of hybrid hydro PV generating plants. Renewable Energy, v.45, p.24-30.

[12-3] Beluco, A. Souza, P.K. Krenzinger, A. (2013) Influence of different degrees of complementarity of solar and hydro availability on the performance of hybrid hydro PV generating plants. Energy and Power Engineering, 5, 332-342.

[12-4] Canales, F.A. Beluco, A. Mendes, C.A.B. (2015) A comparative study of a wind hydro hybrid system with water storage capacity: conventional reservoir or pumped storage plant? Journal of Energy Storage, v.4, p.96-105.

[12-5] Beluco, A. (2012) Three sites for implementation of reversible hydroelectric power plant in the south of the Aparados da Serra, on the north coast of State of Rio Grande do Sul (in portuguese). Hidro & Hydro, n.52, p.32-37. Available at cerpch.unifei.edu.br/wp-content/uploads/revistas/revista-52.pdf#page=32.

[12-6] https://goo.gl/maps/FAgxVYLbF4u.

[12-7] Canales, F.A. Beluco, A. (2014) Modeling pumped hydro storage with The Micropower Optimization Model (Homer), Journal of Renewable and Sustainable Energy, v.6, paper n.043131.

[12-8] Benetti, A.D. Lanna, A.E. Cobalchini, M.S. (2003) Methods for the determination of residual flows in Rivers (in portuguese). Revista Brasileira de Recursos Hídricos, v.8, p.149–160. Available at: www.abrh.org.br/SGCv3/index.php?PUB=1.

[12-9] Braciani, U. (2011) Cost structure for Implementation of electric power generation plants in Brazil (in portuguese). BSc. Thesis in Economic Sciences, Universidade Federal de Santa Catarina (UFSC), Florianópolis, Brazil. Available at tcc.bu.ufsc.br/Economia303023.pdf.

[12-10] Silva, J.S. (2012) Feasibility of electricity generation from ocean waves on the northern coast of Rio Grande do Sul: a study of a hybrid system based on renewable (in portuguese). MSc. Thesis in Water Resources, Universidade Federal do Rio Grande do Sul (UFRGS), Porto Alegre, Brazil. Available at www.lume.ufrgs.br/bitstream/handle/10183/78865/000900392.pdf.

[12-11] Ferrer-Gisbert, C. Ferran-Gonzalvez, J.J. Redon-Santafé, M. Ferrer-Gisbert, P.S. Sanchez-Romero, F.J. Torregrosa-Soler, J.B. (2013) A new photovoltaic floating cover system for water reservoirs. Renewable Energy, v.60, p.63-70.

[12-12] Redon-Santafé, M. Ferrer-Gisbert, P.S. Sanchez-Romero, F.J. Torregrosa-Soler, J.B. Ferran-Gonzalvez, J.J. Ferrer-Gisbert, P. (2013) Implementation of a photovoltaic floating cover for irrigation reservoirs. Journal of Cleaner Production, v.66, p.568-570.

[12-13] Feldman, D. et al. (2014) Photovoltaic system pricing trends: historical, recent and near term projections. National Renewable Energy Laboratory, U.S. Dept. of Energy. Report n.62558. Available at www.nrel.gov/docs/fy14osti/62558.pdf. Accessed on February 23, 2016.

[12-14] Teixeira, L.E. Caux, J. Beluco, A. Bertoldo, I. Louzadam J.A.S. Eifler, R.C. (2015) Feasibility study of a hydro PV hybrid system operating at a dam for water supply in southern Brazil. Journal of Power and Energy Engineering, v.3, n.9, p.70-83.

[12-15] Software HOMER, version 2.68 beta. The Micropower Opyimization Model, Homer Energy. Available at www.homerenergy.com.

[12-16] Lilienthal, P.D. Lambert, T.W. Gilman, P. (2004) Computer modeling of renewable power systems. In: Cleveland, C.J. (ed.) Encyclopedia of Energy, Elsevier, v.1, p.633-647. NREL Report CH-710-36771.

[12-17] Lambert, T.W. Gilman, P. Lilienthal, P.D. (2005) Micropower system modeling with Homer. In: Farret, F.A. Simões, M.G. Integration of Alternative Sources of Energy, John Wiley & Sons, p.379-418. ISBN 0471712329.

[12-18] IRENA, International Renewable Energy Agency (2012) Renewable energy technologies: cost analysis series, Hydropower. Volume 1: Power Sector. Available at www.irena.org/documentdownloads/publications/re_technologies_cost_analysis-hydropower.pdf. Accessed on February 23, 2016.

[12-19] Boccard, N. (2009) Capacity factor of wind power realized values vs. estimates. Energy policy, v.37, n.7, p.2679–2688.

[12-20] Kaldellis, J. K. Kapsali, M. Kavadias, K. A. (2010) Energy balance analysis of wind-based pumped hydro storage systems in remote island electrical networks. Applied energy, v.87, n.8, p.2427–2437.

13. ALGUNS EFEITOS DA COMPLEMENTARIDADE ESPACIAL NO TEMPO NA CONCEPÇÃO DE UM SISTEMA HIBRIDO DE MÉDIO PORTE EÓLICO-HÍDRICO-FOTOVOLTAICO

13.1 Apresentação

Este capítulo, apresenta o *trabalho "Some Effects Of Spatial Complementarity In Time On The Design Of A Medium-Sized Wind Hydro Hybrid System"*, submetido à revista "*Renewable Energy*", em 2019, pela editora ELSIEVER tendo como autores o Prof. Alfonso Risso, o Prof. Alexandre Beluco e a Profa. Rita de Cássia Marques Alves.

Abstract

Energetic complementarity is a growing subject of researchers around the world. It is a concept that can serve as a tool for managing renewable energy resources. Complementarity in time has been studied for some time, but spatial complementarity is still a rather unexplored subject. This work aims to contribute to a better understanding of the influence of spatial complementarity on the performance of hybrid systems. In this work, the spatial complementarity in time is evaluated with the determination of roses of complementarity, applying a method most recently proposed in the specialized literature. The hybrid system under study is a wind hydro hybrid system that is part of the Brazilian Energy System and feeds the northern coast of the State of Rio Grande do Sul, the southernmost State of Brazil. This system contains five hydroelectric plants and fourteen wind farms, but the simulations also included a reversible hydroelectric plant operating in conjunction with photovoltaic panels, still under study. The simulations were carried out with the software ViPOR, developed by NREL of the US Department of Energy. Considering situations with hypothetically more complementary energy resources and less complementary energy resources, compared to the current situation, it was possible to verify that complementarity can contribute to the energy system being up to 30% cheaper.

Keywords

Hybrid systems, hydro PV hydric systems, feasibility analysis, terminal value analysis, valuation, software Homer.

13.2 Introduction

Energetic complementarity is a topic of research that has been growing over the last years, both in the number of articles published and in the number of researchers dedicated to the subject. Energetic complementarity can be considered as a parameter for the operation of

energy systems and can also be seen as a tool for the management of renewable energy resources. This article intends to contribute with knowledge about the effects of spatial complementarity over time on the design of a medium-sized wind hydro PV hybrid system.

Complementarity can be considered over time and-or along space and can be determined in different ways. [13-1] The complementarity between renewable energy resources in one place is called temporal complementarity, while the complementarity between energy resources in different places is called spatial complementarity. Energetic complementarity, according to Beluco [13-2], has three components, namely: time-complementarity, energy-complementarity and amplitude-complementarity.

The next section of this article discusses the determination of time complementarity between the annual energy availabilities of two energy sources. This analysis can be applied for the determination of both temporal complementarity and spatial complementarity.

The subsequent section discusses spatial complementarity in time and its influence on the design of a hybrid system. The work of Risso et al [13-28] proposed that the spatial complementarity can be evaluated with the use of complementary roses. The expression of spatial complementarity in maps is a difficult challenge because it involves the inclusion of various information, such as intensity, distance and direction, at each point evaluated.

This paper evaluates the effects of spatial complementarity over time on a PV wind hydro hybrid system based on simulations performed with ViPOR software. The next section discusses spatial complementarity and its expression through complementary roses, the next section presents the hybrid system being studied and the subsequent section describes the simulations performed with the ViPOR software. Finally, the results are presented and discussed.

13.3 Energetic Complementarity

Energetic complementarity is the characteristic presented by the energy availability of two or more natural renewable resources to complement each other over time and - or space. As stated by Risso et al [13-1], “Temporal complementarity” can be used to refer to the complementarity between energy resources in the same place, while “spatial complementarity” can be used in the case of complementarity between energy resources in different places. In both cases, complementarity has three components, as presented by Beluco et al [13-2], namely time-complementarity, energy-complementarity and amplitude-complementarity.

Fig. **13.1** shows actual energy availability data. The uppermost data, on the left, correspond to typical water availability data in a river section. The lowermost data, on the right, in turn, correspond to the solar radiation incident on a flat horizontal surface. The figure characterizes the mean values of energy and the amplitudes of variation for the two energy

resources. The time-complementarity component evaluates the lag between the maximum or minimum values of energy availability of the energy resources considered.

The energy-complementarity component compares average energy values and a maximum value will be obtained if each resource contributes half of the total annual energy. The amplitude-complementarity component compares the amplitudes of variation of each energy resource and, like the energy complementarity component, a maximum value of complementarity will be obtained if the energy resources compared have the same amplitude variation.

This article deals with the time-complementarity component (here called simply as complementarity in time), which is directly related to the time lag between the maximum or minimum values of energy availability of two renewable resources. Eq. (1) presents the complementarity in time as defined by Beluco et al [13-2]. This equation assigns a linear characteristic to the complementarity in time and other equations can be proposed.

$$\kappa_t = \frac{|d_1 - d_2|}{\sqrt{|D_1 - d_1||D_2 - d_2|}} \qquad (1)$$

In this equation, D is the number of the day (or month) in which the maximum energy availability occurs and d is the day (or month) in which the minimum value occurs. Subscript 1 indicates one of the energy resources while the number 2 indicates the other. The denominator assesses whether energy resources have a 180-day (or six-month) interval between maximum and minimum energy availability, which also affects the complementarity in time.

The application of this equation should not be performed from a mathematically more rigid point of view, as discussed by Beluco [13-4]. Its application must be carried out by a trained human analyst with a good sense of analysis. The evaluation of the energy resources shown in

Fig. **13.1**, for example, indicates a complementarity equal to 2 over 6, that is, equal to 0.3333. The minimum values of energy availability occur in months apart from each other for 2 months.

13.4 Spatial Complementarity in Time

As discussed above, spatial complementarity is the complementarity between energy resources located at different sites. This concept, duly quantified and mapped, can lead to important tools for managing energy resources. The appropriate exploitation of spatial complementarity can contribute to lower cost of installation of power plants and optimization of operation costs of power plants inserted in an interconnected system.

The problem is then the determination of complementarity between operating plants (or sites with energetic potential) in different locations and not in the same place. It is necessary to determine the complementarity in time between energy resources such as those shown in

Fig. **13.1**, but located at different sites. Such a calculation will generate information on complementarities with different sites, placed at different distances, and in different orientations.

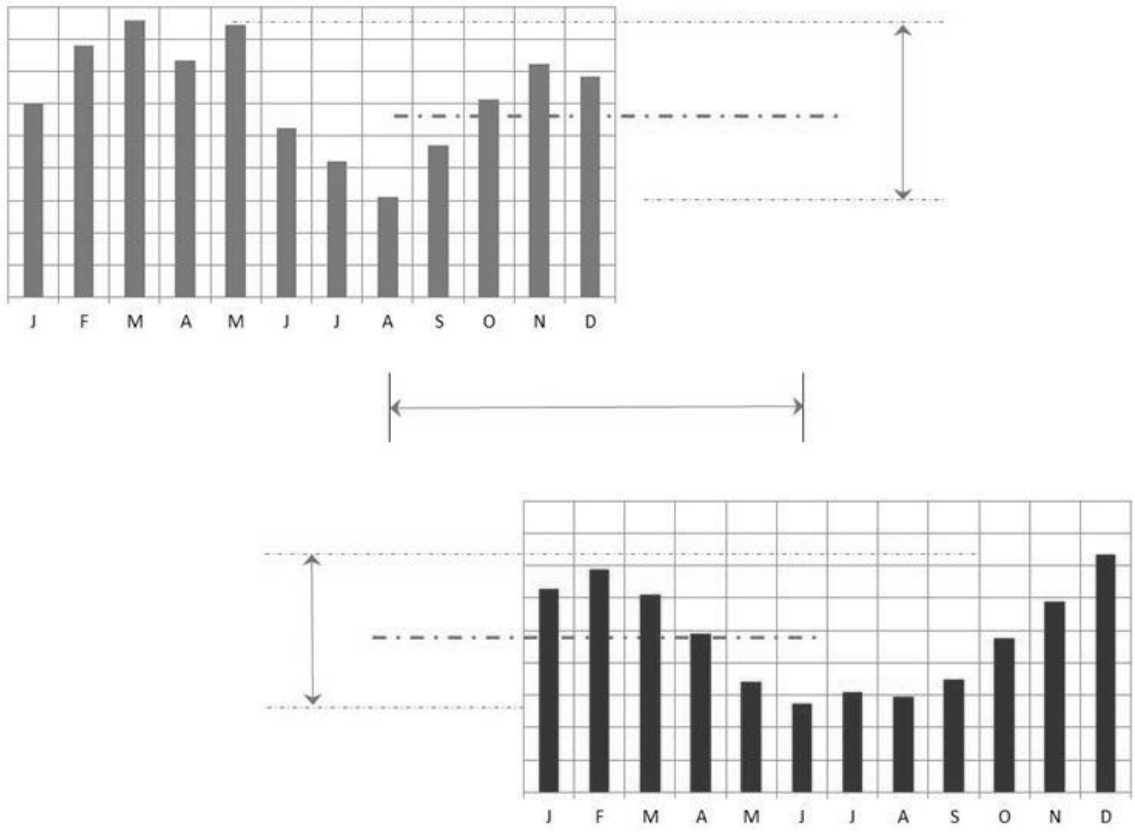

Fig. 13.1. Energy availability for two renewable energy resources and markings indicating the three components of energetic complementarity.

For simplicity, some limitations to this problem will be established, allowing the basic problem of determining spatial complementarity to be solved. This article will then present only the determination of spatial complementarity in time. In addition, a region under study will be modeled with the application of a network of hexagonal cells. Thus, the energy in each cell will be the sum of the energy generated (or available energy resources) on its surface, according to the analysis being undertaken.

The expression of spatial complementarity with the use of complementary roses allows to concentrate in the same figure all the additional information regarding the complementarity in time. In this case, complementarity over time must be characterized in terms of its intensity, its direction and its distance. In addition, a comprehensive study should indicate the spatial

complementarities for different points along a region, differentiating the results for different types of power generation plants.

13.5 PV Wind Hydro Hybrid System under Study

A set of wind farms, hydroelectric power plants and a reversible power plant with photovoltaic generation capacity will be considered as a hybrid system to study the effects of spatial complementarity over time. This hybrid system is located in the north coast region of the State of Rio Grande do Sul and can be located on Google Maps [13-5] and is shown in

Fig. 13.2. A 500 square kilometer cell network was set up to allow this assessment and this figure shows that there are hydroelectric plants in two cells and wind turbines in three cells.

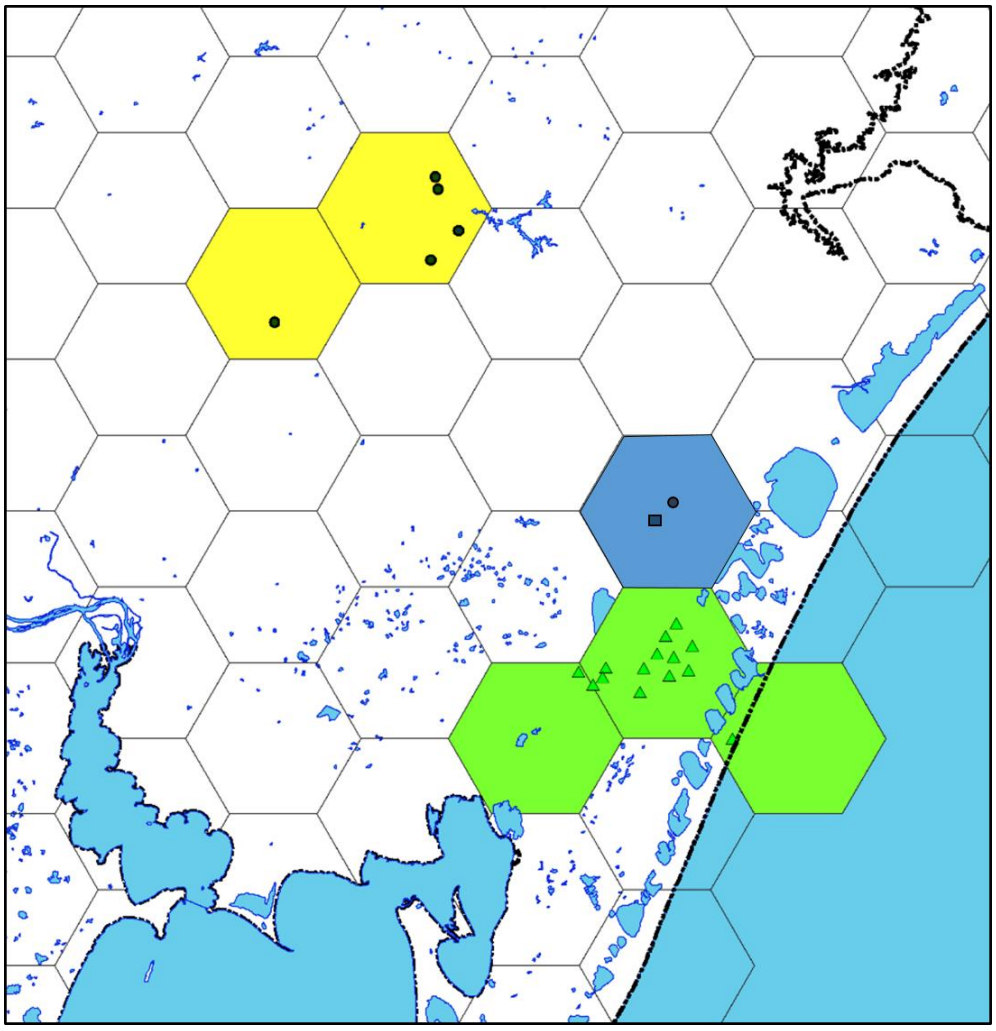

Fig. 13.2. Region of the North Coast of the State of Rio Grande do Sul, with a network of cells of 500 square kilometers established for the determination of the spatial complementarity in

time. The cells in yellow concentrate the hydroelectric power plants, the cells in green the wind farms and the blue cell includes a reversible hydro power plant with PV modules.

Fig. 13.3 and Fig. 13.4 respectively show the locations of the components of the hybrid system identified in the region characterized above. Fig. 13.3 identifies the five hydroelectric power plants with numbers from 1 to 5. In 1 the Herval [13-6] hydro power plant is located, 2 is the Bugres [13-7] hydro power plant, 3 the Canastra [13-8] power plant, 4 the Toca [13-9] power plant and in 5 is located the Passo do Inferno [13-10] power plant.

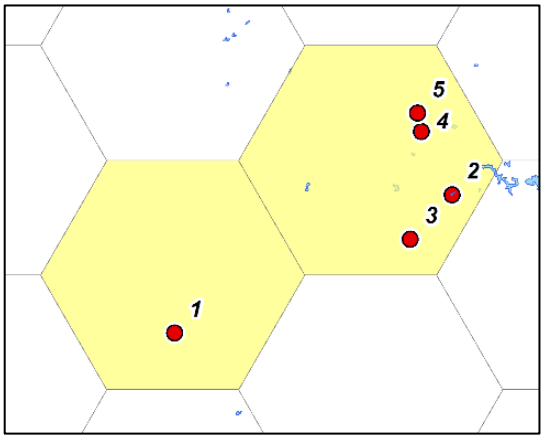

Fig. 13.3. Location of the hydroelectric power plants, numbered 1 to 5, in the yellow cells in Fig. 13.2.

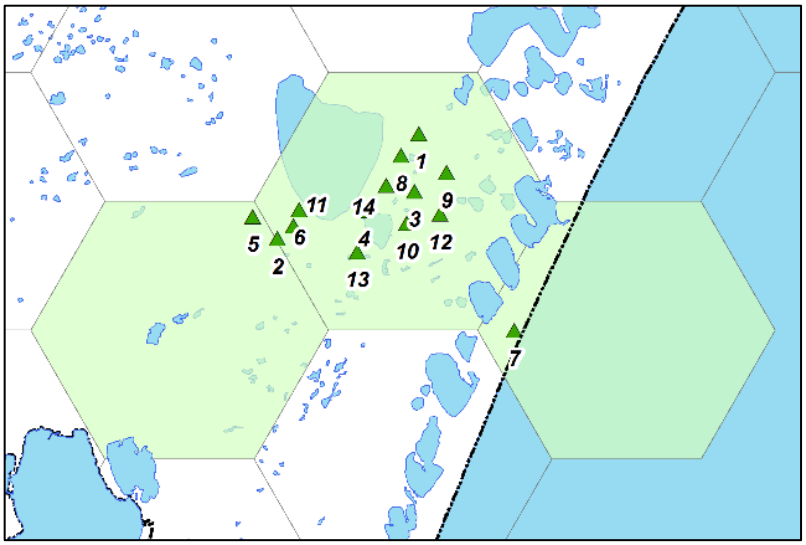

Fig. 13.4. Location of the wind farms, numbered 1 to 14, in the green cells in

Fig. 13.2.

Fig. 13.4 identifies the fourteen wind farms with numbers from 1 to 14. In 1, 8 and 14 are located respectively Sangradouro II [13-11], Sangradouro I [13-18] and Sangradouro III

[13-24]; in 2, 6 and 11 are located respectively Lagoa dos Barros III [13-12], Lagoa dos Barros I [13-16] and Lagoa dos Barros II [13-21]; in 3, 9 and 12 are located respectively Osório I [13-13], Osório II [13-19] and Osório III [13-22]; in 4, 10 and 13 are located respectively Índios III [13-14], Índios I [13-20] and Índios II [13-23]; in 5 is located the Chicolomã [13-15] wind farm and in 7 is located the Cidreira [13-17] wind farm.

The set composed of the reversible hydroelectric power plant and the PV modules on floating structures [13-25] appears in the blue cell. This plant is composed of two reservoirs, one lower and one upper, with the engine room obviously installed near the lower reservoir. Photovoltaic panels are installed on the water surface of the upper reservoir. For that reason, there is two points in the blue cell, with the southwestern point locating the reversible plant and the northeastern point locating the photovoltaic panels.

Fig. 13.5 shows the spatial complementarity in time between hydroelectric power plants and wind farms, Fig. 13.6 shows the complementarity between hydropower plants and PV modules and Fig. 13.7 shows the complementarity between PV modules and wind farms. As can be observed, the best values of complementarity are verified between the hydroelectric plants described in Fig. 13.3 and the wind farms in Fig. 13.4. The PV modules also have good values of complementarity with the hydroelectric plants of Fig. 13.3.

The data for this analysis were obtained with the HidroWeb [13-26] system, available online, and the Wind Atlas [13-27] of the State of Rio Grande do Sul, having been manipulated as proposed by Beluco et al [13-2] for the determination of complementarity in time. Complementary roses were determined as suggested by Risso et al [13-28] from this information of complementarity in time and their respective directions.

The analysis undertaken in this paper considers only the months in which the minimum energy availability occurs in the power plants considered in the study. The purpose of the analysis may induce the choice of a network with smaller cells. The dimensions of the cell network to be adopted should be related to the expected results. A more complete analysis should take into account the other components of complementarity and also evaluate the impact of the use of networks of cells with different dimensions.

13.6 Simulations with ViPOR

The ViPOR software was developed by NREL of the US Department of Energy and is a model that establishes a power distribution system for small and medium-sized power generation systems. ViPOR requires data on the spatial distribution of power plants and consumer loads, as well as their individual power and generation and consumption capacities, and defines, among these consumer loads, which should be connected to the centralized power distribution system and which must be met by autonomous generation sets. Within certain limits, it can also be applied to systems of larger dimensions.

The focus of the ViPOR software is the lease of components of a power distribution

system, not having ability to scale system components such as generators or batteries or other devices. The ViPOR allows to model different types of terrain, with greater or lesser difficulties of transposition of obstacles with transmission and distribution lines reflecting in the corresponding costs of the power system. The ViPOR also allows to simulate the communication with external systems to which the system under study is connected and also allows within certain limits to choose parameters of the optimization models.

The lowest cost distribution system is reached from a sequence of simulations of the system under study with repeated modifications in its parameters. The ViPOR adds successive random changes, adding a new node to the system, changing the position of transformers and components that are connected. Any change that results in lower overall cost is accepted and the solution starts to develop from that change. A rejected change takes the system to its former state. In addition, the advancement of the simulations will make the process less sensitive to changes that are not significant and making the process of identifying a global minimum more robust.

Simulations with ViPOR are usually performed on an annual basis. In this work, however, simulations will also be performed on a semester basis precisely to evaluate the effects of spatial complementarity. A first simulation will be performed with real data, with annual basis, indicating a first design for the system being studied. A second set of simulations will be carried out, now with semester basis, seeking to understand the effects of spatial complementarity. Tab. 13.1 shows the data corresponding to the generating plants and

Tab. 13.2 shows the data related to the consumer loads, inserted in the ViPOR.

In the first set of results, Fig. 13.5 shows the spatial complementarity between hydroelectric power plants and wind farms, Fig. 13.6 shows the spatial complementarity between hydroelectric power plants and the PV modules and finally Fig. 13.7 shows the spatial complementarity between wind farms and the PV modules.

Fig. 13.5 indicates values of spatial complementarity equal to 0.83 and 1.00, and the best complementarities were found between the hydroelectric plants of the westernmost cell and the wind farms. The reversible hydroelectric power plant in the "central" hexagonal cell also presents maximum values of complementarity with the wind farms, in this case also associated to the smaller distances.

Tab. 13.1. Data of the generating plants.

Generating plant	type	#	P [MW]	E [MWh]
Herval	H	1	1.4	11,284
Bugres	H	2	11.1	89,466
Canastra	H	3	42.5	342,550
Toca	H	4	1.0	8,060
Passo do Inferno	H	5	1.3	10,478
			57.3	461,838
Sangradouro II	W	1	29.9	86411
Lagoa dos Barros III	W	2	22.4	64736
Osório I	W	3	50.0	144500
Índios III	W	4	23.0	66470
Chicolomã	W	5	27.2	78608
Lagoa dos Barros I	W	6	22.4	64780
Cidreira	W	7	70.0	202300
Sangradouro I	W	8	50.0	144500
Osório II	W	9	27.6	79764
Índios I	W	10	50.0	144500
Lagoa dos Barros II	W	11	22.4	64736
Osório III	W	12	26.0	75140
Índios II	W	13	29.9	86411
Sangradouro III	W	14	27.6	79764
			478.4	1,382,620
Linha Sete – pumped hydro	H		0.6	5,023
Linha Sete – PV modules	PV		0.1	158

Tab. 13.2. Data of the consumer loads.

Loads	P peak [MW]	E [MWh]
1	12	40,880
2	28	92,710
3	20	68,255
4	10	33,580
5	14	45,990
6	14	48,180
7	7	23,725
8	20	67,890
9	17	56,210
10	25	85,775
11	7	23,725
12	11	35,770
13	13	42,705
14	7	23,725
15	10	33,945
16	9	29,930
17	9	31,390
18	5	17,155
19	6	18,980
20	5	15,330
21	6	18,615
22	8	26,280
23	6	21,900
24	9	29,200
25	22	73,000
26	32	109,500
27	65	219,000
	396	1,333,345

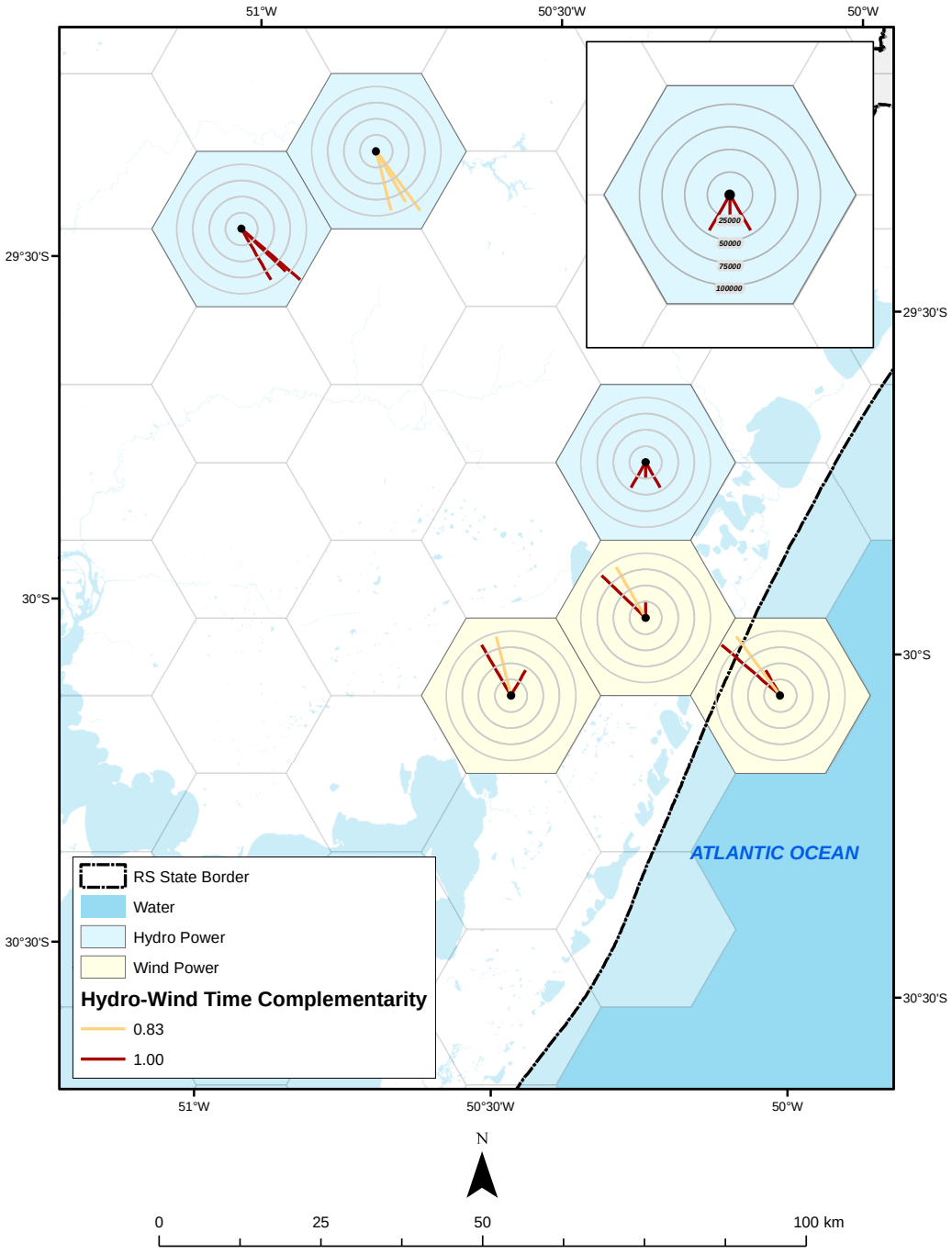

Fig. 13.5. Spatial complementarity in time between hydro and wind energy resources between the power plants indicated in the map of Fig. 13.2.

Fig. 13.6 indicates complementarity values equal to 1.00 between the photovoltaic modules and the northernmost hydroelectric power plants and values equal to 0.83 between the photovoltaic modules and the westernmost power plants. Fig. 13.7 indicates low spatial complementarities in time between photovoltaic modules and wind farms, as would be expected from the results indicated in the two previous figures.

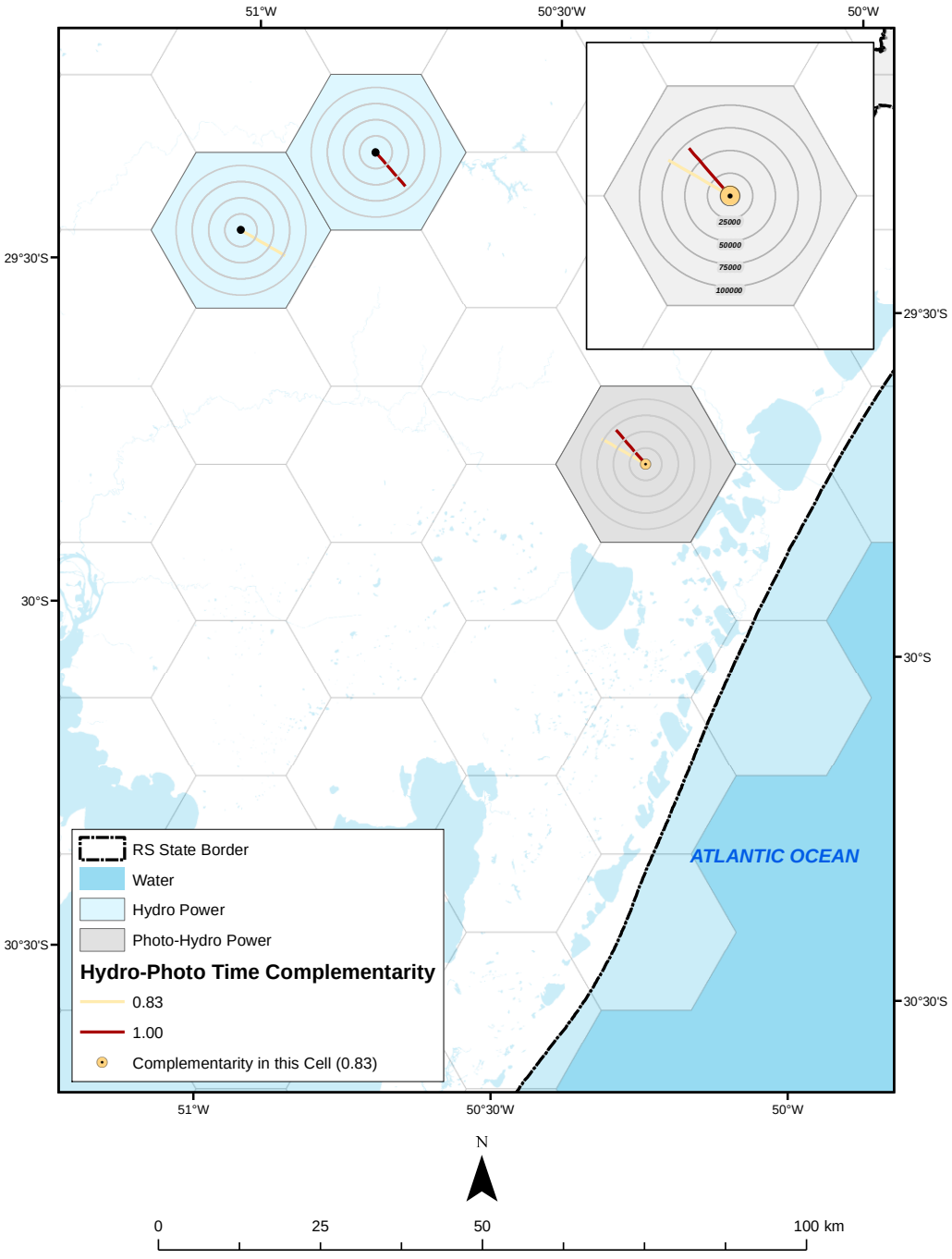

Fig. 13.6. Spatial complementarity in time between hydro and solar PV energy resources between the power plants indicated in the map of Fig. 13.2.

.

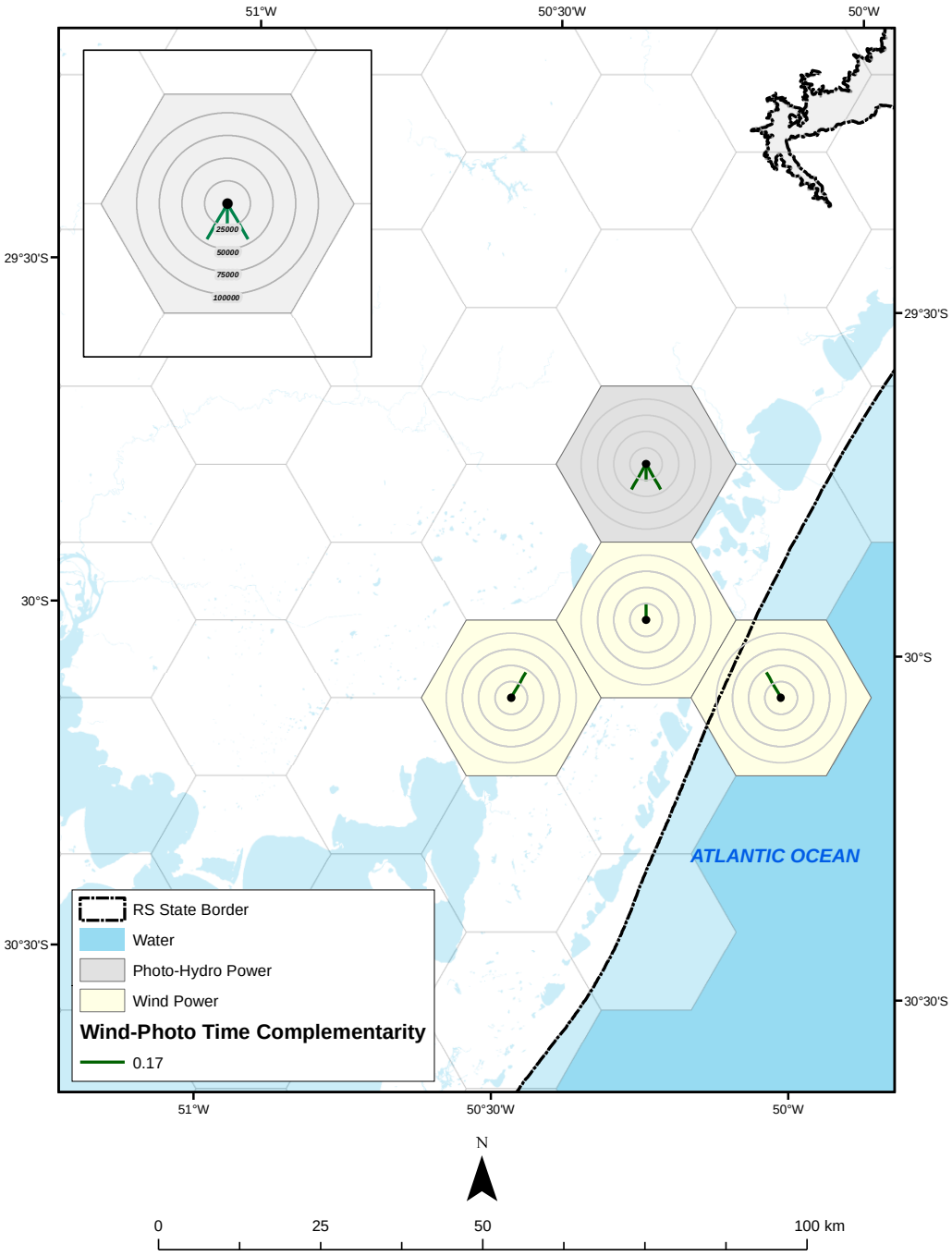

Fig. 13.7. Spatial complementarity in time between wind and solar PV energy resources between the power plants indicated in the map of Fig. 13.2.

. The results obtained with ViPOR are summarized in Fig. 13.8 and detailed in Tab. 13.3. Among the simulations performed, the main differences appeared in the three transmission sections numbered from 1 to 3. Solutions indicating the interconnection of all sources and loads were preferred among all other possible solutions.

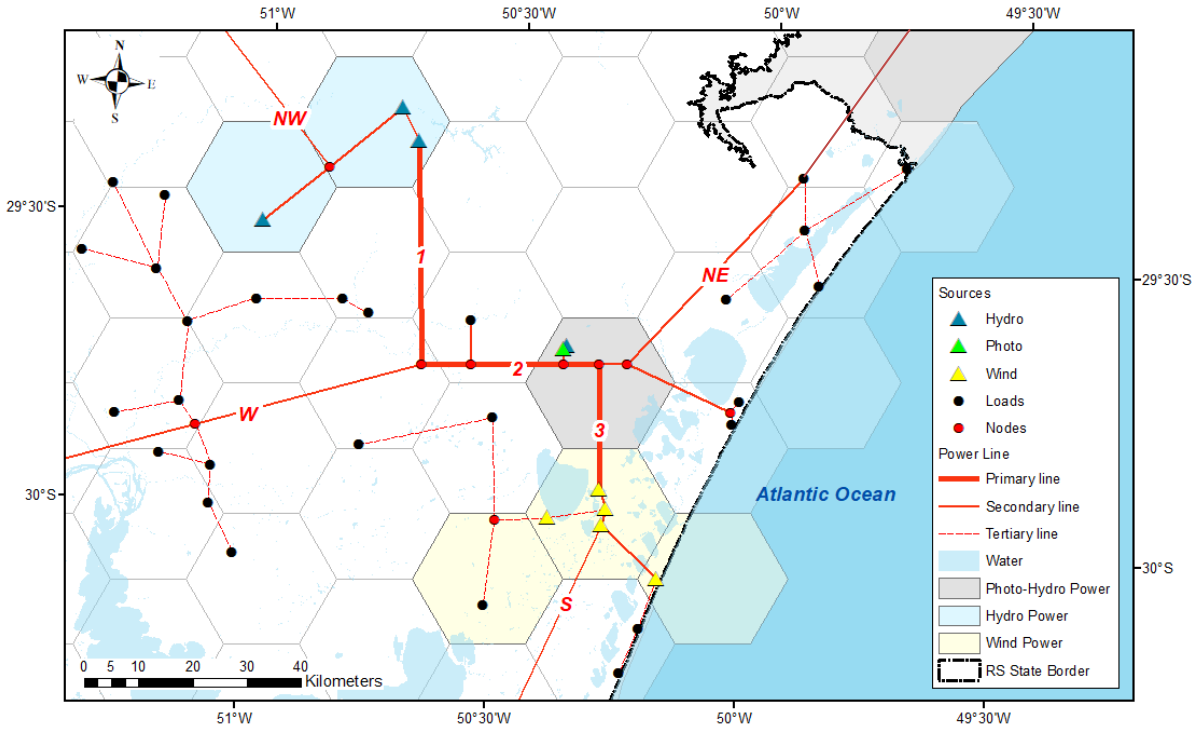

Fig. 13.8. Components of hybrid system under study.

Tab. 13.3. Results of simulation with ViPOR software.

Components of the system	current	maximum	minimum
1	80	60	120
2	60	60	100
3	60	60	100
NW in	20	20	80
NW out	20	20	80
NE in	20	20	80
NE out	20	20	80
W in	20	20	80
W out	20	20	80
S in	0	0	0
S out	0	0	0

The data in Tab. 13.3 indicate that the spatial complementarity in time between water and wind resources indicated in Fig. 13.5 leads to the best solution in which transmission lines 1, 2 and 3 present the lowest costs. The transport capacities for the current situation of complementarity in these lines indicate values of 80 MW for line 1 and 60 MW for the other two lines. A situation of total complementarity would lead to 60 MW of capacity for the three stretches.

A hypothetical situation of zero complementarity between hydroelectric plants and wind farms would lead to the need for lines with a much higher capacity. The results in Tab. 13.3 indicate line 1 with 120 MW of transport capacity and lines 2 and 3 with capacities of 100 MW each line. The availability of energy resources throughout the year in a more balanced way allows the installation of smaller lines, while a concentration of these resources over time in one or another half year requires a greater capacity of the lines to serve the consumers.

Tab. 13.3 also reports data on the import and export capacity of the medium voltage sections around lines 1, 2 and 3, since this simulated system is considered as part of the Brazilian interconnected system. This table shows the power import and export capacities respectively for the north-west (NW), northeast (NE), west (W) and south (S) regions of the large capacity main lines in this system.

The results for the northwest, northeast and west regions were similar. The medium capacity transmission lines should have a capacity of 20 MW for the current situation of spatial complementarity and for a situation of complete complementarity. This capacity should be high and equal to 80 MW if spatial complementarity equals zero.

This higher capacity related to a worse complementarity is related to the need to import energy from the interconnected system to meet the consumer loads located in the simulated system. These imports are naturally intended to offset the concentration of energy available in one part of the year and the energy drought in the other part of the year.

The simulations did not take into account the possibility of energy import and energy export in the southern region, since it would only feed consumers in the region to the town of São José de Norte in an extensive region where there is little energy consumption and in which the generation of energy through wind farms was not simulated in this study.

13.7 Conclusions

This paper studied the influence of spatial complementarity on the design of a medium-sized hybrid system in the north coast of the State of Rio Grande do Sul. The software used in this study was the ViPOR, which allowed the simulation of loads and generating plants along of a region by identifying its spatial locations and differentiating the dimensions of the structures for the distribution of available energy.

The simulations showed that the current situation of spatial complementarity between hydroelectric plants and wind farms leads to results quite similar to a hypothetical situation of total complementarity. The simulations also showed that a hypothetical situation of zero complemetarity would require lines to transport energy with almost twice the capacity of the current lines.

Spatial complementarity will influence the hybrid system design based on renewable resources, eventually contributing to lower installed energy transport capacities, as the resources employed present better values of spatial complementarities. Certainly the interconnected systems currently in operation already take advantage of the complementarity to exploit available resources, however a better knowledge of the mechanisms associated with complementarity will allow a better use of the resources still available, both in the design of hybrid systems and in the establishment of rules of operation.

13.8 References

[13-1] Risso, A., Beluco, A. (2017) Bases for a methodology assessing time complementarity in space. Energy and Power Engineering, 9, 527-540.

[13-2] Beluco, A., Kroeff, P.K., Krenzinger, A. (2008) A dimensionless index evaluating the time complementarity between solar and hydraulic energies. Renewable Energy, 33, 10, 2157-2165. http://dx.doi.org/10.1016/j.renene.2008.01.019

[13-3] Beluco, A., Souza, P.K., Livi, F.P., Caux, J. (2015) Energetic complementarity with hydropower and the possibility of storage in batteries and water reservoirs. In: Sørensen, B. (Ed.) Solar Energy Storage, Academic Press, London, UK, 155-188. http://dx.doi.org/10.1016/B978-0-12-409540-3.00007-4

[13-4] Beluco, A. (2015) A concept of boundaries of performance for analysis of hybrid systems based on complementary energy resources. In: Prasad, R. Shivakumar, B.G. Sharma, U.C. Energy Management; Energy Science and Technology, Vol.12; Houston, TX, USA, Studium Press LLC, p.459-483.

[13-5] https://goo.gl/maps/3ezz3m9fm2M2

[13-6] https://goo.gl/maps/PBxDo9kEcWB2

[13-7] https://goo.gl/maps/EDKWw5MWBqC2

[13-8] https://goo.gl/maps/6cVRAGuTSaQ2

[13-9] https://goo.gl/maps/KMP31dzwJVR2

[13-10] https://goo.gl/maps/kyzFbHgbLK22

[13-11] https://goo.gl/maps/SmsbLgJwmvK2

[13-12] https://goo.gl/maps/Ex7F6y9gvPG2

[13-13] https://goo.gl/maps/m5ULeACSvDk

[13-14] https://goo.gl/maps/SL4pigs7bJC2

[13-15] https://goo.gl/maps/2hAFUGbdhEw

[13-16] https://goo.gl/maps/APib4Vvdcyu

[13-17] https://goo.gl/maps/df18LiQZL5F2

[13-18] https://goo.gl/maps/oM6iEMDhB6k

[13-19] https://goo.gl/maps/upE7VUgMkL92

[13-20] https://goo.gl/maps/jiGXfV1P4ez

[13-21] https://goo.gl/maps/eGhduuoqAXJ2

[13-22] https://goo.gl/maps/tLi8HmLnN9r

[13-23] https://goo.gl/maps/kdNYG9dtTNP2

[13-24] https://goo.gl/maps/xFjnUWVJBBx

[13-25] Risso, A., Canales, F.A., Beluco, A., Rossini, E.G. (2016) A PV hydro hybrid system with pumped storage capacity installed in Linha Sete, Aparados da Serra, southern Brazil. In: Kishor, N., Fraile-Ardanuy, J. (org.) Modeling and Dynamic Behaviour of Hydropower Plants, London, UK, The Institution of Engineering and Technology, 208-225.

[13-26] Water Resources National Agency (ANA); HidroWeb, Brazilian Water Resources Database.
Available in www.hidroweb.ana.gov.br, accessed on August 22, 2017.

[13-27] Mines and Energy State Secretary, Rio Grande do Sul Wind Atlas.
Available in minasenergia.rs.gov.br/atlas-eolico-2016-03, accaessed on August 22, 2017.

[13-28] Risso, A., Beluco, A. (2018) Evaluating spatial complementarity in time with complementarity roses. Energies, submitted for publication.

14. CONSIDERAÇÕES FINAIS

Este capítulo apresenta uma síntese das conclusões apresentadas ao longo dos artigos que compõem esta tese, assim como uma panorâmica de futuras abordagens provenientes deste trabalho.

14.1 Conclusões

De forma geral foi feita a proposição de uma metodologia para a quantificação da complementaridade espacial no tempo e para sua expressão gráfica através de mapas.

O primeiro artigo apresentou um primeiro passo no processo de obtenção do método proposto, sugerindo a avaliação da complementaridade espacial através de um gráfico, determinado pela avaliação da complementaridade no tempo entre dois locais diferentes, mostrando a complementaridade espacial como uma função da distância.

Entre as limitações desse primeiro método, destaca-se o fato de que esse gráfico não distingue as direções indicadas e também apresenta apenas as máximas complementaridades em cada distância representada. É necessário qualificar a informação de complementaridade espacial com informações de direção e sentido.

Dentro das limitações desse processo, esse artigo apresenta um mapa contendo informações de complementaridade entre algumas usinas hidrelétricas e algumas fazendas eólicas situadas no entorno do litoral norte do Estado do Rio Grande do Sul, discutindo algumas das influências da complementaridade espacial sobre sistemas de geração de energia.

O segundo artigo propõe um método realmente eficaz para quantificação de complementaridade espacial no tempo, propondo sua avaliação por meio de rosas de complementaridade. As rosas de complementaridade são compostas por linhas direcionadas de um ponto de origem a um ponto de destino, cujos recursos energéticos foram comparados no sentido de identificar complementaridade espacial.

Os comprimentos das linhas que compõem as rosas de complementaridade indicam a distância entre os pontos cujos recursos energéticos foram comparados. As cores das linhas estabelecem as intensidades da complementaridade no tempo entre os recursos energéticos dos dois pontos considerados. Uma rosa de complementaridade é composta então por um conjunto de linhas em diferentes direções, indicando as complementaridades para o entorno do ponto considerado.

Por outro lado, a base de dados que contém a localização das fontes dos diferentes recursos de geração de energia é composta por uma rede georreferenciada interligada, o que permite identificar a localização dos pontos complementares a uma fonte específica.

Esse artigo ainda apresenta um mapa para o Estado do Rio Grande do Sul, indicando a complementaridade espacial entre um conjunto de usinas hidrelétricas e um conjunto de fazendas eólicas. Nesse mapa, é identificada por exemplo a forte complementaridade espacial no tempo entre usinas hidrelétricas no rio Uruguai e fazendas eólicas no litoral norte do Estado do Rio Grande do Sul.

No último artigo, as simulações efetuadas no ViPOR, mostraram que a atual situação de complementaridade espacial entre usinas hidrelétricas e parques eólicos leva a resultados bastante semelhantes a uma situação hipotética de complementaridade total. As simulações também mostraram que uma situação hipotética de zero complementaridade exigiria que as linhas transportassem energia com quase o dobro da capacidade das linhas atuais.

A complementaridade espacial influenciará no desenho do sistema híbrido a partir de recursos renováveis, contribuindo para a diminuição das capacidades de transporte de energia instalada, uma vez que os recursos empregados apresentam melhores valores de complementaridade espacial. Certamente os sistemas interligados atualmente em operação já aproveitam a complementaridade para explorar os recursos disponíveis, porém um melhor conhecimento dos mecanismos associados à complementaridade permitirá um melhor aproveitamento dos recursos ainda disponíveis, tanto na concepção de sistemas híbridos quanto no estabelecimento de recursos disponíveis das regras de operação.

14.2 Abordagens futuras

A abordagem inovadora deste trabalho abre caminho para várias novas linhas de pesquisa. Entre as questões a serem exploradas, podem ser citadas:

[1] O aperfeiçoamento do método para quantificação e para expressão gráfica da complementaridade espacial no tempo e sua extensão também para as outras componentes, a complementaridades de energia e a complementaridade entre as amplitudes.

[2] O estudo da relação entre a complementaridade espacial e a distância abrangida em sua determinação, inserindo na determinação da complementaridade o conceito de distância de viabilidade para os empreendimentos de geração.

[3] A aplicação exaustiva do método em estudos, por exemplo, sobre a complementaridade energética entre diversos recursos renováveis ao longo do território brasileiro e ao longo do continente sul-americano.

[4] O estudo mais aprofundado da influência da complementaridade energética sobre a performance de sistemas híbridos de geração e de sistemas híbridos de armazenamento de energia.

[5] A construção de uma plataforma de simulação e de otimização de sistemas híbridos de geração de energia, mais abrangente que o software Homer e incluindo conceitos de complementaridade energética.